

CHARACTERIZATION OF T CELL ANTIGEN COUPLERS

**CHARACTERIZATION OF THE CORECEPTOR DOMAIN OF T CELL
ANTIGEN COUPLERS IN CANCER IMMUNOTHERAPY**

By KENNETH ANTHONY MWAWASI, B.Sc, M.Sc

A Thesis Submitted to the School of Graduate Studies in Partial
Fulfillment of the Requirements for the Degree Doctor of Philosophy

McMaster University © Copyright by Ken Mwawasi, January 2020

McMaster University DOCTOR OF PHILOSOPHY (2020) Hamilton,
Ontario (Medical Sciences)

TITLE: Characterization of the Cytoplasmic Domain of T Cell Antigen
Couplers in Cancer Immunotherapy

AUTHOR: Kenneth A. Mwawasi, B.Sc. M.Sc. (McMaster University)

SUPERVISOR: Dr. Jonathan L. Bramson

PAGES: xvi, 132

Lay Abstract

Cancer is the leading cause of death in Canada, and it is expected that 2 in 5 Canadians will develop some form of cancer in their lifetime. The immune system presents an intriguing alternative method to treat tumours since immune cells such as T cells can circulate through the body and seek and destroy harmful cells, including tumours. Here, we focus on the T cell Antigen Coupler (TAC), a genetically engineered receptor that our laboratory originally designed that directs T cells to recognize and destroy specific cancer cells. This thesis looks at the inner workings of the receptor, specifically a part called the inner tail, and how this feature contributes to how the TAC works. Our results show that removing the tail increases the T cell's ability to safely clear different tumours in living organisms, bringing us a step closer in designing new and safe treatments for cancer patients.

ABSTRACT

Activating the immune system in the therapeutic treatment of cancer is rapidly growing and has demonstrated tremendous success. One such method is engineering T cells with chimeric antigen receptors (CARs) to specifically direct them in targeting tumours, however this has been associated with several toxicities that may be linked to the synthetic nature of the CAR. To address this, our laboratory created the T Cell Antigen Coupler (TAC), an alternative receptor that redirects T cells in a more natural TCR-dependent fashion.

The TAC consists of three components: the antigen-binding domain that recognizes a tumour antigen, a TCR-recruitment domain that co-opts the native CD3-TCR complex and a CD4 co-receptor domain. The TAC displays unique biology, specifically in the increased antitumor infiltration and clearance of solid malignancies without any of the observed host toxicities seen with CARs.

The functionality of the TAC was shown to be dependent on both the antigen binding and TCR-recruitment domains, however the co-receptor domain remains relatively uninvestigated despite evidence in the literature indicating its importance in endogenous T cell activation. This thesis seeks to better understand the biology of the TAC receptor by investigating the contributions of co-receptor domain.

In **Chapter 3**, we replaced the CD4 co-receptor domain with CD8 variants and showed that the TAC retains functionality.

In **Chapter 4**, we removed the cytosolic domain of the TAC in its entirety (creating a “tailless TAC”) and observed increased *in vivo* efficacy.

In **Chapter 5**, we evaluated the tailless TAC in different cancer models and consistently observed increased *in vivo* efficacy compared to the full length TAC.

These results demonstrate an increase in the *in vivo* functionality of the TAC receptor when the cytoplasmic tail is removed, giving us further insights into the mechanisms behind the unique biology of the TAC receptor.

ACKNOWLEDGEMENTS

I would first and foremost like to extend my genuine gratitude to my supervisor Dr. Jonathan Bramson for giving me the opportunity to do exciting and impactful research in his laboratory. I originally came to his laboratory with minimal cancer biology or immunology experience, and I truly appreciate his decision in taking me on as a doctoral student despite this. The training and experience I received under his supervision have exceeded all my expectations from when I first joined the lab, and throughout the years he has continuously challenged me to improve my craft as a scientist. Choosing a laboratory and supervisor is possibly the most important decision a student will make in graduate school, and I can confidently say it was the best decision I made.

I would also like to thank all the members of my supervisory committee, Dr. Dawn Bowdish, Dr. Carl Richards and Dr. Martin Stampfli. Their knowledge and diverse immunological backgrounds helped me view and approach my science from different perspectives and I'm grateful for their patience and insights.

I feel honoured and privileged to have worked with many intelligent, fun, diverse and remarkable individuals in the Bramson lab, all of which have positively impacted me in some fashion. I would like to thank the members of the HITS team for their expertise on flow cytometry, the laboratory technicians for the technical assistance (especially with regards to the mouse work) and my fellow graduate students, past and present, who have embarked on this incredible journey with me.

I owe my deepest and heartfelt gratitude to my family who have supported me as I pursued my goals and ambitions. Their encouragement and support have been a continuous source of inspiration and I cannot imagine completing this chapter of my life without them. Thank you Mom and Dad for always believing in me.

TABLE OF CONTENTS

Preliminary Pages

Half Title Page.....	i
Title Page	ii
Descriptive Note.....	iii
Lay Abstract.....	iv
Abstract.....	v
Acknowledgements	vi
Table of Contents	vii-ix
List of Figures.....	x-xi
List of Tables.....	xii
List of Abbreviations	xiii-xv
Declaration of Academic Achievement	xvi

Main Text

CHAPTER 1 – INTRODUCTION.....	1
1.1 Cancer.....	2
1.1.1 <i>Biology and Etiology</i>	2
1.1.2 <i>Current Treatments and Limitations</i>	3
1.2 The Immune System and Cancer.....	4
1.2.1 <i>Innate and Adaptive Immunity</i>	4
1.2.2 <i>Immune Surveillance of Tumours</i>	5
1.3 T Cell Biology.....	5
1.3.1 <i>T Cell Development and Central Tolerance</i>	5
1.3.2 <i>Peripheral Migration and Antigen Experience</i>	7
1.3.3 <i>Signaling Involved in T Cell Activation</i>	11
1.3.4 <i>Models of T Cell Activation</i>	12
1.3.5 <i>Structural Insights into T Cell Activation: Immunological Synapse</i>	13
1.3.6 <i>Activated T cell Fates and Dénouement</i>	15
1.4 Cancer Immunotherapy.....	18
1.4.1 <i>Mechanisms of Tumour Escape from the Immune System</i>	18
1.4.2 <i>Cancer Vaccines</i>	19
1.4.3 <i>Monoclonal Antibody Based Therapies</i>	21
1.4.4 <i>Oncolytic Viruses and Vaccines</i>	22
1.4.5 <i>Adoptive Cell Transfer</i>	22
1.5 MHC-Independent Synthetic T Cell Receptors.....	23
1.5.1 <i>Chimeric Antigen Receptors</i>	23

1.5.2 <i>T Cell Antigen Coupler (TAC) Receptor</i>	29
1.6 Thesis Objectives.....	32
CHAPTER TWO – MATERIALS AND METHODS.....	33
2.1 Genetic Cloning of TAC Constructs.....	34
2.1.1 <i>Transmembrane and Intracellular Tail Constructs</i>	34
2.1.2 <i>Antigen Binding Domain Constructs</i>	34
2.2 Plasmid Propagation and Preparation from <i>E. coli</i>	37
2.2.1 <i>E. coli Chemical Competent Cell Preparation</i>	37
2.2.2 <i>E. coli Transformation</i>	37
2.2.3 <i>Large Scale Plasmid Preparation</i>	38
2.3 Cell Lines and Tissue Culturing.....	38
2.3.1 <i>Human Embryonic Kidney 293TM (HEK293TM)</i>	38
2.3.2 <i>Adherent Tumour Lines</i>	38
2.3.3 <i>Nonadherent Tumour Lines</i>	39
2.4 HEK293TM Transient Transfection.....	39
2.5 Lentivirus Production.....	39
2.6 Manufacturing of Engineered T Cells.....	40
2.6.1 <i>T Cell Transduction and Upscaling</i>	40
2.6.2 <i>Enrichment of Engineered T cells (NGFR Selection)</i>	40
2.6.3 <i>Cryopreservation of Engineered T cells</i>	40
2.7 Cell Phenotyping.....	41
2.8 <i>In vitro</i> T Cell Functionality Assays.....	42
2.8.1 <i>Intracellular Cytokine Stimulation</i>	42
2.8.2 <i>Killing/Cytotoxicity Assay</i>	42
2.8.3 <i>Proliferation Assay</i>	43
2.9 Jurkat Immunofluorescence Microscopy.....	43
2.10 <i>In vivo</i> Tumour Modeling.....	44
2.10.1 <i>Mice</i>	44
2.10.2 <i>KMS-11 Model and Monitoring</i>	44
2.10.3 <i>OVCAR-3 Model and Monitoring</i>	44
2.10.4 <i>NALM-6/JEKO-1 Model and Monitoring</i>	44
2.11 Statistical Analyses.....	45
CHAPTER THREE – SUBSTITUTION OF THE CD4 TAC ANCHOR WITH CD8.....	45
VARIANTS	
Introduction.....	46
Results.....	47
Discussion.....	60
CHAPTER FOUR – CHARACERIZATION OF THE TAILLESS TAC.....	63
Introduction.....	64

Results.....	65
Discussion.....	81
CHAPTER FIVE – FUNCTIONALITY OF THE TAILLESS TAC USING DIFFERENT ANTIGEN BINDING DOMAINS	85
Introduction.....	86
Results.....	87
Discussion.....	97
CHAPTER SIX – GENERAL DISCUSSION	99
6.1 Summary of Research Findings.....	100
6.2 Biological Implications.....	101
6.2.1 <i>Diminished Surface Expression of the Tailless TAC</i>	101
6.2.2 <i>Increased in vivo Efficacy of the Tailless TAC</i>	102
6.3 <i>In vitro</i> Evaluation of Future Receptors.....	105
6.4 Future Considerations in TAC Design.....	107
6.5 Closing Remarks.....	110
REFERENCES	111

LIST OF FIGURES

CHAPTER ONE: INTRODUCTION

Figure 1.1 – Peptide-MHC interaction with the TCR-CD3 complex and associated co-receptor	8
Figure 1.2 – Co-receptor intracellular domains	10
Figure 1.3 – Simplified scheme of signal 1 and signal 2 convergence	12
Figure 1.4 – Schematic of Chimeric Antigen Receptors (Generations 1-3)	24
Figure 1.5 – Single chain variable fragment composition from antibody structure	25
Figure 1.6 – T Cell Antigen Coupler (TAC) design mimics the TCR-CD3 complex	30

CHAPTER TWO: MATERIALS AND METHODS

Figure 2.1 – DNA backbone of the <i>pCCL</i> vector	34
--	----

CHAPTER THREE: SUBSTITUTION OF THE CD4 TAC ANCHOR WITH CD8 VARIANTS

Figure 3.1 – Schematic of the CD8 TAC constructs	47
Figure 3.2 – CD8 TAC constructs express on the surface of T cells and functionally lyse target cells <i>in vitro</i>	48
Figure 3.3 – CD8 TAC constructs secrete similar cytokines as the CD4 TAC upon antigen stimulation	50
Figure 3.4 – Schematic of TAC intracellular tail mutants	51
Figure 3.5 – TAC mutants retain <i>in vitro</i> functionality	52-53
Figure 3.6 – The Her2 DARPins as ligand binding domains for the TAC receptors are expressed on HEK293TM and exhibit different binding properties	55
Figure 3.7 – DARPins exhibit differential expression and functionality as the antigen binding domain of the TAC receptor on T cell	56
Figure 3.8 – <i>In vitro</i> functionality of the G3-AVD mutant TAC variants despite poor surface expression	57-59

CHAPTER FOUR: CHARACTERIZATION OF THE TAILLESS TAC RECEPTOR

Figure 4.1 – Schematic representation of anti-BCMA huUCHT1 Y177T scaffold TAC constructs	66
Figure 4.2 – Diminished surface expression of the tailless TAC	67
Figure 4.3 – Cellular trafficking of the TAC receptor	68
Figure 4.4 – Abrogated <i>in vitro</i> cytokine production of the Tailless TAC	69
Figure 4.5 – <i>In vitro</i> proliferation and cytotoxicity of the tailless	70

TAC is not abrogated	
Figure 4.6 – The tailless TAC displays <i>in vivo</i> efficacy.....	71-72
Figure 4.7 – The tailless TAC displays <i>in vivo</i> efficacy.....	73
Given a higher initial tumour burden	
Figure 4.8 – Schematic representation of TAC intracellular.....	74
Tail truncation constructs	
Figure 4.9 – Intracellular tail truncation constructs exhibit.....	75-76
Higher surface expression and <i>in vitro</i> functionality than	
The tailless TAC	
Figure 4.10 – The TAC _{Δ488-525} truncation displays similar.....	77-78
<i>In vivo</i> efficacy to the tailless TAC	
Figure 4.11 – The tailless TAC outperforms the TAC _{Δ488-525} truncation.....	78
<i>In vivo</i> when mice are re-challenged with BCMA ⁺ JEKO-1 tumour cells	
Figure 4.12 – Characterization of the role of the palmitoylation.....	79
Cysteines on surface expression and functionality	
Figure 4.13 – The 2A truncation TAC phenocopies the surface.....	80
Expression and <i>in vitro</i> functionality (cytokine production) of	
The full-length TAC	

CHAPTER FIVE: FUNCTIONALITY OF THE TAILLESS TAC USING DIFFERENT ANTIGEN BINDING DOMAINS

Figure 5.1 – Schematic representation of Her-2 specific TAC.....	87
Intracellular tail truncation constructs	
Figure 5.2 – <i>In vitro</i> cytokine production of the Her2-specific.....	88-89
Tailless TAC is not abrogated despite diminished surface expression	
Figure 5.3 – The tailless TAC displays increased <i>in vivo</i> efficacy.....	90
Compared to other TAC constructs against Her2 ⁺ OVCAR tumours	
Figure 5.4 – Schematic representation of CD19-specific TAC constructs.....	91
Figure 5.5 - CD-19 specific tailless TAC displays abrogated surface.....	92-93
Expression, but similar <i>in vitro</i> cytokine production profile compared	
To the full-length TAC	
Figure 5.6 – The tailless TAC displays increased <i>in vivo</i> efficacy compared.....	94-95
To other TAC constructs against CD19 ⁺ NALM-6 tumour cells	
Figure 5.7 – Both TAC-engineered T cells can control the tumour.....	95-96
Burden from a CD19 ⁺ tumour re-challenge	

CHAPTER SIX: GENERAL DISCUSSION

Supplementary Figure S1 – Type 1 cytokine receptors in T cells.....	108
Supplementary Figure S2 – Antigen-dependent JAK-STAT signaling.....	109
<i>In TAC T cells</i>	

LIST OF TABLES

CHAPTER TWO: MATERIALS AND METHODS

Table 1.0 – Gene products used to clone TAC and DARPin constructs.....	35-37
Table 2.0 – List of cloning primers used.....	37
Table 3.0 – List of antibodies used.....	40-41

CHAPTER THREE: SUBSTITUTION OF THE CD4 TAC ANCHOR WITH CD8 VARIANTS

Table 4.0 – Affinities of different anti-Her2 DARPins.....	54
---	----

CHAPTER FOUR: CHARACTERIZATION OF THE TAILLESS TAC RECEPTOR

Table 5.0 – Organelle markers for IF trafficking of the tailless TAC.....	67
--	----

LIST OF ABBREVIATIONS

Ab - antibody
ACT – adoptive cell therapy/transfer
ADC – antibody drug conjugates
ADCC - antibody-dependent cellular cytotoxicity
AF – AlexaFluor
AICD – activation induced cell death
APC – antigen presenting cell/ Allophycocyanin
ATP - adenosine triphosphate
BCMA – B cell maturation antigen
BFA – Brefeldin A
BiTE - bi-specific T cell engager
BSA – bovine serum albumin
BV421 - brilliant violet 421
CAIX - carbonic anhydrase IX
CAR – chimeric antigen receptor
CCL# - chemokine (C-C motif) ligand#
CCR# - C-C chemokine receptor #
CD# - cluster of differentiation
CDC - complement dependent cytotoxicity
CLP - common lymphoid progenitor
CMP – common myeloid progenitor
CRS – cytokine release syndrome
CTL – cytotoxic T lymphocyte
CTLA-4 - cytotoxic T lymphocyte associated antigen 4
Ctrl – control
DAPI - 4',6-diamidino-2-phenylindole
DARPin - designed ankyrin repeat protein
DC – dendritic cell
DDR – DNA damage response
DMEM – Dulbecco's Modified Eagle Medium
DMSO - Dimethyl sulfoxide
DNA – deoxyribonucleic acid
dSMAC – distal supermolecular activation center
ECM – extracellular matrix
EDTA - Ethylenediaminetetraacetic acid
EF1 α – elongation factor 1 alpha
ER – endoplasmic reticulum
FBS – fetal bovine serum
FITC - Fluorescein isothiocyanate
GPI - glycosylphosphatidylinositol

HEK – human embryonic kidney
HER2 - human epidermal growth factor receptor 2
HEPES - 4-(2-hydroxyethyl)-1-piperazineethanesulfonic acid
HEVs – high endothelial venules
HSC – hematopoietic stem cell
ICAM-1 – intracellular adhesion molecule 1
ICS – intracellular cytokine stain
IF – immunofluorescence
IFN γ – interferon gamma
IgG – Immunoglobulin G
IL – Interleukin
IS – immunological synapse
ITAM - immunoreceptor tyrosine-based activation motif
ITK – inducible T cell kinase
i.v. – intravenous
JAK – Janus kinase
K_D - dissociation constant
KLGR-1 - killer-cell lectin like receptor G1
LAG3 - lymphocyte activating gene 3
LAT – linker for activation of T cells
LB - lysogeny broth
Lck – lymphocyte specific c-src kinase
LFA-1 – lymphocyte function associated antigen 1
mAb – monoclonal antibody
MC - microcluster
MDSCs - Myeloid derived suppressor cells
MFI – mean fluorescence intensity
MHC – major histocompatibility complex
MOI – multiplicity of infection
NCK - non catalytic region of tyrosine adapter kinase 1
NEAA – Nonessential amino acids
NK - natural killer
NGFR – nerve growth factor receptor
NOD – non-obese diabetic
NS – no stimulation
OD₆₀₀ – optical density at 600 nm
OV – oncolytic virus/vaccine
P/S – penicillin/streptomycin
PAMPs – pathogen associated molecular patterns
PBMC – peripheral blood mononuclear cells
PBS – phosphate buffered saline
PD-1 - programmed cell death-1

PE - Phycoerythrin
PFA - paraformaldehyde
PGK - phosphoglycerate kinase
PI3K - phosphoinositide 3-kinase
PKC - protein kinase C
PLC γ 1 – phospholipase C gamma 1
PMA - phorbol 12-myristate 13-acetate
PSCA - prostate stem cell antigen
pSMAC – peripheral supermolecular activation center
STAT - Signal Transducer and Activator of Transcription proteins
SCID - Severe combined immunodeficiency
scFv – single chain variable fragment
SH# – Src homology #
SPICE – simplified presentation of incredibly complex evaluations
STAT - signal transducer and activator of transcription proteins
RAG – recombination activating gene
RNA - ribonucleic acid
RPM – revolutions per minute
RPMI - Roswell Park Memorial Institute medium
TAA - tumour associated antigen
TAC – T cell antigen coupler
T_{CM} – central memory T cell
TCR – T cell receptor
T_{EM} – effector memory T cells
Tfh - T follicular helper
Th – T helper
TIL – tumour infiltrating lymphocyte
TM – transmembrane
TNF α – tumour necrosis factor alpha
TRAC - T cell receptor α constant
Treg – regulatory T cell
TSA – tumour specific antigen
YFP – yellow fluorescent protein

DECLARATION OF ACADEMIC ACHIEVEMENT

Kenneth A. Mwawasi has produced all content described in this thesis apart from the following:

- **Figure 1.1** and **Supplementary Figure S2** were originally produced by Arya Afsahi and adapted for this thesis by Ken Mwawasi with permission from the original creator.
- The anti-Her2 UCHT1 CD4 TAC constructs (both parent and 4A) introduced in **Figure 3.4** were originally cloned and created by Chris Helsen
- The proliferation and cytotoxicity experiments for the anti-BCMA TACs shown in **Figure 4.5** were performed by Ying Wu
- The phenotype and ICS data shown in **Figure 5.5** were generated from experiments conducted by Bojana Bojovic. Raw flow cytometry data was compiled and analyzed by Ken Mwawasi
- All *in vivo* tumour modeling including tumour (re)challenge, adoptive cell transfer and monitoring described in **Section 2.10** were performed by Craig Aarts and Chris Baker. These data are shown in **Figures 4.6, 4.7, 4.10, 4.11, 5.3, 5.6 and 5.7**. Joni Hammill and Bojana Bojovic provided technical assistance in manufacturing some of the engineered T cells for these experiments.

CHAPTER ONE

INTRODUCTION

1.1 CANCER

1.1.1 Biology and Etiology

Cancer is a term that encompasses over 100 related diseases defined by uncontrolled cell division with the potential to spread and invade surrounding tissue¹. It is widely believed to arise when cells experience genomic damage² and evade cellular mechanisms that prevent programmed cell death, progressively proliferating them into neoplastic cancer cells in a process called carcinogenesis². It is the leading cause of mortality in Canada, and it is estimated that 2 in 5 Canadians will develop cancer in their lifetime³.

Carcinogenesis caused by genetic damage can be the result of abnormal endogenous cellular processes (which in some cancers is inherited⁴) such as errors in DNA replication, epigenetic hypomethylation of oncogenes and attack from free radicals generated during metabolism or exogenous factors such as ultraviolet radiation and chemical carcinogens^{2,5-7}. Normal cells employ tissue specific homeostatic mechanisms that tightly control proliferation and programmed cell death (apoptosis), allowing for rapid expansion of new cells in tissues that require ongoing turnover (such as the epithelial lining of the intestines) or maintenance of a non-dividing state, such as the neurons in adult mammal brains^{2,8}. When the damage to DNA during carcinogenesis affects the genes controlling proliferation and cell death, the cell escapes these homeostatic mechanisms, allowing the growth and expansion of cancerous progeny and generally leading to the formation of tumours^{1,2}.

The neoplastic cells eventually proliferate and interact with surrounding stromal cells, fibroblasts, and immune cells to establish the tumour microenvironment, a heterogeneous and critical local niche where the tumor exists with these other cell populations⁹. Fibroblasts are non-epithelial, non-vascular cells in the connective tissue associated with wound healing that are appropriated by the neoplastic cells in the tumour microenvironment to remodel the extracellular matrix (ECM), a network of fibronectin, proteoglycans, laminins and collagen, allowing for the metastasis of cancer cells to other tissues^{10,11}. The growing mass of the tumour increases oxygen demands of the tumour microenvironment, often leading to its hypoxic state¹². This hypoxic signal is detected by adjacent blood vessels, stimulating the creation of new blood vessels (angiogenesis) to the tumour microenvironment. This tumour vasculature is often abnormal in their structure and function, consisting of heterogenous, uneven and chaotically branched vessels that leak escaping fluid and increase interstitial fluid pressure^{12,13}. This leads to uneven blood flow and limits the ability chemotherapeutic drugs and immune cells to reach the tumour mass¹³.

The biological traits shared by all cancers were summarized in 2000 by Hanahan and Weinberg (termed *the six hallmarks of cancer*¹⁴): self-sufficiency in growth signals,

sustained angiogenesis, insensitivity to inhibitory growth signals, evading apoptosis, metastasis capabilities and limitless replicative potential. Although the chronology and mechanisms of acquiring these traits vary significantly across cancer types, the transformation of a normal cell into a cancer encompasses all six hallmarks.

In 2011, Hanahan and Weinberg updated the hallmarks of cancer to include two new hallmarks: abnormal metabolism and **evasion of the immune system**¹⁵, the latter hallmark being most pertinent to this thesis. It was recognized that tumor cells possessed these traits, allowing them to grow in mass, appropriate local blood vessels and fibroblasts, evade immune clearance, and metastasize to different organs. They noted that our understanding of cancer and the tumour microenvironment is growing, and recognize additional underlying hallmarks may be added as we better understand the myriad of phenotypic complexities among different cancers¹⁵.

1.1.2 Current treatments and limitations

The three main treatments for cancer are surgery, radiation therapy and systemic treatment – the latter being an umbrella term that encompasses chemotherapy, targeted therapy, hormonal treatment and immunotherapy (discussed in detail in **Section 1.4**)¹⁶. The choice of treatment generally depends on the specific cancer and its stage of progression. For instance, 49% of patients with stage I breast cancer (non-metastasized, tumour smaller than 2 cm) are treated with a combination of surgery and radiation therapy, while 56% of stage IV patients (tumour metastasized to other organs) receive a combination of chemotherapy and radiation therapy¹⁶.

Surgery is a medical procedure used to examine, remove or repair tissue and is the first-line treatment for patients with solid tumours^{17,18}. The primary goal of surgery is the complete physical clearance and resection of the tumour. Surgery is primarily effective against cancer that is localized and has not spread to surrounding tissue¹⁸. As stated earlier other treatments such as chemotherapy and radiation therapy can be used alongside surgery as an adjuvant (after surgery) or neoadjuvant (before surgery) therapy^{18,19}.

Radiation therapy uses high energy x-rays or other photons to create ionizing particles in cells that lead to DNA damage, cell cycle arrest and, eventually, cell death²⁰. DNA damage inflicted by ionizing radiation triggers the DNA Damage Response (DDR) in cells, which halts the cell cycle (preventing progeny cells from receiving damaged genetic material) and allows DNA damage repair machinery to function. When repair fails, the DDR triggers apoptosis^{20–22}. Normal cells are generally successful in repairing the damage caused by ionizing radiation, while cancer cells (due to genetic instability, primarily in the DDR) are susceptible to it²².

Unlike surgery and radiation therapy where the application is directed at the site of the tumour, systemic therapies are administered in the blood and travel throughout the body. They include chemotherapeutic drugs, which inhibit the growth of rapidly proliferating cells through various mechanisms of actions. For instance, alkylating agents

covalently bind an alkyl group to the guanine bases of DNA, while anthracyclines intercalate DNA base pairs, thereby preventing unwinding by DNA topoisomerase²³.

Despite the vast improvements in patient outcomes over the past 50 years with these therapies¹⁶, they are not without their limitations. The complete debulking of a tumour may not be possible via surgery when the tumour is too big, has grown too close to nearby organs or if the patients' general pre-operation health is poor¹⁸. Furthermore, surgery tends to only be effective in the early stages of cancer before the tumour metastasizes to other organs¹⁶. Hypoxia of the tumour microenvironment also limits the effectiveness of radiation therapy, as it is hypothesized that DNA damage by ionization is chemically fixed by molecular oxygen²¹. Furthermore, hypoxia and poor delivery to the tumour microenvironment via abnormal angiogenesis also negatively impacts the effectiveness of some chemotherapeutic drugs which require oxygen to function and require proper systemic delivery to the tumour site via blood vessels²⁴.

1.2 THE IMMUNE SYSTEM AND CANCER

Advancements in our understanding of the immune system and its relation to cancer has led to the exponential rise of cancer immunotherapy (or immune oncology) as the new pillar of cancer therapy²⁵. It utilizes the ability of the immune system to circulate throughout the body and recognize and destroy target cells expressing certain antigens with high specificity. In this section, basic principles of immunology will be discussed with a focus on T lymphocytes in the context of cancer clearance and immune surveillance.

1.2.1 Innate and adaptive immunity

Innate immunity provides the “first line of defense” against pathogens and toxins, and includes anatomical physical barriers such as gut and skin epithelia that prevent foreign entities from the external world from entering the internal milieu of the host²⁶. In addition to acting as a physical barrier, detection of these pathogens and toxins can also trigger the surface epithelia produce a wide variety of chemicals that not only have anti-microbial properties but also mediate the cellular response to infection²⁷. This immediate cellular response is provided by innate immune cells that recognize certain molecular motifs expressed by foreign microbes called pathogen associated molecular patterns (PAMPs) and become activated²⁶. The cell subsets associated with this arm of immunity include dendritic cells, natural killer cells (NK), macrophages, neutrophils, eosinophils, basophils, and mast cells.

The next line of defense is the adaptive immune response, in which individual clonal T and B lymphocytes recognize very specific molecular structures termed antigens by the expression of antigen-specific receptors on their cell surface²⁸. Unlike innate immune cells, T and B lymphocytes can recognize a large repertoire of antigens due to the gene segment rearrangement of their antigen-specific receptors during initial

development, allowing for an exponentially higher pool of these individual receptors than genetically encoded in the genome^{26,28}. Not only can these clones rapidly proliferate in response to their antigens, a major hallmark of the adaptive immune system is the induction of immunological memory. After initial activation, a small subset of antigen experienced cells remain, allowing for a rapid and robust response in the event of re-exposure²⁶.

Clearance of infection involves coordinated responses from a network of cells that encompass both arms of the immune system in order to maintain physiological homeostasis.

1.2.2 Immune surveillance of tumours

In addition to targeting foreign non self-pathogens and toxins, the immune system plays a major role in cancer control²⁵. History is replete with evidence of tumours regressing after episodes of infectious diseases as early as the late 1800s: in 1868 Wilhelm Busch, a German surgeon intentionally infected cancer patients with the bacteria that caused erysipelas (skin rash) and noted a shrinkage of their tumours²⁵. In the 1890s, William Coley continued this line of investigation when he too observed that a sarcoma patient whose tumour relapsed after several surgeries had no trace of cancer for seven years after an erysipelas infection²⁹. He hypothesized that the infection was somehow responsible for the tumour regression, and refined this early vaccination strategy by injecting patients with two strains of killed bacteria: *S. pyogenes* and *S. marcescens* (subsequently known as Coley's toxins) and observed tumour regression in sarcoma patients^{25,29}. As the discoveries of several immunological mechanisms were made during the 20th century such as the role of histocompatibility complex in the role of transplant rejection³⁰, tolerance³¹, the role of interferon in viral interference³², and the chemical structure of antibodies³³⁻³⁵, our understanding of how and which immune cells contribute to carcinogenesis increased exponentially.

A landmark discovery in immune surveillance occurred in 2001 when investigators observed that immunodeficient mice lacking functional T and B lymphocytes (i.e. SCID and Rag2^{-/-} mutants) treated with the highly carcinogenic methylcholanthrene developed sarcomas at a much higher rate than wildtype mice^{36,37}. Additional clinical studies showed that the presence of T cells (specifically effector memory, which will be discussed in detail in **Section 1.3.6**) in tissues displaying early signs of metastatic colorectal cancer is associated with the absence of pathological metastatic invasion and with prolonged survival³⁸. T lymphocytes clearly play an important role in immune surveillance, and understanding this role requires a deep dive into the basics of T cell biology, as discussed in the following section.

1.3 T CELL BIOLOGY

1.3.1 T cell development and central tolerance

All classes of human blood cells including red blood cells and leukocytes originate in the bone marrow from hematopoietic stem cells (HSCs) expressing CD34. HSCs can differentiate into two classes of progenitors: common lymphoid progenitors (CLPs) that give rise to T cells, B cells and NK cells and common myeloid progenitors (CMPs) that eventually give rise to granulocytes, macrophages, platelets and erythrocytes^{26,39,40}. A hallmark of HSCs is their ability of self-renewal, which CLPs lose during the differentiation process⁴¹.

One of the hallmarks of T cells is expression of the T cell receptor (TCR) on the cell surface, a unique heterodimer of disulfide-linked type I glycosylated membrane proteins: TCR α and TCR β . CLPs destined for the T cell fate migrate to the thymus where they acquire their TCR and differentiate following three major events: T cell receptor (TCR) $\alpha\beta$ rearrangement, positive selection, and negative selection⁴². While T cells are generally CD4⁺ or CD8⁺, referring to the expression of the coreceptor on their cell surface (discussed below), they enter the thymus as double negative CLPs (CD4⁻CD8⁻) as they begin their “education” in this site⁴³. Diversity in clonal TCRs arise from the rearrangement of gene segments from germline DNA, a mechanism beyond the scope of this document but described in detail elsewhere^{44,45}. The TCR β chain is assembled first, and then associates with an invariant pre-TCR α (pT α) chain as well as CD3 molecules (consisting of CD3 $\epsilon\gamma$, CD3 $\epsilon\delta$ and CD3 $\zeta\zeta$ dimers)⁴⁶ to form a pre-TCR complex. The thymocytes then undergo a process called β -selection, where only cells that generated a functional TCR β chain will receive antigen independent survival signals and proliferate and differentiate into double positive cells (CD4⁺CD8⁺)^{26,47}.

At this stage, the cells begin to quiesce, rearrangement of the TCR β loci ceases, and rearrangement of the TCR α chain commences. Interaction with host peptide-MHC is then evaluated: TCRs with sufficient binding affinity to peptide-MHC receive **positive selection** signals, ensuring that recognition is restricted to host MHC. However, TCRs that bind with too strongly with host peptide-MHC (i.e. high interaction affinity) undergo **negative selection** and receive apoptotic death signals to ensure that the T cells do not auto-react to host antigens in the periphery^{26,48}. The range of this affinity threshold between positive and negative selection for TCR-pMHC interaction is a dissociation constant (K_D) of 0.1-500 μ M⁴⁹. The thymocytes that survive death by neglect from positive selection and avoid apoptosis from negative selection mature into either a single positive CD4 or CD8 T cell, depending on their recognition of MHCII or MHCI (discussed below), respectively. Thymocytes then exit the thymus and enter the periphery as a mature, naïve T cells with functional clonal TCRs (~30,000 molecules per cell)⁵⁰.

Collectively, negative and positive selection in the thymus is known as **central tolerance**, a process that is believed to ensure the host T cells can recognize host MHC while limiting the generation of T cells that recognize self-peptides, which could lead to autoimmune disease. Of course, some potentially auto-reactive T cells do escape and

enter the periphery. There also exist peripheral tolerance mechanisms that aim to prevent autoimmunity that will be discussed throughout the remainder of **Section 1.3**.

1.3.2 Peripheral migration and antigen experience

Mature, naïve T cells need to interact with their cognate antigen to elicit an effector response. These antigens are peptides that are processed and presented by major histocompatibility complex (MHC) molecules on the surface of antigen presenting cells (APCs). To present antigens to T cells, APCs first degrade proteins into peptides and load them on MHC molecules: MHCI for CD8⁺ T cells and MHCII for CD4⁺ T cells (**Figure 1.1**). MHCI is expressed by all nucleated cells, and peptides loaded onto this complex (8-10 amino acids in length) are derived endogenously from the endoplasmic reticulum, whereas peptides loaded onto MHCII are 13-25 amino acids in length and are derived exogenously from endosomes of professional antigen presenting cells^{51,52}.

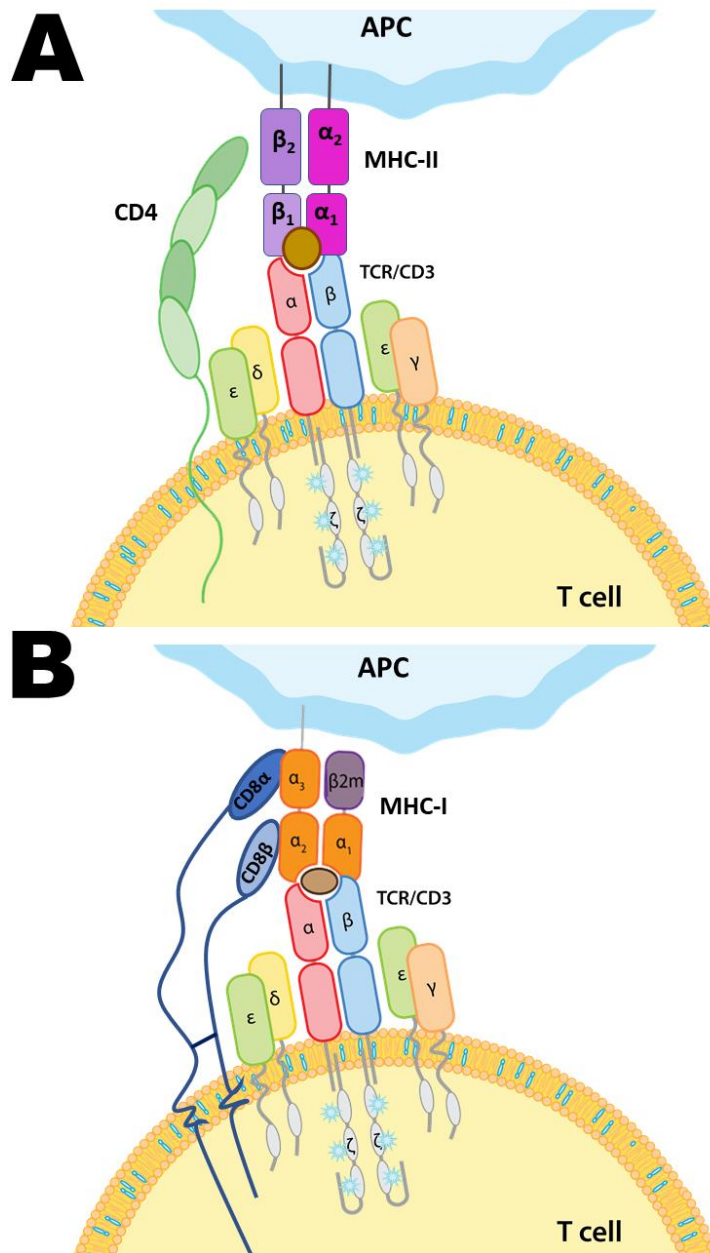


Figure 1.1 – peptide-MHC interaction with the TCR-CD3 complex and associated co-receptor

T cells recognize their clonal antigen by interaction of peptide-displayed by the MHC complex with the TCR and the associated co-receptor. (A) A CD4⁺ T cell recognizes peptides presented by MHC-II complexes. The CD4 complex interacts with the β_2 component of MHC-II. (B) A CD8⁺ T cell recognizes peptides displayed by MHC-I complexes. The CD8 co-receptor is a heterodimer in which CD8 α interacts with the α_3 component of MHC-I while CD8 β interacts with the α_2 component of MHC-I.

Figure adapted from Arya Afsahi

Given that a single T cell only occupies one-hundred-trillionth of the volume of an adult human⁵³, and each T cell is specific for a single peptide-MHC, this feat requires the precise migration of both T lymphocytes and APCs in the same spatial location, mostly secondary lymphoid organs such as lymph nodes⁵³. Naïve T cells enter lymph nodes from the bloodstream via the high endothelial venules (HEVs), specialized vessels containing tall and plump endothelia and thick basal lamina, as opposed to the flat endothelia and thin basal lamina of other venules⁵⁴. Constitutive expression of chemokines CCL19 and CCL21 at these sites contributes to migration of naïve T cells via interaction with CCR7 on their surface⁵⁵. Interaction of CD62L (L-selectin) on the surface of T cells with complex carbohydrates on HEVs allows for the rolling and tethering of the lymphocytes⁵⁶. CCL21 interaction with CCR7 also activates lymphocyte associated antigen 1 (LFA-1) on the surface of T cells, which binds strongly to the intracellular adhesion molecules (ICAMs) of the vascular endothelium, thereby allow complete arrest and entry of the naïve T cell into the lymph node⁵⁵. A naïve T cell spends 8-12 hours exploring a single lymph node. If it does not experience its specific peptide-MHC, it exits lymph node via the efferent lymphatics and returns to circulation through the thoracic duct where it begins the homing cycle again⁵⁷.

Regardless of MHCI or MHCII peptide presentation, TCR $\alpha\beta$ engage the complex in a similar fashion: although both TCR $\alpha\beta$ variable regions make contact with invariant regions of the MHC, TCR α specifically engages the peptide at its N-terminus while TCR β engages it at the C-terminus⁵⁸. As earlier stated, this interaction is relatively weak (K_D of 0.1-500 μM)⁴⁹ and is accompanied by the interaction of either the CD4 or CD8 coreceptor with MHCII or MHCI, respectively.

The CD4 coreceptor is a type I transmembrane glycoprotein consisting of 4 immunoglobulin-like extracellular domains (D1-D4) connected by a short stalk, transmembrane domain and an intracellular domain. Of the extracellular domain, only the membrane distal D1 motif interacts with MHCII, while the D2-D4 motifs provide the rigidity during antigen ligation⁵⁹. In addition to anchoring the coreceptor to the membrane, the 13 amino-acid long transmembrane domain may have important structural roles for T cell activation⁶⁰. A study that replaced the glycines in the conserved GGxxG motif (present in several other transmembrane proteins) with bulkier side chains found that CD4⁺T cells produced less cytokine in response to antigen stimulation, despite no difference in surface expression compared to the wildtype CD4 coreceptor⁶¹. The CD4 intracellular domain (or cytoplasmic tail) has been heavily characterized in the literature due to its role in T cell signaling (**Figure 1.2**). The domain contains a C-terminal CXCP motif that specifically binds the Lck signaling kinase in the presence of a zinc ion cofactor⁶². The intracellular domain also contains two membrane proximal cysteine residues that have been shown to be important sites for post translational palmitoylation. Palmitoylation of

these cysteines contributes to the localization of the CD4 receptor into membrane specific microdomains that enhance antigen-induced signaling, leading to T cell activation and proliferation⁶³.

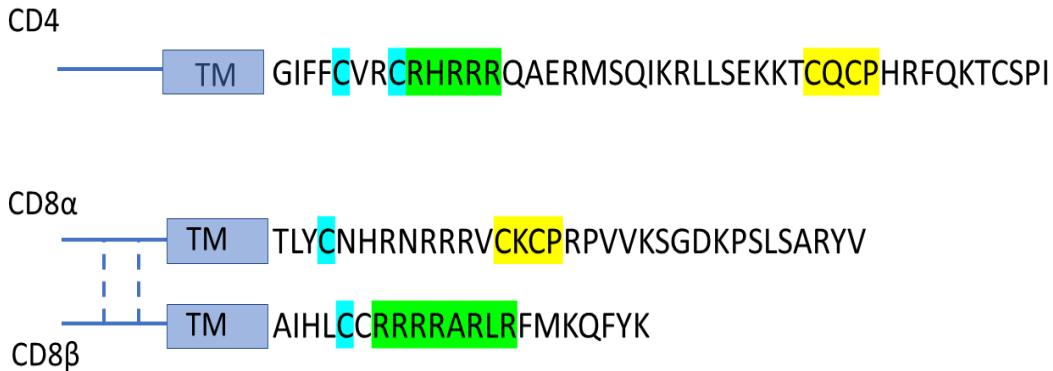


Figure 1.2 Co-receptor intracellular domains

Intracellular domains for the CD4, CD8 α and CD8 β co-receptors are shown. The CD4 monomer contains two-membrane proximal cysteines that undergo posttranslational palmitoylation (blue), an arginine rich domain (green) important for membrane compartmentalization and a CXCP motif responsible for Lck binding (yellow). CD8 is an $\alpha\beta$ heterodimer (joined by two di-sulfide bonds in the extracellular domain, shown as dotted lines) containing similar residues in its intracellular domain. The α stalk specifically contains the CXCP motif and interacts with Lck while the β stalk contains the arginine rich domain.

The CD8 coreceptor differs from CD4 not only in MHC recognition, but also in structure. CD8 is a transmembrane dimer primarily consisting of heterodimeric α and β chains (CD8 $\alpha\beta$), but can also exist as homodimeric α chains (CD8 $\alpha\alpha$) in certain lymphocyte populations⁶⁴. CD8 $\beta\beta$ homodimers have been reported, but they do not bind to MHC and their significance is currently not known⁵⁹. The extracellular domain of both CD8 isoforms interact with MHCI, however CD8 β is also involved in receptor orientation as its shorter length requires a T cell membrane proximal position during antigen engagement⁶⁵. The stalk region of CD8 also appears to play larger structural and functional roles than the CD4 stalk region. Although there is little sequence similarity between both stalk domains, they both contain two conserved cysteine residues that form disulfide bonds with the adjacent cysteine residues on the other stalk leading to dimerization of the coreceptor⁶⁶. Interestingly, replacement of only the α stalk with the β stalk in CD8 $\alpha\alpha$ homodimers leads to antigen-induced cytokine production similar to that of the CD8 $\alpha\beta$ heterodimer, suggesting that the β domain enhances *in vitro* functionality⁶⁶. Similar to CD4, the intracellular domain of CD8 α contains a CXCP motif that binds Lck in the presence of a Zn²⁺ cofactor^{62,67} (**Figure 1.2**). Although both CD8 α and CD8 β cytoplasmic tails contain cysteine palmitoylation sites, palmitoylation is not involved in the association of the coreceptor in specific membrane microdomains associated with T

cell activation. Instead, CD8 β contains an arginine rich motif in its intracellular domain (**Figure 1.2**) that is responsible for this compartmentalization⁶⁸.

1.3.3 Signaling involved in T cell activation

T cells that emerge from the thymus are termed “naïve” and possess little functionality. Upon stimulation by specific peptide antigen, the naïve T cells differentiate and acquire effector function (cytolysis, cytokine production) and memory function (capacity to rapidly expand upon re-exposure to antigen). The initial activation of naïve T cells requires two signals: i) peptide-MHC interaction with the specific clonal TCR and ii) ligation of costimulatory molecules.

Despite numerous experimental studies, the relationships between peptide-MHC interaction, signal transduction and T cell activation remain controversial. While the proximal events are debated in the literature, it is understood that TCR ligation leads to the Lck dependent phosphorylation of the immunoreceptor tyrosine-based activation motifs (ITAMs) in the CD3 ζ chain⁶⁹. Phosphorylation of these motifs leads to the recruitment of another cytoplasmic tyrosine kinase, ZAP-70, due to the high affinity interaction of its SH2 domains to the phosphorylated tyrosine residues on the ITAMs. ZAP-70 is subsequently phosphorylated by Lck, leading to its activation and the downstream phosphorylation of the linker for the activation of T cells (LAT) and the SH2-domain-containing leukocyte protein of 76 kDa (SLP-76) proteins⁷⁰. The consequence of these intracellular signaling events is the activation of biochemical pathways such as PLC γ 1, PI3K and Ras which ultimately contribute to T cell activation^{71,72}.

The second signal necessary to achieve naïve T cell activation comes from costimulatory ligands. Costimulatory receptors on the surface of the T cell such as CD28 and 4-1BB interact with cognate costimulatory ligands, such as CD80/CD86 and 4-1BBL, respectively²⁶. A subset of hematopoietic cells, known as **antigen presenting cells (APCs)**, express these co-stimulatory molecules in the presence of danger or pattern associated molecular patterns to promote activation of naïve T cells that recognize antigens present in relevant environments. Co-stimulatory receptors play several roles in signal transduction leading to cell proliferation and survival and converge with TCR-peptide-MHC signaling to achieve this. For instance, the phosphorylation of SLP-76 initiated by signal 1 ultimately causes the recruitment and phosphorylation PLC γ which requires Itk, a kinase that is recruited by the costimulatory receptor, CD28^{26,73}. Itk is activated by Lck phosphorylation, thereby recruiting it to the LAT-SLP76 scaffold, and allowing it to phosphorylate PLC γ ²⁶. In this instance, signaling through PLC γ is only achieved simultaneously with both signal 1 (recruitment) and signal 2 (activation) (**Figure 1.3**). PLC γ activation leads to the increase of intracellular Ca²⁺ through Inositol trisphosphate (IP₃) production, thereby activating calcineurin which acts on the Nuclear factor of activated T-cells (NFAT) transcription factor to translocate into the nucleus and transcribe genes associated with proliferation and cytokine production⁷³.

When naïve T cells are exposed to their relevant MHC/peptide (i.e. signal 1) in the absence of costimulation (i.e. signal 2), T cells become anergic: a hyporesponsive state with low proliferative capacity which is one way potentially auto-reactive T cells are controlled in the circulation through peripheral tolerance^{74,75}.

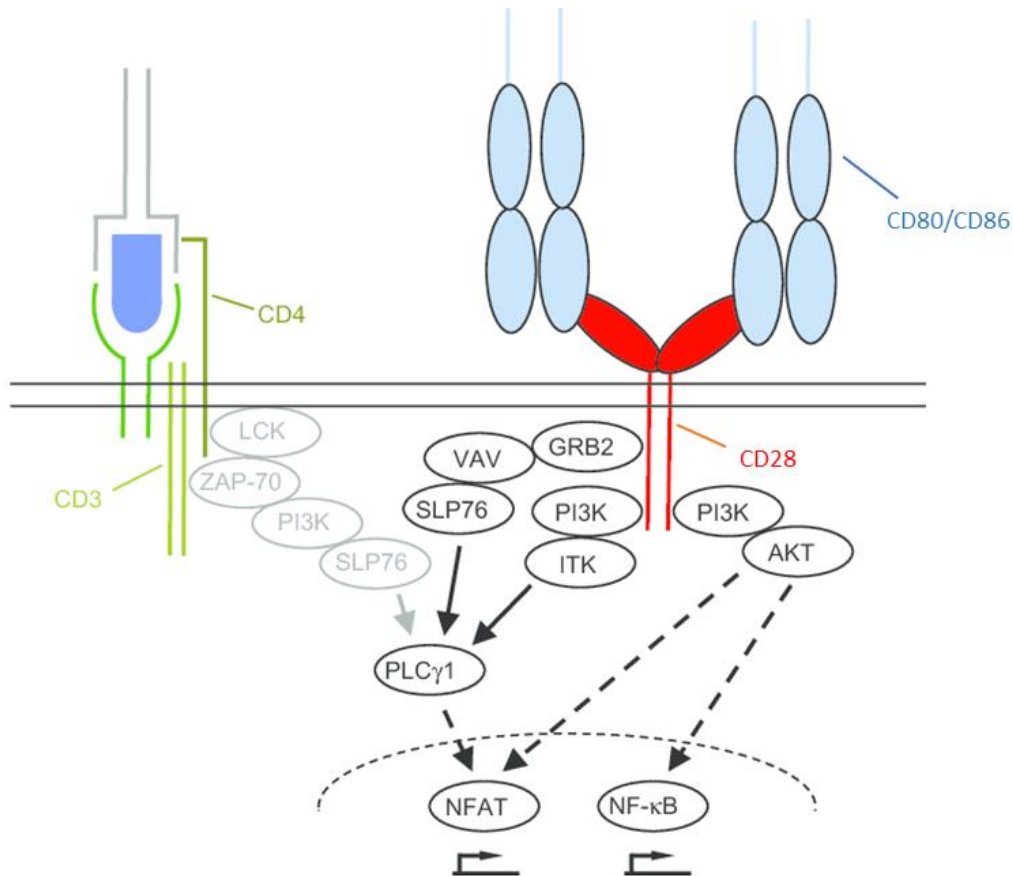


Figure 1.3 Simplified scheme of Signal 1 and Signal 2 convergence⁷⁶

During TCR/coreceptor-pMHC interaction (signal 1), phosphorylation of the CD3 ζ ITAMS by Lck initiates a signaling cascade (see text for details) that eventually recruits PLC γ to the signalosome. Co-stimulatory interaction of CD28 and CD80/CD86 recruits ITK, which is also phosphorylated and activated by Lck. Active Itk phosphorylates PLC γ , thereby leading to its activation.

1.3.4 Models of T cell activation

Early biochemical models of T cell activation involved the initial compartmentalization of Lck associated CD4/CD8 and ITAM containing TCR-CD3 complex. Evidence suggests that the CD4/CD8 co-receptors reside in lipid rafts, a liquid-ordered micro domain in the membrane containing tightly packed sphingolipids (such as ceramide and sphingomyelin) and cholesterol⁷⁷. The TCR resides in the glycerophospholipid-rich

bilayer which comprises most the plasma membrane⁷⁸. Upon peptide-MHC engagement, Lck (by virtue of association with the coreceptor) is brought in close proximity with the TCR-CD3 complex, allowing for the phosphorylation of its ITAMs by Lck due to the clustering of signaling molecules and kinases⁷⁹. This “Lck juxtaposition” model was supported by the fact that both CD4 and CD8 intracellular tails interact with Lck^{62,67}, both coreceptors and Lck reside in lipid rafts in resting cells^{63,68,80} while only antigen engagement lead to the localization of the TCR-CD3 complex into these rafts^{78,81,82}, and mutant versions of Lck⁸³, CD4⁶³, and CD8⁶⁸ that did not associate into lipid rafts lead to abrogated or diminished T cell activation.

This model however is not without its contradictions. There are some TCR $\alpha\beta$ variants that interact with peptide-MHC with such high affinity that they can trigger T cell activation without the need of a coreceptor⁸⁴. These high affinity TCRs bind to their peptide-MHC with >100 fold greater affinity ($K_D \sim 1-10$ nM) than conventional TCR $\alpha\beta$, and therefore dispute the assertion that Lck is only involved in activation when brought into close proximity to the TCR-CD3 complex by the coreceptor⁸⁵. Furthermore, Lck itself exists in two conformations (active and closed) depending on its phosphorylation state. As a member of the Src family of kinases, Lck contains four Src-homology (SH) domains each independently important for either structure or functionality of the protein⁸⁵. These domains include the membrane distal SH1 catalytic site of the enzyme responsible for phosphorylation, an SH2 domain responsible for binding to phosphorylated tyrosines, an SH3 domain that interacts with proline-rich regions and a myristoylated and palmitoylated N-terminal SH1 domain important for membrane anchoring^{86,87}. Enzymatic activity of Lck is regulated by the phosphorylation of two key tyrosine sites: Tyr394 in the SH1 domain and Tyr505 at the C-terminal end. When Tyr505 is phosphorylated, it causes the intramolecular rearrangement of the C-terminal tail whereby it interacts with its own SH2 domain, causes a clamped or closed conformational state unable to function enzymatically. Conversely, trans autophosphorylation of Tyr394 promotes an open/active conformation⁸⁷. Approximately 40% of total Lck is in the active form, however neither TCR-peptide-MHC engagement nor coreceptor interaction alter the ratio of active to inactive Lck^{87,88}. Therefore, most of the Lck the coreceptors juxtapose are in the inactive state and do not contribute to signaling.

Other T cell activation models have been proposed that attempt to consolidate the data in the literature, which are briefly discussed below⁷⁷:

TCR conformational change

Upon peptide-MHC ligation, conformational changes are induced in the TCR-CD3 complex that either stabilize the interaction with peptide-MHC or expose motifs that are recognized by signaling molecules. One of these conformational changes is the exposure of a proline-rich region in CD3 ϵ , leading to recruitment and direct binding of the Nck adapter protein through its SH3 domain^{89,90}. Nck, which also contains an SH2 domain that

binds to phosphorylated tyrosines, interacts with SLP-76 and the actin rearrangement associated Wiskott–Aldrich syndrome protein (WASP) and likely provides a link between T cell signaling and cytoskeleton remodeling at the T-cell-APC interface^{89,91}.

Peptide-MHC ligation has also been shown to keep CD3 ζ in a rigid conformation that protects the tail from proteolytic degradation, thereby sustaining signaling during antigen engagement⁹².

Furthermore, cholesterol has been shown to interact with TCR β , keeping it in an inactive conformation that cannot be phosphorylated. The TCR spontaneously detaches from cholesterol, leading to a primed conformation that can be phosphorylated and contribute to T cell signaling. Interaction with peptide-MHC stabilizes the primed conformation, suggesting an allosteric regulation of T cell activation by antigen interaction and cholesterol⁹³.

Kinetic proofreading

This phenotypic model proposes that T cell activation is proportional to the number of TCRs that have bound to peptide-MHC for a sufficient amount of time to lead to signal transduction⁷⁷. This depends on the association/dissociation constants of the interaction, where an agonistic interaction will lead to a longer dwell time, thereby allowing time for the numerous steps involved in signal transduction (i.e. antigen ligation, ITAM phosphorylation, ZAP70 involvement, etc)⁹⁴. Nonspecific interactions will have higher dissociation rates and will not have a long enough dwell time for the signal to persist. The kinetic proofreading model also suggests that all of the intermediary steps within the signaling cascade can be reversed by dissociation of the TCR from peptide-MHC⁹⁵.

Kinetic segregation

This model proposes that kinases and phosphatases are in passive equilibrium within the membrane of a resting T cell. The ITAMs are passively phosphorylated by signaling kinases, such as active Lck, and passively dephosphorylated by phosphatases, such as CD45, therefore, on balance, no signal is transmitted. Upon peptide-MHC interaction, multiple TCR-CD3 complexes cluster with their agonistic peptide-MHC. The kinetic clustering of these signaling molecules serves two purposes: 1) it physically separates them from phosphatases that would otherwise prevent signaling by dephosphorylation and 2) it clusters ITAMs together, allowing Lck to passively phosphorylate multiple motifs within the same area, thereby leading to signal transduction^{77,94,96}.

1.3.5 Structural insights into T cell activation – immunological synapse

Immediately ensuing the cellular engagement between the T cell and the target cell is the spatial reorganization of membrane proteins into a specialized structure at the interface of the contact site, referred to as the immunological synapse (IS)⁹⁷. The role of the synapse is to spatially coordinate signaling molecules and organize the secretion of

lytic granules onto the target cell in the case of cytotoxic T cells. The structure was first visualized and characterized by fluorescence microscopy two decades ago showing that two concentrated rings of proteins formed at the T cell-APC interface in a distinctive bull's-eye pattern: an inner ring containing high concentration of TCR and CD4/CD8 co-receptors called the central supramolecular activation complex (cSMAC) and an outer ring containing the integrin LFA-1 called the peripheral supramolecular activation complex (pSMAC)⁹⁸. A third outermost ring called the distal supramolecular activation complex (dSMAC) containing proteins with large ectodomains such as CD43 and CD45 surrounds the inner ring to complete the structure of the IS⁹⁹.

The original model of T cell activation by IS formation involves signal transduction originating from the cSMAC, as accessory proteins such as protein kinase C (PKC) and Lck were co-localized in the region along with a high TCR concentration⁹⁸. However, it was subsequently determined that the activated forms of these signaling proteins were only present in the pSMAC, and not the cSMAC, suggesting that although TCRs were more concentrated in the cSMAC, active TCRs were mainly present in the pSMAC ring⁹⁹. Work involving recombinant pMHC and ICAM-1 (binding partner for LFA-1) conjugated to artificial planar lipid bilayer surfaces allowed formation of the cSMAC and pSMAC at the T cell and bilayer interface to be visualized and followed in detail. Upon contact, the TCRs began aggregating in microclusters (MCs), and these MCs associated with several signaling molecules such as Lck, ZAP-70, SLP76 and LAT in the pSMAC. Over time, the MCs migrated centripetally to the cSMAC, but the associations with the activated accessory molecules were lost^{100,101}. It was then proposed that signaling occurs and is sustained in the pSMAC, while the cSMAC (devoid of active kinases) most likely serves as a site for TCR internalization and degradation, which is important for the long-term attenuation of T cell function^{97,102}. The hypothesis that the cSMAC serves as a termination site is further supported by the strong colocalization of Cbl-b (ubiquitin ligase) and LBPA (late endosomal marker) in the region^{99,103}.

With the advancement of high resolution microscopy, research into IS formation and function has increased dramatically⁹⁹. Work conducted by electron microscopy revealed that TCRs in resting T cells exist in linear oligomers of 2-10 complexes called nanoclusters (NCs), which are undetectable by standard microscopy since NCs are smaller than the wavelength of visible light (roughly 0.2 μm)¹⁰⁴. In addition to electron microscopy, super-resolution fluorescence microscopy such as high-speed photoactivated localization microscopy (hsPALM) further demonstrated that TCRs exist in nanoclusters in dormant T cells, and aggregate into microclusters (visible by standard light microscopy) upon antigen engagement^{105,106}. Signaling molecules such as LAT were also found to exist in nanoclusters (independent of the TCR), and aggregated with TCR nanoclusters to form activation microclusters in the pSMAC region of the IS¹⁰⁶.

1.3.6 Activated T cell fates and dénouement

A mature, naïve T cell encountering its associated antigen (along with adequate co-stimulation) for the first time experiences a series of biochemical, genetic, metabolic and proliferative events called T cell priming, which ultimately leads to the production of expanded T cell clones containing a mixed population of short lived effector cells and long-lived memory cells¹⁰⁷. Priming occurs in three phases¹⁰⁸: in the first phase, the mature naïve T cell recognizes its agonistic peptide-MHC displayed by an APC, likely a dendritic cell, in a lymph node. The T cell then undergoes a series of transient interactions with the APC lasting 2-8 hours, which leads to decreased lymphocyte motility and the upregulation of the early activation marker CD69¹⁰⁹. In the second phase, the T cell makes long lasting stable contacts with the APC lasting approximately 12 hours. At this stage, the T cell begins to produce cytokines such as IL-2 and IFN γ as well as upregulates activation markers such as the α subunit of the IL-2 receptor (CD25)^{108,110}. Finally, the last phase begins 24 hours after initial antigen experience, where the T cell begins to dissociate from the APC, rapidly migrates, vigorously proliferates, and begins to downregulate CD25 and CD69¹¹¹.

CD4⁺ T cells polarize into a broad class of “helper” T cells during priming. These cells support the immune system by the robust production and secretion of cytokines and chemokines that can activate neighbouring immune cells and/or recruit specific cell subsets to a site of infection¹¹². The effector subsets include T helper (such as Th1, Th2 and Th17), T follicular helper (Tfh), and regulator T cells (Tregs). The former migrate to nonlymphoid tissues in order to regulate the anti-microbial actions of other immune cells at the site of infection, while Tfh cells travel to B cell follicles where they induce germinal center responses that aid in the production of antibodies^{112,113}. Tregs play an important role in attenuating inflammatory processes, which if unchecked, can result in overexuberant immune responses associated with immunopathology and auto immune diseases^{112,114}. Differentiation into these different fates depends on the cytokine environment/milieu during priming, which is often referred to as “signal 3”¹¹⁵. For instance, the generation of IFN γ and IL-12 during intracellular viral infections polarizes CD4⁺ T cells to the Th1 subset during priming. This subset is characterized by the large production of IFN γ and TNF α , which feed back into the cytokine environment and promote neighbouring immune cells such as macrophages and dendritic cells to activate their antigen presentation phenotype, among other outcomes¹¹². Similarly, the presence of IL-4 commonly produced during extracellular parasitic infections¹¹⁶ polarizes the CD4⁺ T cells to the Th2 subset, which produce IL-4, IL-5, and IL-13 that activate neighboring eosinophils, mast cells, and basophils, which specialize in the elimination of parasites^{112,117}.

Naïve CD8⁺ T cells differentiate into cytotoxic T lymphocytes (CTLs) (also known as killer T cells) that specialize in eradicating intracellular pathogens. The cytokine priming environment drives CD8⁺ T cell differentiation into short-lived effector cells that immediately deal with the infection within the first 15 days of initial antigen experience

or long lived memory cells that persist in the periphery and robustly respond to future similar infections. Pro-inflammatory cytokines, specifically IL-2, IFN γ and IL-12 drive the development of the effector phenotype, which includes low expression of the IL-7 receptor (CD127)¹¹⁸, high expression of the killer-cell lectin like receptor G1 (KLRG-1)¹¹⁹ and increased transcription of effector genes perforin and granzyme¹²⁰. These effectors specialize in the delivery of cytotoxic granules into target cells that ultimately lead to the apoptosis of those cells. Upon immunological synapse formation with the target cells, CTLs secrete perforin, a pore-forming protein, into the membrane of the target cell. This causes membrane perturbations that lead to a calcium flux, eventually causing the target cells to rapidly uptake anything bound to its outer membrane¹²¹. CTLs also secrete granzymes, a class of serine proteases that are endocytosed during the calcium flux that ultimately trigger three different apoptosis pathways, leading to target cell death^{121,122}. Apoptosis of target cells can also be initiated by the ligation of CTL Fas ligand (FasL) to the target cell Fas protein (CD95/TNFRSF6), a type I transmembrane member of the tumour necrosis receptor (TNFR) family^{26,123}. With regards to signal 3 for CD8⁺ T cells, cytokines IL-7, IL-15 and IL-21 tend to drive the polarization of the memory phenotype¹¹².

Following activation, naïve T cells proliferate vigorously and subsequently undergo a unique process after priming and proliferation called contraction (approximately 7-15 days after initial priming), where most of the effector cells die off via apoptosis, and a small pool of memory cells remain^{124,125}. Memory cells exist in two broad classes: effector memory (T_{EM}) and central memory (T_{CM}). T_{EM} cells tend to circulate in the periphery, have relatively low proliferative capacity but display rapid effector function (i.e. Granzyme B and IFN γ production). T_{CM} cells conversely migrate into secondary lymphoid organs and display high proliferative capacity after antigen re-exposure which results in asymmetrical division where most daughter acquire an effector phenotype while some daughter retain the T_{cm} phenotype, presumably to maintain immunological memory¹¹².

The difference in lifetime of an effector T cell (approximately two weeks) compared to a memory T cells (months-years) is highlighted in their metabolism^{126,127}. Effector T cells display high glucose intake and use glycolysis as the primary energy source pathway, whereas memory cells metabolize lipids through β -oxidation in the mitochondria to generate ATP¹²⁸.

A key component to proper memory formation is the absence of antigen stimulation after the effector phase. Constant antigen exposure such as in chronic infections and cancer can manifest another T cell fate: exhaustion. An exhausted T cell is characterized by low proliferative potential, abrogated cytokine production and an increase in inhibitory surface receptors such programmed cell death-1 (PD-1), lymphocyte activating gene 3 (LAG3), and cytotoxic T lymphocyte associated antigen 4 (CTLA-4)⁷⁴. These inhibitory receptors on the surface of tumour cells counteract TCR stimulation and suppress T cell function, giving the impression of a cell that is “exhausted”. Exhausted T

cells can be rescued from their quiescent state by the targeted blockade of inhibitory receptors and induction of the CD28 co-stimulatory pathway¹²⁸.

1.4 CANCER IMMUNOTHERAPY

1.4.1 Mechanisms of tumour escape from the immune system

T cells are powerful immunological agents that maintain physiological homeostasis, which includes circulating throughout the body where they recognize and destroy neoplastic cells. The host immune cells and nascent tumor cells are believed to co-exist in a dynamic interplay called immunoediting¹²⁸, which ultimately determines the tumour fate. Immunoediting is suggested to occur in three phases: elimination, equilibrium, escape (the “three Es”).

Elimination

Initially described as the original concept of immunosurveillance¹²⁹, elimination is the host protective phase of immunoediting where immune cells eliminate neoplastic cells. Initiation of host defenses begin when the immune system is alerted to the danger signals created by the growing tumour. As stated in **Section 1.1.1**, two hallmarks of cancer are sustained angiogenesis (creation of abnormal blood vessels to the tumour mass) and invasive tumour growth^{14,15}, both of which cause aggressive stromal remodeling that potentially leads to the production of these pro-inflammatory “danger signals”^{129,130}. In addition to the chemokines released by the tumour cells themselves¹³¹, these danger signals summon innate immune cells (such as NK cells and macrophages) to the tumour microenvironment where they engage with the tumour and begin to produce IFN γ , a cytokine critical for the anti-tumour response¹³². This ultimately creates an innate immune response feedback loop, where IFN γ stimulates tumour-infiltrating macrophages to produce IL-12, which stimulates tumour infiltrating NK to produce more IFN γ , which act on the macrophages again¹²⁹. Tumour destruction by the innate cells releases tumour antigens and danger associated molecular patterns, such as intracellular ATP¹³⁰, which eventually drive the adaptive immune response when APCs pick up these antigens and present them to naïve T cells as previously described. During the elimination phase, the balance towards anti-tumour immunity is achieved¹³².

Equilibrium

In this stage, carcinogenesis is kept dormant, as constant selective pressures on cancer cells by the immune system contains, but does not completely eliminate, neoplastic cells undergoing mutations caused by genetic instability (described in **Section 1.1.1**)¹³². Although many of the neoplastic cells are destroyed during the elimination phase, new variants arise carrying mutations that subject them to increased immune resistance¹²⁹. In terms of cytokine mediators, the equilibrium phase appears to strike a balance between anti-tumour cytokines, such as IL-12, and tumour promoting cytokines, such as IL-23¹³³. The equilibrium phase is the longest of the three phases, and

it has been predicted that there can be a 20 year gap between initial carcinogen exposure and clinical detection of the tumour in certain solid cancers^{129,134}.

Escape

In the final phase of immunoediting, cancer cell variants selected in the equilibrium phase acquire the ability to grow in an immunologically intact environment. This breach of the host's immune system can be achieved by several possible molecular immunosuppressive mechanisms: for instance, tumours can escape CTL recognition by selection of variants that lost their T cell specific antigens¹³⁰ and/or downregulation of MHC-I¹³⁵. Additionally, tumour cells may upregulate coinhibitory ligands (i.e. PD-L1) that interact with inhibitory receptors on T cells (i.e. PD-1) and lead to T cell exhaustion and lack of cytotoxic potential¹³⁵. Tumour cells can also upregulate antiapoptotic molecules such as FLICE-inhibitory protein (FLIP) and BCL-X_L which decrease sensitivity to FasL^{136,137}.

Several subsets of immune cells can promote tumour escape. Myeloid derived suppressor cells (MDSCs) suppress the activity of T cells specifically through mechanisms such as the production of arginase, which depletes available L-arginine in the local environment suppressing T cell proliferation¹³⁸ and CD3-TCR complex expression¹³⁹. Additionally, MDSCs produce high amount of reactive oxygen species, creating oxidative stress in the tumour microenvironment that has been shown to downregulate CD3 ζ expression¹⁴⁰ and trigger signaling related to abnormal angiogenesis¹⁴¹. Macrophages of the M2 phenotype are also associated with the progression of tumour growth as they promote matrix remodeling, tissue repair and angiogenesis¹⁴². Additional immune cells involved in carcinogenesis and the escape phase (neutrophils, Tregs, etc) have been described in detail elsewhere^{132,143,144}.

Despite the barriers presented by tumour escape mechanisms, research on the molecular and biochemical mechanisms of immunology and cancer biology, in addition to clinical observations has led to the development of immunotherapies that aim to overcome these challenges. These therapies harness and augment the power of the immune system to treat cancer malignancies, and because of their efficacies and unrealized future potentials, cancer immunotherapy was labelled the "breakthrough of the year" in 2013 by Science magazine¹⁴⁵. Several examples of cancer immunotherapies are discussed below.

1.4.2 Cancer vaccines

Similar in utility as the vaccines that harness immunological memory to protect against infectious diseases, cancer vaccines aim to initiate or amplify host lymphocyte responses against evolving tumours^{146,147}. The basic mechanism of action is to activate APCs to pick up and present either tumour associated antigens (TAAs) or tumour-specific antigens (TSAs) and then migrate to the lymph nodes. There, the APCs may activate naïve

lymphocytes with TCRs recognizing these antigens in order to destroy neoplastic cells through T cell biology previously described¹⁴⁸.

The choice of antigen is critical, and can be divided into four types: i) overexpressed/aberrantly expressed self, ii) germline self in somatic cells, iii) foreign (i.e. viral), and iv) mutated/neoantigen¹⁴⁹. Among TAAs, overexpressed self includes the human epidermal growth factor receptor 2 (HER2) that is present in normal tissues but upregulated in metastatic breast cancer¹⁵⁰, while germline self in somatic antigens include MAGE-A1, which is a germline gene normally repressed in somatic cells, but can become re-expressed in tumours^{151,152}. Within TSAs, foreign antigens include oncoviral antigens such as the HPV E6/E7 antigens in cervical cancer, while mutated/neoantigens are those caused by the genetic instability of tumours and present altered epitopes (amino acid change, posttranslational modifications, etc)¹⁴⁸. TSAs present novel antigens not educated against during central tolerance development of T cells in the thymus, while TAAs are difficult to target due to central tolerance mechanisms and therefore require methods to “break tolerance” to elicit a T cell response. Some of these methods include the addition of strong adjuvants in the vaccine, such as pathogen associated molecular patterns, provide additional co-stimulation and use repeated vaccinations with the same antigen¹⁵³. Nevertheless, because TAAs are still expressed on normal tissue, therapies targeting them may elicit “on-target off-tumour” toxicity, where normal cells expressing the antigen (even at lower levels) are targeted and destroyed¹⁴⁸.

There are three main cancer vaccination platforms. The first are cellular vaccines, which include either killed cancer cells or autologous APCs (ex. dendritic cell vaccines) preloaded with the antigen of interest¹⁵³. The second class are molecular vaccines that are composed of macromolecules (peptides, DNA, RNA) and an adjuvant. Peptide vaccines <15 amino acids can activate CD8⁺ T cells but do not effectively activate CD4⁺ helper T cells, which are necessary for full CTL functionality¹⁴⁸. To address this, multivalent synthetic long peptides (30+ residues in length) have been shown to induce both CD4⁺ and CD8⁺ T cells and are preferentially processed by APCs thereby providing adequate co-stimulation^{154,155}. DNA and RNA molecular vaccines are relatively inexpensive and simple to manufacture. Extracellular DNA also has the advantage of being a potent immune stimulant and therefore their need for an additional adjuvant is less critical^{148,156}. RNA is susceptible to degradation by ubiquitous RNases, but degradation can be mitigated by chemical modification of the RNA such as incorporation of pseudouridine as a modified nucleoside that stabilizes secondary structure and increases RNA rigidity^{157,158}. The third platform of cancer vaccines are viral vector vaccines, which are attenuated viruses that boost the activation of APCs through their pathogen associated molecular patterns (Discussed further in **Section 1.4.4**).

To date, regardless of the platform, most cancer vaccines have targeted TAAs that are abnormally expressed by cancer cells instead of TSAs which are truly unique

antigens¹⁴⁸. Because of central tolerance mechanisms previously discussed, these cancer vaccines stimulate activation and proliferation of less than 1% of total circulating CD8⁺ T cells, while effective antiviral vaccines (such as the Dryvax smallpox vaccine) can stimulate activation and expansion of viral-specific CD8⁺ T cells comprising as much as 40% of the total pool^{148,159}, which may explain the poor clinical outcomes observed with cancer vaccines.

1.4.3 Monoclonal antibody based therapies

Monoclonal antibody (mAb) based therapy is one of the most successful therapeutic strategies for both hematological and solid cancer malignancies of the last two decades¹⁶⁰. The initial development of hybridoma technology¹⁶¹ as well as the multiple proteomic, genomic and bioinformatic approaches¹⁶⁰ to characterize cancer cell surface antigens (also known as the “surfaceome”) has paved the way for the discovery and clinical investigation of many mAbs with various different mechanisms of actions. One class of mAbs are those that recognize antigens expressed by tumour cells (tumour-targeting antibodies). These antigens range from glycoproteins expressed on certain hematological cells such as CD20¹⁶², growth factor receptors such as EGFR¹⁶³ and stromal and extracellular matrix antigens such as fibroblast activating protein (FAP)¹⁶⁴. Mechanisms of action for tumour-targeting antibodies can also vary considerably: for instance, rituximab (anti-CD20 mAb) can clear B cell malignancies by complement dependent cytotoxicity (CDC) and antibody-dependent cellular cytotoxicity (ADCC)¹⁶⁵. Binding of Cetuximab to EGFR blocks many receptor-dependent transduction pathways, leading to apoptosis, receptor internalization (downregulation), cell cycle arrest and inhibition of angiogenesis¹⁶⁶.

Another class of mAb based therapy is the bi-specific antibody, an artificially made antibody with two different antigen binding sites. These antibodies have the mechanistic potential to link two moieties from different cells together in the same molecule, thereby creating functionalities that otherwise would not occur without the bi-specific antibody¹⁶⁷. A well-known variant of a bispecific antibody is the combination of fragments from anti-CD3 and anti-CD19 mAbs yielding a structure known as the bi-specific T cell engager (BiTE) blinatumomab where one arm of the molecule binds to CD3 on the surface of the T cell, while the other arm binds to CD19, a surface biomarker for many leukemias and lymphomas¹⁶⁸. This dual interaction engages the otherwise unstimulated T cell to destroy the CD19⁺ cell¹⁶⁹.

A third class of mAb based therapies are the checkpoint blockade antibodies. As described in **Sections 1.3.6 and 1.4.1**, T cells can express inhibitory receptors that when ligated, can lead to T cell exhaustion and an abrogation of anti-tumour efficacy. Monoclonal antibodies against these inhibitory/checkpoint receptors and their ligands prevent T cell inhibition, enabling the T cell to fight the tumour. For instance, after T cell activation, CTLA-4, a protein normally found in intracellular stores, migrates to the

immunological synapse and interacts with B7 molecules (CD80/CD86) with higher affinity and avidity than CD28, thereby inhibiting co-stimulatory signaling^{160,170}. The monoclonal antibody ipilimumab specifically binds to CTLA-4 and prevents its interaction with CD80/CD86, and therefore prevents T cell inhibition¹⁷¹. Checkpoint blockade inhibitors exist against other checkpoint pathways; as examples, PD-L1 (expressed on tumors) is targeted by atezolizumab¹⁷² and PD-1 (expressed on T cells) is targeted by nivolumab¹⁷³.

1.4.4 Oncolytic viruses and vaccines

Oncolytic viruses (OVs) are attenuated yet replication-competent viruses that preferentially infect, replicate in, and eventually lyse tumour cells¹⁷⁴. A major advantage of this therapy against solid tumours is the *in-situ* effect¹⁷⁵: viral replication in cancer cells lead to their eventual necrosis, which unlike the organized programmed cell death of apoptosis, leads to the release of intracellular contents due to membrane disruptions¹⁷⁶. These contents include danger associated molecular patterns (ex. intracellular DNA and ATP) and tumour antigens (both tumour associated antigens and possible neoantigens that may have occurred during carcinogenesis): both components necessary to activate APCs to pick up protein antigens, process and present them on MHC and activate T cells. OVs preferentially infect and replicate in cancer cells due to the anti-viral mechanisms that are disrupted in neoplastic cells: while anti-viral responses include suppression of translation, induction of apoptosis and decreased proliferation, cancer cells tend to have increased translation, limited apoptosis and increased proliferation¹⁷⁷.

Oncolytic virus vaccines (OV vaccines) are derivatives of OVs that have been engineered to encode and express tumour antigens that will be picked up and processed by APCs during virus replication, therefore directing an antigen-specific response^{178,179}. A major challenge for OV vaccines is the relatively weak immunogenicity of the engineered tumor antigen relative to the highly immunogenic viral antigens, resulting in a skewing of the T cell response towards the virus antigens¹⁷⁹. To address this, a heterologous prime-boost strategy can be employed¹⁸⁰ where the host is first immunized against the tumor antigen using a vaccine platform unrelated to the OV vaccine (in our experience, recombinant adenovirus works well) followed by a boost with the OV vaccine (in our experience, recombinant rhabdoviruses are highly effective). Such prime-boost strategies have shown great promise in pre-clinical models and are currently being tested in humans.

1.4.5 Adoptive Cell Transfer

The previously described immunotherapies aim to either develop (vaccination) or augment (checkpoint blockade) an endogenous T cell response against tumours. These strategies ultimately require *in situ* activation and proliferation of T cells in patients who are often immunocompromised, which can be a challenging limitation¹⁸¹. Further, as noted earlier, the availability of T cells reactive against the tumor is limited through the mechanisms of *central* and *peripheral* tolerance. To overcome these limitation, adoptive

cell transfer (ACT) was developed as a means of treating patients with large numbers of tumor-specific T cells produced in the laboratory^{182–184}. Several ACT strategies have been employed in the clinic with varying success: for instance, the infusion of autologous *ex vivo* expanded tumour infiltrating lymphocytes (TILs) in patients with metastatic melanoma has shown cancer regression in approximately half of all patients following intensive pre-conditioning with chemotherapy and radiation^{185,186}. These lymphocytes are obtained and isolated from the surgical excision of a solid tumour (due to them being in complex with the tumour, along with other immune cells), grown in culture dishes containing T cell growth factors (such as IL-2) and allowed to expand *ex vivo* before ultimately being reinfused into the patient¹⁸⁷. These lymphocytes are understood to have higher immunological reactivity against solid tumours compared to non-infiltrating lymphocytes¹⁸⁸. Another ACT strategy involves engineering bulk populations of T cells with single high affinity transgenic TCRs. This immunotherapy has been used with moderate success against melanomas expressing MART-1 or gp100 antigens^{189,190}.

1.5 MHC-Independent Synthetic T Cell Receptors

All therapeutic strategies that rely on T cells are limited by the downregulation of MHC-I by cancer cells, which is common outcome of immunoediting¹⁹¹. In this section, we will discuss synthetic antigen receptors, which are designed to direct T cell immunity against tumors in the absence of TCR-MHC interaction.

1.5.1 Chimeric Antigen Receptors

Overview and history

Chimeric antigen receptors (CARs) are recombinant transmembrane proteins containing an antigen binding domain linked to a hinge and transmembrane domain and fused to one or more intracellular signaling domains that are proving to be effective in directing T cells to cancer-specific targets in an MHC independent manner (**Figure 1.4**)¹⁹². T cells are engineered to express CAR using standard gene transfer methods; both viral and non-viral methods can be used. The CAR model arose from the observation that fusing the extracellular domain of CD8 α co-receptor to the intracellular CD3 ζ chain yielded a synthetic receptor that could activate a T cell independently of the TCR¹⁹³. The first generation of CARs contained a single chain variable fragment (ScFv – discussed in detail below) covalently ligated to the CD3 zeta chain¹⁹⁴. While first-generation CARs could trigger T cells to elaborate robust cytotoxic function and cytokine production *in vitro*, these first-generation CARs yielded disappointing clinical results in cancer patients, as they exhibited limited persistence and anti tumour activity^{181,195,196}. Second generation CARs contained an additional co stimulatory domain such as CD28 or 4-1BB and proved to be much more effective *in vivo* than first generation CARs due to their greater signaling strength and persistence^{197–201}. A third generation of CARs, containing two or more co stimulatory domains in addition to the CD3 ζ signaling domain has been described and may to confer even greater potency in targeting antigen-specific cancer cells, although

research is ongoing^{202,203}. The design of chimeric antigen receptors is critical for their function, and each modular domain which will be discussed in detail below²⁰⁴.

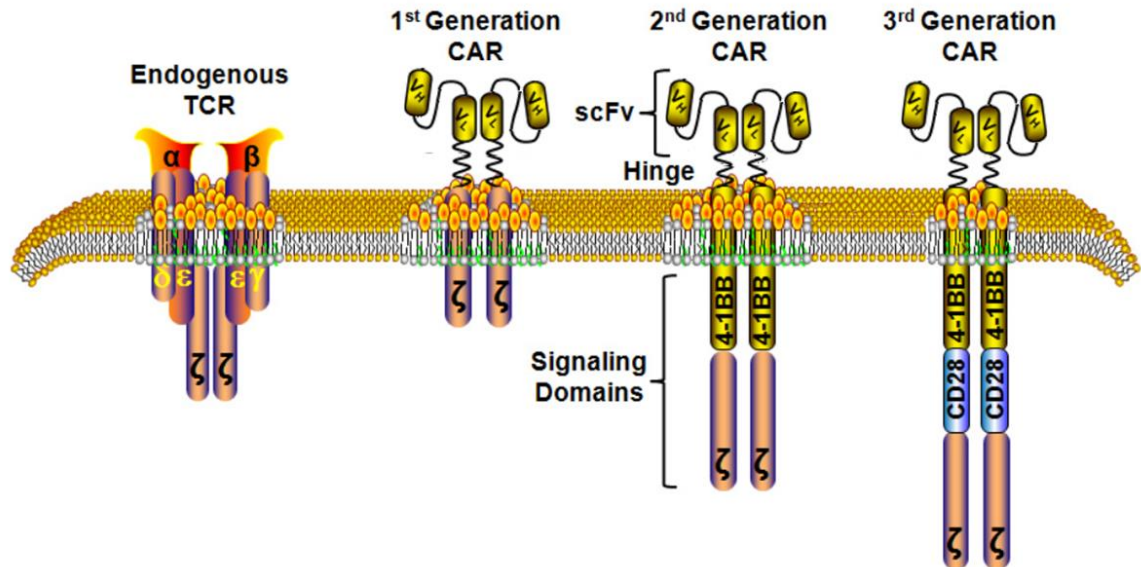


Figure 1.4 – Schematic of Chimeric Antigen Receptors (Generations 1-3)¹⁹²

The three generations of CARs are shown compared to the endogenous TCR-CD3 complex within the T cell membrane. All generations of CARs contain an extracellular antigen binding domain (shown here as a scFv of heavy and light chains) that redirects the engineered T cell against a tumour antigen in an MHC independent manner linked to a hinge and transmembrane domain. All generations of CARs also contain an intracellular CD3 ζ domain necessary for signal 1 transduction. Second generation CARs contain a single intracellular co-stimulatory domain necessary for signal 2 transduction (shown here as 4-1BB) while third generation CARs have two or more intracellular co-stimulatory domains.

Antigen binding domain

Recognition of cancer target cells by CAR T cells is determined by the antigen binding domain, an extracellular protein-binding moiety usually consisting of a single chain variable fragment (scFv) specific for a tumour antigen (**Figure 1.5**). The feasibility of the scFv, which is composed of an antibody's variable light (V_L) and heavy (V_H) chains linked by a short peptide linker and retaining recognition and affinity of the parent antibody was first demonstrated in 1988 by purifying the single chain from *E. coli* and characterizing its properties *in vitro*^{205,206}. Based on the structure of an antibody, it is not unreasonable to assume that the NH_2 - V_L -linker- V_H - $COOH$ peptide chain orientation would most closely resemble that of the parent antibody and therefore always confer greater recognition and affinity, however some scFv confer higher specificity with the opposite orientation^{204,207}. Due to their flexibility, glycine-serine repeats are the most widely used linkers as they allow for the independent folding of individual immunoglobulin chains without interference^{208,209}. Serine is specifically responsible for forming hydrogen bonds

with water molecules in aqueous solutions, which creates a hydration shell that prevents glycine from forming potential hydrophobic interactions with nearby proteins²⁰⁸. The generally accepted linker length is 15-20 amino acids, therefore many CAR constructs use $(\text{Gly}_4\text{Ser})_3$ or $(\text{Gly}_4\text{Ser})_4$ scFv linkers²⁰⁴. Short linkers are known to cause scFv clustering, which can cause spontaneous CAR-mediated signaling in the absence of antigen, also known as tonic signaling, that can lead to premature exhaustion of the CAR-T cells and poor anti-tumor activity^{210–212}.

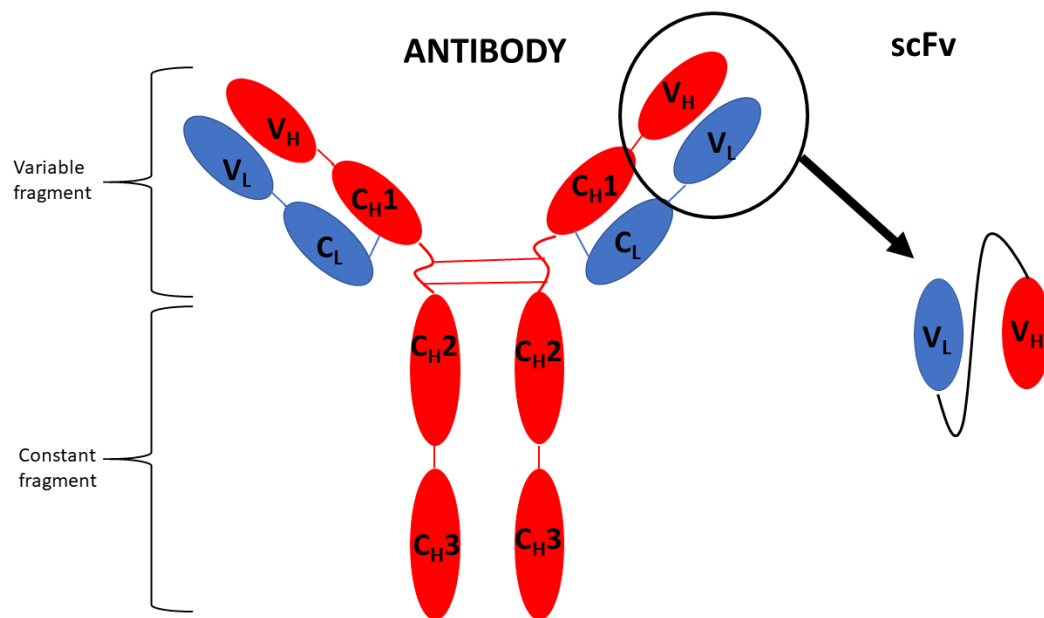


Figure 1.5 Single chain variable fragment composition from antibody structure

The scFv is generated by linking the heavy (V_H , red) and light (V_L , blue) chains from the variable fragment (antigen recognizing) of an antibody with a linker (black). The constant fragment is not included within the scFv.

The main advantage of a scFv is that recognition is MHC independent, and therefore not susceptible to MHC-I downregulation common to cancer cells¹⁹¹. Although this suggests that targets can now only be surface antigens (therefore lowering the total number of available potential targets), scFvs against peptide-MHC epitopes have been characterized in the context of CAR T cells (“TCR mimic CARs”) ²¹³. Therefore, flexibility exists with regards to the choice of antigen to target.

As with many protein-protein interactions, affinity of the scFv with the tumour antigen also appears to play an important role in CAR functionality. ScFvs tend to have higher affinities for their antigens ($K_D \sim$ nanomolar range) than endogenous TCR $\alpha\beta$ recognition of peptide-MHC ($K_D \sim$ micromolar range)²¹⁴. CAR functionality has been

shown to be proportional to affinity, where the low affinity binders cannot stimulate comparable T cell functionality to high affinity binders of the same single chain, suggesting each binder has a lower limit that must be achieved for full functionality^{215,216}. Furthermore, increasing affinity past a certain threshold does not appear to improve CAR functionality (especially for high density antigens), suggesting that there is also an upper limit to affinity and T cell response^{217,218}.

Although most CARs employ scFvs, other protein-binding moieties can be used as the antigen binding domain. One example is designed ankyrin repeat proteins (DARPs) which have been used in our laboratory to recognize tumour targets in the context of CAR T cells²¹⁹. DARPs specific for different cancer antigens have also successfully been used in tandem on a single CAR construct to generate multi-specific tumour recognition, and this strategy is favourable over tandem scFvs since DARPs are less likely to aggregate and lead to tonic signaling²²⁰. CARs specific for IL13R α 2, an antigen upregulated on glioblastoma cancers, have utilized IL13 muteins as antigen binding domains. These muteins contained either single or double amino acid substitutions within the IL13R α 2 recognition motif of IL13 that increased the affinity of this interaction and displayed high *in vivo* efficacy against established glioblastoma cancer²²¹.

Hinge (spacer) domain

The hinge (or spacer) is an extracellular sequence that links the antigen binding domain to the transmembrane domain. While the selection of this domain might appear inconsequential since, in theory, it does not participate in any protein-protein interactions, direct signal transduction or membrane retention, the field is replete with evidence of that the hinge has significant impact on CAR function, both *in vitro* and *in vivo*. Most hinges in CAR constructs are derived from the extracellular domains of immunoglobulin G (IgG), CD28 or CD8 α ²⁰⁴. One caveat of using an unmodified IgG hinge is that it retains the ability to bind Fc-Receptor bearing cells through the CH2 domain, thereby leading to off-target T cell activation or activation induced cell death (AICD) of the CAR T cells^{222–225}. To circumvent this, many groups have mutated or deleted the Fc-receptor interacting domain^{224,226}.

The length of the hinge is also an area of intense research and appears to be dependent on the tumour antigen's position and accessibility. Some groups have noted that CAR T cells are more potently activated when the tumour antigen rests closer to the tumour cell membrane^{227,228}. This observation is supported by the kinetic segregation model of T cell activation^{95,97} and has led to the hypothesis that a shorter hinge length allows for a physically tighter association between the antigen binding domain and the tumour antigen within the immunological synapse that excludes large phosphatases such as CD45^{204,229}. Nevertheless, in some cases a longer hinge is necessary if the epitope is relatively inaccessible with a short hinge^{222,230,231}. Therefore, hinge length is often empirically optimized for each target and antigen binding domain.

Finally, an observation often overlooked is the homodimerization of CARs (displayed in **Figure 1.4**). CD8 α and CD28 receptors for instance form endogenous homodimers on the surface of T cells^{64,232}, and this dimerization in the context of chimeric antigen receptors (which has previously been demonstrated)²³³ might be important for signaling as early CARs using CD4 (monomer) as a hinge displayed inferior response to antigen stimulation²³⁴.

Transmembrane domain

The transmembrane domain consists of 20-25 primarily hydrophobic amino acids in an α -helical secondary structure responsible for anchoring the receptor in the T cell membrane. It is the least studied domain of the CAR, mainly because these domains are used concomitantly either with the hinge (i.e. CD8 α hinge and transmembrane domains) or with intracellular signaling domains (i.e. CD28 transmembrane and membrane proximal signaling domains)²³⁵. Nevertheless, CD4, CD28, CD8 α , and CD3 ζ transmembrane domains have all been used in previous CAR constructs with no discernable differences observed²⁰⁴.

Intracellular domains

The intracellular domains of the CAR supply the activation signals following antigen engagement. In the context of the 2-signal model of T cell activation, the intracellular CD3 ζ domain, present in the majority of CAR constructs, provides “signal 1”. It is believed that the failure of first-generation CARs was the lack of costimulatory signals. Thus, current generation CARs include domains from costimulatory receptors (ex. CD28, CD137) to deliver “signal 2” and considerable optimization has occurred in the field, although the optimal configuration remains to be determined. The inclusion of a costimulatory domain does little to improve *in vitro* cytolytic function compared to a first generation CAR, however CAR T cell proliferation²³⁶, *in vivo* tumour clearance²³⁷ and *in vivo* persistence²³⁸ are markedly enhanced.

CD28 and 4-1BB/CD137 are the most commonly used costimulatory domains in CAR T cells and their head to head performance have been extensively studied²⁰⁴. In preclinical mouse models, CD28-based CAR-T cells displayed rapid effector functions (i.e. higher tumour killing kinetics), but lower persistence compared to the 4-1BB-based CAR-T cells^{237–239}. Conversely, the 4-1BB-CAR displayed delayed tumour killing kinetics *in vivo* but expanded over time and eventually led to tumour destruction. Metabolic analysis²⁴⁰ of these CAR T cells revealed that the CD28-based CAR-T cells primarily used glycolytic metabolism upon antigen stimulation, a phenotype common for effector T cells, whereas the 4-1BB-based CAR-T cells used fatty acid oxidation upon antigen stimulation, a phenotype common to memory T cells. The immediate effector functions of the CD28-based CAR-T cells appear to be supported by glucose metabolism, while the long term persistence of the 4-1BB-based CAR-T cells is supported by oxidative metabolism. Similar

results have been observed clinically where CD28-based CAR T cells recognizing CD19 have shown potent anti tumour efficacy, but only limited persistence^{241,242}. Conversely, the corresponding 4-1BB-based CAR-T cells displayed similarly potent anti-tumour efficacy and were found to persist for up to several years in patients^{243,244}.

Results using third generation CARs, which contain 2 costimulatory domains (usually CD28 and 4-1BB combination) have varied in preclinical studies: some have shown increased efficacy compared to second generation CARs, others have shown no difference, others have shown lower efficacy and one study even reported AICD in their third generation CAR (not observed in second generation CARs of individual co-stimulatory domains)²⁰⁴. It remains to be seen whether third generation CARs will confer a clinical benefit and what impact having multiple costimulatory domains will have on CAR T cell functionality. The majority of clinical studies and product candidates employ second-generation CAR-T cells with only a single costimulatory domain.

Extrinsic components

Successful expression and functionality of CAR T cells also depend on extrinsic factors not specific to the receptor design but relating to its transduction and subsequent transcription and translation. One of these factors is the method by which the CAR is introduced into the T cell. This has primarily been achieved by stable genomic integration through the use of γ -retroviral or lentiviral vectors²⁰⁴. Although both viruses integrate into random transcriptionally accessible sites, γ -retroviruses tend to integrate near transcriptional start sites and near proto-oncogenes, thereby running the risk of insertional mutagenesis and/or dysregulation^{245–247}. Non-viral methods for gene transfer have been used to express CARs in T cells, specifically by transposon systems like Sleeping Beauty and transient methods such as RNA electroporation^{248,249}.

Another important extrinsic factor to consider is the promoter: how the transgene is regulated and transcribed once it is in the cell. This is generally impacted by the type of transgene vector used, and the choice can be consequential. For instance, it was noted that antigen-independent signaling (i.e. tonic signaling) could be reduced by lowering the surface expression of the CAR which was achieved by exchanging the powerful elongation factor 1 α (EF-1 α) promoter with either the cytomegalovirus (CMV) or phosphoglycerate kinase 1 (PGK) promoter, which lead to lower surface expression of the CAR²⁵⁰.

Challenges for CAR T cell therapies

Although CAR T cell therapy has demonstrated considerable clinical success against hematological malignancies^{251–253}, clinical and biological challenges remain, especially with regard to solid tumours²⁵⁴. The most frequent and serious adverse event related to CAR T cell therapy is cytokine release syndrome (CRS), which is the systemic, abrupt and rapid release of cytokines into the blood from immune cells affected from the

immunotherapy. The pathophysiology of CRS occurs in two steps: First, the CAR T cells produce pro-inflammatory cytokines, such as IFN γ and TNF α , following engagement of the tumor cells. Second, these pro-inflammatory cytokines activate innate immune cells such as macrophages to release additional cytokines such as IL-1, IL-6 and IL-10 which exacerbates the toxicity²⁵⁵. Clinical presentation of CRS ranges from flu-like symptoms (fever, fatigue, headache, rash, arthralgia, and myalgia) to more severe cases of hypotension, circular shock, vascular leakage and multi-organ system failure²⁵⁵. Low grade CRS is treated with antihistamines, fluids and antipyretics. Higher grade CRS is treated with anti-IL-6 monoclonal antibodies (siltuximab and clazakizumab, or tocilizumab which binds the IL-6 receptor), as IL-6 is elevated in serum of patients with CRS following CAR T cell therapy²⁵⁶.

Another complication is neurotoxicity that has been associated with CD19-targeted CAR T cell therapy. Although the mechanism of action is not completely understood, neurotoxicity appears to be associated with CRS, as elevated levels of IL-6 and IFN γ have been found in both the blood and the cerebrospinal fluid, which suggests a possible compromise of the blood-brain barrier²⁵⁶. Clinical symptoms include delirium, headache, language disturbance, tremor, transient focal weakness, behavioral disturbances, ataxia, peripheral neuropathy, visual changes and generalized weakness, seizures, and acute cerebral edema. Cerebral edema is an especially serious and life threatening condition that involves fluid build up in the brain, causing an increase in intracranial pressure²⁵⁶. Corticosteroids are the first-line of treatment against CAR T cell induced neurotoxicity: dexamethasone specifically has excellent central nervous system penetration and is the gold standard of treatment of cerebral edema and neurotrauma for several groups²⁵⁷.

There is also evidence of “on-target off-tumour” toxicity of CAR T cells, when the engineered T cells recognize a TAA also present on normal tissue and attack it. For instance, treatment of metastatic renal cell carcinoma with CAR T cells recognizing carbonic anhydrase IX (CAIX, an antigen overexpressed in this type of cancer) lead to tumour clearance, but also severe liver toxicity in several patients. It was suggested that the CAR T cells also targeted CAIX expressed by bile duct epithelial cells, even if they were expressed at lower levels than the renal cell carcinoma cells²⁵⁴.

1.5.2 T Cell Antigen Coupler (TAC) Receptor

While traditional CARs activate T cells by their recombinant CD3 ζ and co stimulatory domains, work in the Bramson laboratory sought to develop an alternate method in T cell redirection that did not rely on the incorporation of signaling domains into the chimeric receptor. We hypothesized that CAR toxicities are linked to the synthetic nature of the receptor design, and that a more controlled response could be achieved by signaling through the endogenous framework of the TCR. To this end, the T cell antigen coupler (TAC) receptor²⁵⁸ was developed with the idea of recapitulating the natural

activation of a T cell (**Figure 1.6**) but in an MHC independent and TAA specific manner. The TAC co-opts the endogenous TCR-CD3 complex and signals through the natural CD3 ζ ITAMS on this complex, rather than having intrinsic signaling domains of its own. The TAC is modular in design and contains three central features: i) an antigen binding domain that recognizes a tumour associated antigen ii) a CD3 binding domain that recruits the TCR-CD3 complex to the receptor and iii) a CD4 co-receptor anchor which affixes the receptor into the membrane.

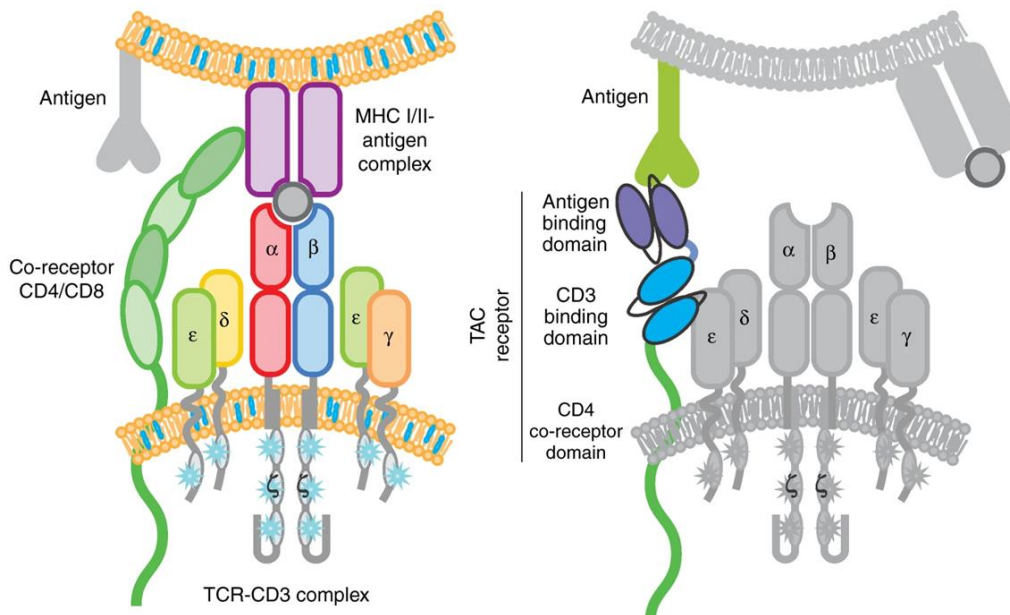


Figure 1.6 – T Cell Antigen Coupler (TAC) design mimics the TCR-CD3 complex²⁵⁸

Left, the natural TCR-CD3 complex interacting with an MHC-II molecule on the surface of a professional APC. The CD4 co-receptor interacts with the MHC at the different site from where TCR $\alpha\beta$ binds to the peptide on the MHC. Right, TAC engages a tumour associated antigen via its antigen recognition domain on the surface of the cancer cell in an MHC-independent manner. The TAC co-opts the TCR-CD3 complex through a CD3 binding domain and is anchored into the cell membrane with the CD4 co-receptor domain.

Our laboratory has published experimental evidence of the efficacy and unique biology of TAC-engineered human T cells: we observed enhanced *in vivo* anti-tumour efficacy and decreased off-tumour toxicity compared to first and second generation CARs, most notably in a solid tumour model. Given the same antigen binding domain, we observed lower tonic signaling in TAC T cells compared to both CD28 and 4-1BB-CAR T cells, supporting the hypothesis that the natural activation pathway is more controlled. This idea is further supported in the literature by the efficacy and biology of T cell receptor fusion constructs (TRuCs), which comprise an antibody-based binding domain fused to the endogenous T cell receptor²⁵⁹. TRuCs also had evidence of lower tonic signaling

(antigen independent phosphorylation of CD3 ζ) yet displayed improved *in vivo* liquid tumor .

With regards to the modular design of the TAC receptor, our laboratory has demonstrated the broad utility of the receptor by targeting several different cancer antigens, namely Her2 (breast cancer), CD19 (B cell lymphoma) and BCMA (multiple myeloma) using different binders such as scFvs and DARPins. Unlike CARs however, the TAC does not contain any endogenous signaling domains within its design, and therefore requires recruitment of the TCR-CD3 complex to provide signal transduction through the ITAMS. It achieves this by containing a CD3-binding domain, and specifically binding to CD3 ϵ using the UCHT1 scFv²⁶⁰. CD3 ϵ was chosen as the binding site due to its outer orientation in the TCR and the well characterized interactions with other anti-CD3 antibodies such as L2K, OKT3²⁶¹ and F6A^{258,261}. Similar to the antigen recognition domain, the CD3 binding domain is absolutely necessary for TAC functionality, and the choice of the scFv also affects functionality: for instance, TAC receptors using F6A and L2K showed poor surface expression and cytokine production upon antigen stimulation. UCHT1 displayed preferred properties (surface expression and cytokine production) and was therefore used in the TAC platform.

The TAC is also unique in that it also does not contain costimulatory moieties within the receptor design, similar to the first generation CAR. The TAC however has demonstrated enhanced *in vivo* activity against a solid tumour model (Her2⁺ OVCAR-3) in a head-to-head experiment comparing anti-Her2 TACs to first and second generation (CD28 costimulatory domain) anti-Her2 CARs. Therefore, despite the specific lack of costimulatory signaling within the TAC, it displays the *in vivo* efficacy and persistence often not observed in first generation CARs. It is interesting to note that TRuCs, which similarly signal through the TCR complex and do not contain costimulatory domains, also show high *in vivo* efficacy and persistence comparable to second-generation CARs. It is unclear how signaling through the entire endogenous TCR complex within the context of a synthetic antigen receptor provides enough signaling breadth (signals 1 and 2) necessary for *in vivo* persistence.

Given that the TAC recruits and signals through the endogenous TCR-CD3 complex, the final component of the TAC design is the CD4 anchor/co-receptor domain, consisting of the CD4 hinge, transmembrane domain and intracellular tail. In addition to anchoring the receptor within the T cell membrane, the anchor incorporates co-receptor properties necessary for natural T cell activation such as Lck recruitment for ITAM phosphorylation and membrane partitioning important for receptor clustering during antigen engagement (described in **Section 1.3.3**). Of the three modular TAC components, the anchor/co-receptor domain is the least characterized. Our laboratory was interested in refining the TAC technology by first understanding the specific contributions this domain provides to the functionality of the receptor. By doing so, we hoped to gain

further insights in some of the unique features that the receptor displayed, such as a lack of tonic signaling, *in vivo* persistence despite a lack of co-stimulatory domains, and high activity against solid tumours.

1.6 THESIS OBJECTIVES

Overview and scope

The work described in this thesis aimed to characterize the modular features of the TAC receptor. Specifically, the focus of this thesis was on the TAC anchor/CD4 co-receptor domain. The TAC was designed with the aim of recapitulating natural T cell activation, and therefore the CD4 co-receptor was used as an anchor based on the biological understanding of co-receptor function at the time (described in **Section 1.3.2**); however, the contribution of this domain with regards to TAC functionality was not known.

Objective 1 Substitution of the CD4 with CD8

The use of CD4 as the TAC anchor to recapitulate natural T cell activation was rationalized based on the monomeric structure of CD4. Given that T cells have two natural co-receptors that serve similar functions, we were interested in evaluating the modular design of the TAC receptor by replacing the CD4 co-receptor with CD8 and observing the resulting phenotype and functionality. We were also interested in determining whether these intracellular features were necessary for TAC functionality, as they are in the biology of natural T cell activation. The objective was to determine if the CD4 co-receptor could be functionally replaced with the CD8 co-receptor, and if the domains within these receptors were critical for TAC functionality.

Objective 2 Functionality of the “tailless” TAC

We continued characterizing the CD4 anchor by removing the cytoplasmic domain/tail in its entirety, thereby creating a “tailless” TAC. We examined the phenotype and functionality of this new TAC receptor compared to the parent TAC in order to gain further insight into the components necessary for TAC functionality.

Objective 3 Functionality of the tailless TAC across different antigen binding domains

Finally, we wanted to validate the previous results across different antigen binding domains and cancer models to ensure that the outcomes we observed were consistent across all TAC platforms and not unique to a single model.

CHAPTER TWO

MATERIALS AND METHODS

2.1 GENETIC CLONING OF TAC CONSTRUCTS

2.1.1 Transmembrane and intracellular tail constructs

Sequences for human *cd8 α* and *cd8 β* genes were obtained from GenBank. The nucleotide moieties of all CD8 TAC constructs including the CD8 Δ R, CD8 Δ L, and CD8 Δ LR mutants were ordered from GenScript and subcloned into a *pUC57* vector containing the CD4 TAC (prepared by another member of the lab) after the CD4 moiety was digested out. This plasmid was confirmed by DNA sequencing at MOBIX. The entire DARPin-UCHT1-CD8 Alpha/Alpha+R/Beta+Lck TAC constructs were then digested out of *pUC57* using the *Ascl* and *NheI* restriction enzymes (New England Biolabs), and cloned into the *pCCL* lentivirus transfer vector (graciously provided by Dr. Megan Levings, University of British Columbia) using T4 DNA Ligase (New England Biolabs). The nucleotide sequences of all other intracellular TAC constructs including the CD4 truncations, tailless, and 4A were ordered from GenScript and cloned into the *pCCL* vector as previously described. The DNA backbone of the *pCCL* vector is shown in **Fig. 2.1**. Double stranded nucleotide sequences and primers used are shown in **Table 1.0** and **Table 2.0**, respectively.

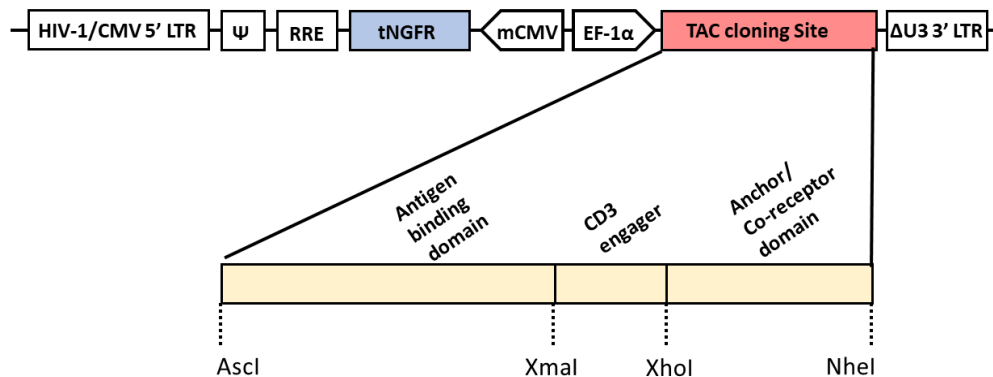


Figure 2.1 DNA backbone of *pCCL* vector²⁵⁸

The bi-directional *pCCL* lentivirus transfer vector DNA backbone contains a truncated nerve growth factor receptor (tNGFR, blue) gene under control of the mCMV promoter serving as a transduction control. The TAC cloning site (red) under control of the EF-1 α promoter is contained in between the *Ascl* and *NheI* restriction digest sites. Each component of the TAC (antigen binding domain, CD3 engager, anchor) can be swapped using the appropriate restriction sites.

2.1.2 Antigen binding domain constructs

Nucleotide sequences for the DARPin antigen binding domains (G3-A, G3-AVD, G3-HAVD) were obtained from Zahnd et al 2007 and ordered from GenScript²⁶². Sequences were amplified with primers containing *Ascl* and *XmaI* restriction digest sites (**Table 1.0**) and cloned into the *pCCL* vector as previously described. All anti-CD19 and the anti-BCMA 2A Δ 488-525 truncation constructions were cloned into the TAC cloning site of *pCCL* by GenScript in its entirety, and the plasmids were delivered to us by GenScript.

PCR product	Double stranded DNA sequence (5'-3')	Type of DNA	Supplier/Vendor
CD8 TAC Alpha	CTCGAGCTGCGCCAGAGGCGTCCCGGCCAGCGGCGGG GGGCGCAGTGCACACGAGGGGGCTGGACTTCGCCTCTG ATATCTACATCTGGGCGCCCTTGGCCGGGACTTGTGGG GTCCTTCTCCTGTCCTGTTATCACCCCTTACTGCAACC ACAGGAACCGAAGACGTGTTTGCAAATGTCCCCGGCCT GTGGTCAAATCGGGAGACAAGCCCAGCCTTTCGGCGAG ATACGTCTAATGAGCTAGC	Gene synthesis	GenScript
CD8 TAC Alpha+R	CTCGAGCTGCGCCAGAGGCGTCCCGGCCAGCGGCGGG GGGCGCAGTGCACACGAGGGGGCTGGACTTCGCCTCTG ATATCTACATCTGGGCGCCCTTGGCCGGGACTTGTGGG GTCCTTCTCCTGTCCTGTTATCACCCCTTACTGTCCT GCCGGCGGAGGAGAGTTTGCAAATGTCCCCGGCCTGTG GTCAAATCGGGAGACAAGCCCAGCCTTTCGGCGAGATA CGTCTAATGAGCTAGC	Gene synthesis	GenScript
CD8 TAC Beta+Lck	CTCGAGAAGAAGTCCACCCTCAAGAAGAGAGTGTCCCG GTTACCCAGGCCAGAGACCCAGAAGGGCCCACTTTCTA GCCCCATCACCCCTGGCCTGCTGGTGGCTGGCGTCCTGG TTCTGCTGGTTTCCCTGGGAGTGGCCATCCACCTGTGCT GCCGGCGGAGGAGAGCCTGCAAATGTCCCCGGCTTCGT TTCATGAAACAATTTTACAAATGATAAGCTAGC	Gene synthesis	GenScript
CD8 Δ R TAC	CTCGAGAAGAAGTCCACCCTGAAGAAACGGGTGTCCCG GCTGCCAGACCCGAGACACAGAAGGGCCCTGAGCA GCCCTATCACCCCTGGGACTGCTGGTGGCCGGCGTGCTG GTGCTGCTGGTGTCTCTGGGAGTGGCCATCCACCTGTGC TGCGCCTGCAAGTGCCCCAGACTGCGGTTTCATGAAGCA GTTCTACAAGTGATGAGCTAGC	gBlock®	IDT
CD8 Δ LR TAC	CTCGAGAAGAAGTCCACCCTGAAGAAACGGGTGTCCCG GCTGCCAGACCCGAGACACAGAAGGGCCCTGAGCA GCCCTATCACCCCTGGGACTGCTGGTGGCCGGCGTGCTG GTGCTGCTGGTGTCTCTGGGAGTGGCCATCCACCTGTGC TGCGCCAGACTGCGGTTTCATGAAGCAGTTCTACAAGTG ATGAGCTAGC	gBlock®	IDT
G3-A DARPin	ATGGATTTCCAGGTCCAGATTTTCTCCTTCTGCTGATTT CCGCAAGCGTCATTATGTCACGGGGCTCCGACCTGGGC AAAAAGCTGCTGGAGCCGCTAGGGCCGGGCAGGACG ATGAAGTGAGAATCCTGATGGCCAACGGGGCTGACGTG AATGCTAAGGATGAGTACGGCCTGACCCCTGTATCTG GCTGTGTCACACGGCCATCTGGAGATCGTGGAAGTCCT GCTGAAAAACGGAGCCGACGTGAATGCAGTCGATGCCA TTGGGTTCACTCCTCTGCACCTGGCAGCCTTATCGGAC ATCTGGAGATTGCAGAAGTGCTGCTGAAGCACGGCGCT GACGTGAACGCACAGGATAAGTTCGAAAAACCGCTTT TGACATCAGCATTGGCAACGGAAATGAAGACCTGGCTG	gBlock®	IDT

	AAATCCTGCAGAACTGAATGAACAGAACTGATTAGC GAAGAAGACCTGAAC		
G3-AVD DARPin	ATGGATTTCCAGGTCCAGATTTTCTCCTTCTGCTGATTT CCGCAAGCGTCATTATGTCACGGGGCTCCGACCTGGGC AAAAAGCTGCTGGAGCCGCTAGGGCCGGGCAGGACG ATGAAGTGAGAATCCTGATGGCCAACGGGGCTGACGTG AATGCTAAGGATGAGTACGGCCTGACCCCTGTATCTG GCTGCTTTCATCGGCCATCTGGAGATCGTGAAGTCTG CTGAAAAACGGAGCCGACGTGAATGCAGTCGATGCCAT TGGGTTCACTCCTCTGCACCTGGCAGCCTTTATCGGACA TCTGGAGATTGTGAAGTGTGCTGCTGAAGCACGGCGCTG ACGTGAACGCACAGGATAAGTTCGAAAAACCGCTTTT GACATCAGCATTGACAACGGAAATGAAGACCTGGCTGA AATCCTGCAGAACTGAATGAACAGAACTGATTAGCG AAGAAGACCTGAAC	gBlock®	IDT
G3-HAVD DARPin	ATGGATTTCCAGGTCCAGATTTTCTCCTTCTGCTGATTT CCGCAAGCGTCATTATGTCACGGGGCTCCGACCTGGGC AAAAAGCTGCTGGAGCCGCTAGGGCCGGGCAGGACG ATGAAGTGAGAATCCTGATGGCCAACGGGGCTGACGTG AATGCTAAGGATGAGTACGGCCTGACCCCTGCACCTG GCTGTGCACACGGCCATCTGGAGATCGTGAAGTCTT GCTGAAAAACGGAGCCGACGTGAATGCAGTCGATGCCA TTGGGTTCACTCCTCTGCACCTGGCAGCCTTTATCGGAC ATCTGGAGATTGTGAAGTGTGCTGCTGAAGCACGGCGCT GACGTGAACGCACAGGATAAGTTCGAAAAACCGCTTT TGACATCAGCATTGACAACGGAAATGAAGACCTGGCTG AAATCCTGCAGAACTGAATGAACAGAACTGATTAGC GAAGAAGACCTGAAC	gBlock®	IDT
TAC _{Δ516-525}	GGGATCCTCGAGAGCGGACAGGTGCTGCTGGAATCCAA TATCAAAGTCTGCCACTTGGTCTACCCCGTGCAGCC TATGGCTCTGATTGTGCTGGGAGGAGTCGAGGACTGC TGCTGTTTATCGGGCTGGGAATTTTCTTTTTCGCTGCGCT GCCGGCACCGGAGAAGGCAGGCCGAGCGCATGAGCCA GATCAAGCGACTGCTGAGCGAGAAGAAAACCTGTCAGT GTCCCTGATAAGCTAGCGATCCC	gBlock®	IDT
TAC _{Δ488-525}	GGGATCCTCGAGAGCGGACAGGTGCTGCTGGAATCCAA TATCAAAGTCTGCCACTTGGTCTACCCCGTGCAGCC TATGGCTCTGATTGTGCTGGGAGGAGTCGAGGACTGC TGCTGTTTATCGGGCTGGGAATTTTCTTTTTCGCTGCGCT GCTGATAAGCTAGCGATCCC	gBlock®	IDT
TAC 4A	AGCGGACAGGTGCTGCTGGAATCCAATATCAAAGTCT GCCACTTGGTCTACCCCGTGCAGCCTATGGCTCTGAT TGTGCTGGGAGGAGTCGAGGACTGCTGCTGTTTATCG GGCTGGGAATTTTCTTTGCCGTGCGCGCCCGGCACCGG AGAAGGCAGGCCGAGCGCATGAGCCAGATCAAGCGAC	Gene synthesis	GenScript

	TGCTGAGCGAGAAGAAAACCGCTCAGGCTCCCATAGA TTCCAGAAGACCTGTTACCCATTTGATAA		
TAC _{Δ488-525} 2A	AGCGGACAGGTGCTGCTGGAATCCAATATCAAAGTCCT GCCCACTTGGTCTACCCCGTGCAGCCTATGGCTCTGAT TGTGCTGGGAGGAGTCGCAGGACTGCTGCTTTATCG GGCTGGGAATTTCTTTGCCGTGCGCGCCTGATAA	Gene synthesis	GenScript

Table 1.0 – Gene products used to clone TAC and DARPin constructs

PCR product	Forward Primer (5'-3')	Reverse Primer (5'-3')
CD8 Alpha	GGGATCCTCGAGCTGAGGCCCGA	GGGATCGCTAGCTCATCACACGTATC
CD8 Beta	GGGATCCTCGAGAAGAAGTCCACCC	GGGATCGCTAGCTCATCACTTGTAGAA
DARPin	GGGATCGGCGGCCATGGATTTCCAGG TCCAGATTT	GGGATCCCCGGGGTTCAGGTCTTCTTCGC TAATC
CD8ΔLck	GGGATCCTCGAGAAGAAGTCCACCC	GGGATCGCTAGCTCATCATTTGTAAAATT GTTTCATGAAACGAAGCCGGCCCTTCTC CGCCGG
TAC _{Δ516-525}	GGGATCCTCGAGAGCGGACAGGTGCTG CTG	GGGATCGCTAGCTTATCAGGGACACTGAC AGGTTTTCT
TAC _{Δ488-525}	GGGATCCTCGAGAGCGGACAGGTGCTG CTG	GGGATCGCTAGCTTATCAGCAGCGCACGC AAAAGAAAA

Table 2.0 – List of cloning primers used in this thesis

2.2 Plasmid Propagation and Preparation from *E. coli*

2.2.1 *E. coli* chemical competent cell preparation

E. coli TURBO (NEB) were cultivated in aerobic conditions at 37°C in Lysogeny Broth (LB) (1% w/v bacto-tryptone, 0.5% w/v bacto-yeast extract, 1% w/v NaCl) shaking at 250 RPM overnight. Cells were inoculated in a 1:50 ratio into new LB broth and incubated at 37°C and 250 RPM until an optical density at 600 nm (OD₆₀₀) of 0.5 was obtained. Cells were then incubated on ice for 15 minutes and harvested at 1,500 x g for 10 minutes at 4°C. The cells were resuspended in ice cold 10 mM MgSO₄ and incubated on ice for 30 minutes. The cells were harvested as previously described and incubated on ice with 50 mM CaCl₂ for 30 minutes. The cells were harvested and resuspended in ice cold 50 mM CaCl₂ supplemented with 15% (v/v) glycerol. The cells were aliquoted in 55 μL fractions and stored at -80°C.

2.2.2 *E. coli* transformation

Chemically competent *E. coli* cells were thawed on ice and incubated with 1 μL of the ligation reaction from Section 2.1 on ice for 20 minutes. Cells were then heat shocked for 42 seconds at 42°C and then plated on LB 1.5% (w/v) agar supplemented with 100

µg/mL ampicillin overnight at 37°C. Individual colonies were selected for screening and large scale propagation.

2.2.3 Large scale plasmid preparation

Single bacterial colonies transformed with the *pCCL* plasmids from Section 2.2.2 were inoculated in 500 mL LB and incubated at 37°C and 250 RPM overnight. Plasmids were extracted and purified from the bacterial cells using the PureLink™ HiPure Plasmid Maxiprep Kit (Thermo Fisher) according to the manufacturer's guidelines with the following exceptions:

- Bacterial cell pellets were harvested at 8,000 x g for 4 minutes at room temperature
- Soluble plasmid DNA was separated from insoluble cell debris by centrifugation at 12, 000 x g for 10 minutes at room temperature
- Precipitated DNA was harvested in 70% ice cold ethanol at 15, 000 x g for 4 minutes at 4°C

Purified DNA was diluted 1/100 in ddH₂O and quantified using the NanoVue™ Plus Spectrophotometer (VWR)

2.3 Cell lines and tissue culturing

2.3.1 Human Embryonic Kidney 293TM (HEK293TM)

HEK293TM (generously donated by Dr. Megan Levings, University of British Columbia) were cultured in Dulbecco's Modified Eagle Media (DMEM) supplemented with 10% heat-inactivated fetal bovine serum (FBS), 10 mM HEPES, 2 mM L-glutamine, 100 U/mL Penicillin/100 µg/µL Streptomycin (Sigma Aldrich) at 37°C and 5% CO₂ in sterile T150 flasks until confluency. Cells were split by removing the media, washing the monolayer with 1 mL of sterile PBS, and incubating cells with 5 mL of Trypsin-EDTA at 37°C and 5% CO₂ for 5-10 minutes. Trypsin-treated cells were then added to a new T150 flasks containing HEK293TM media in a 1:6 ratio. For long term storage, confluent cells were treated with Trypsin and harvested at 500 x g for 5 minutes. The cells were then resuspended in 5 mL of FBS and counted by mixing a 1:1 ratio of cells with 0.4% Trypan Blue. A 10 µL aliquot of this solution was added to a single chamber of a Bright-Line Hemocytometer (Hausser Scientific) and the number of cells in each corner square were added and averaged to determine the concentration of HEK293TM cells according to the manufacturer's guidelines. Cells were then mixed with a 1:1 volume of 20% sterile Dimethyl sulfoxide (DMSO) in FBS and added in 1 mL aliquots in Nunc™ Biobanking Cell Culture Cryogenic Tubes (Thermo Fisher) and incubated for at least 16 hours at -80°C in a Mr. Frosty™ freezing container (Thermo Fisher). Cryogenic tubes were then moved to liquid phase nitrogen tank for long-term storage.

2.3.2 Adherent tumour lines: A549, SKOV-3, SKBR-3, LOXIMVI, OVCAR-3

Adherent tumour lines A549, SKOV-3, SKBR-3, LOXIMVI and OVCAR-3 (originally obtained from Dr. Karen Mossman, McMaster University) were cultured in complete Roswell Park Memorial Institute 1640 (cRPMI, Thermo Fisher) media containing 10% heat-inactivated FBS, 10 mM HEPES, 2 mM L-glutamine and 100 U mL Penicillin/100 µg/µL Streptomycin at 37°C and 5% CO₂ in sterile T150 flasks until confluency. Cells were passaged into new T150 flasks and stored in long-term liquid phase nitrogen as described above in **Section 2.3.1**.

2.3.3 Nonadherent tumour lines: KMS-11, NALM-6, K562, Jurkat, JEKO-1

Nonadherent tumour lines KMS-11, NALM-6, K562, Jurkat E6.1 and JEKO-1 were cultured in T150 flasks in cRPMI media at 37°C and 5% CO₂. Cells were split 1:4 into a new T150 flasks containing fresh cRPMI media upon cell confluency and inspection of the culture media. Cells were stored long term in liquid phase nitrogen as described in **Section 2.3.1**.

2.4 HEK293TM Transient Transfection

HEK293TM cells were plated in HEK293TM media (**Section 2.3.1**) at 100,000 cells/well in a 24-well plate overnight at 37°C and 5% CO₂. The next day, the following two transfection mixtures were prepared and incubated at room temperature for five minutes (each transfection mixture serves one well containing HEK293TM cells).

Mixture 1: 48 µL OPTIMEM (Thermo Fisher) + 2 µL Lipofectamine2000 (Thermo Fisher)

Mixture 2: 50 µL OPTIMEM + 0.8 µg of *pCCL* DNA

Both mixtures were combined and incubated for 20 minutes at room temperature and subsequently added to separate HEK293TM wells. Cells were incubated for at least 48 hours at 37°C and 5% CO₂ prior to flow cytometry analysis as described in **Section 2.7** using antibodies against human IgG and NGFR/CD271 described in **Table 3.0**.

2.5 Lentivirus Production

HEK293TM cells were seeded at a concentration of 8x10⁶ cells per 15 cm radius cell culture dish (three dishes per lentivirus) and incubated overnight at 37°C and 5% CO₂ in HEK293TM media. The next day, media was removed and supplemented with similar media containing 50 µg/mL Normocin in lieu of P/S. Cells were transfected with 60 µg *pMD2G*, *pRSV-Rev*, *pMDLg-pRRE* and *pCCL* (construct specific) vectors and 1.5% Lipofectamine 2000 in OptiMEM media and incubated at 37°C and 5% CO₂ overnight. The media was replaced with DMEM containing 1 mM sodium butyrate and incubated for another 30-48 hours. Viral particles were concentrated by either:

i) Ultracentrifugation

28,000 RPM using the Beckman Coulter SW 32 Ti rotor; virus was resuspended to a final volume of 150 µL and aliquoted for storage at -80°C.

ii) Amicon® filtration

1,450 x g in Amicon® Ultra-15 Centrifugal Filter Units (Thermo Fisher) for 30 minutes at 4°C. Virus was concentrated to a volume of approximately 200 µL/filter unit and aliquoted for storage at -80°C

Virus aliquots were titrated by transducing 30,000 HEK293TM cells with 2×10^{-3} - 2×10^{-6} virus dilutions and incubating at 37°C+5%CO₂ for three days. Transduced HEK293TM cells were quantified as %transfection control positive by flow cytometry, and the viral titer was calculated (in transduction units/mL) as (#cells transduced x %positive cells by flow cytometry x dilution factor)/100.

2.6 Manufacturing of engineered T cells

2.6.1 T cell transduction and upscaling

Peripheral blood mononuclear cells (PBMCs) were extracted using Ficoll-Paque-Plus gradient centrifugation (GE Healthcare) from healthy McMaster Adult cohort (MAC) donors or from commercial Leukopak (HemaCare) leukapheresis products, and incubated with Dynabeads™ human T activator αCD3/αCD28 beads (Thermo Fisher) at a 0.8:1 bead:PBMC ratio for 24 hours in T cell media consisting of RPMI 1640, 10% heat-inactivated FBS, 10 mM HEPES, 2 mM L-glutamine, 1 mM sodium pyruvate, 55 µM 2-Mercaptoethanol, 1X non-essential amino acids (NEAA, Gibco) and 100 U/mL Penicillin/100 µg/µL Streptomycin at 37°C and 5%CO₂. The media was additionally supplemented with 1.5 ng/mL human IL-2 and 10 ng/mL human IL-7 (PeproTech). Cells were transduced with lentiviruses described in **Section 2.5** with a MOI of 2-4 the following day. Every 2-3 days, transduced cells were counted and upscaled to larger flasks at a concentration of 1×10^6 cells/mL in T cell media supplemented with human IL-2 and IL-7. After two weeks, cells were phenotypically analyzed as described in **Section 2.7**.

2.6.2 Enrichment of engineered T cells (NGFR selection)

T cells were enriched for engineered/NGFR⁺/CD271⁺ cells seven days after αCD3/αCD28 activation (**Section 2.6.1**) using the EasySep™ Human CD271 Positive Selection Kit II (StemCell Technologies) as per manufacturer's instructions with the following alterations:

- Cells were washed for a minimum of four times
- Enriched cells were counted and seeded at a concentration of 1×10^6 cells/mL in T cell media supplemented with IL-2 and IL-7 after the enrichment process

T cells were then upscaled as described in **Section 2.6.1**.

2.6.3 Cryopreservation of engineered T cells

After the culturing period, engineered T cells were counted as described in **Section 2.3.1**, harvested at 500 x g for 5 minutes, washed with 20 mL sterile PBS and harvested again. Cells were resuspended in ice-cold CryoStor® CS10 (StemCell

Technologies) at concentrations of $2-7 \times 10^7$ cells/mL and 1 mL/cryovial. Cells were incubated in CryoStor solution for 10 minutes at 4°C, then transferred to a Mr. Frosty™ freezing container, where they were then incubated at -80°C for at least 16 hours. Cryogenic tubes were then moved to liquid phase nitrogen tank for long-term storage.

2.7 Cell phenotyping of surface-expressed proteins

5×10^5 HK393TM, Jurkat E6.1 or primary T cells were washed with 2 mL of FACS-EDTA buffer: PBS supplemented with 1% (w/v) bovine serum albumin (BSA, Roche) and 2.5 mM Ethylenediaminetetraacetic acid (EDTA). Cells were harvested at 500 x g for 5 minutes, and the cells were incubated with 250 ng of Fc-tagged protein (Her2-Fc, BCMA-Fc, or CD19-Fc, R&D Systems) or anti-myc antibody (see **Table 3.0**) for 30 minutes at room temperature in FACS-EDTA buffer. Cells were washed with 2 mL of FACS-EDTA, harvested at 500 x g for 5 minutes and incubated with antibodies against human IgG, CD4, CD8, TCR $\alpha\beta$, and CD271/NGFR specified in **Table 3.0** for 30 minutes at room temperature for 30 minutes. Cells were washed with 2 mL FACS-EDTA, harvested at 500 x g for 5 minutes and fixed with 2% paraformaldehyde (PFA) in FACS-EDTA for 20 minutes at room temperature. Cells were washed one final time with 2 mL FACS-EDTA, harvested at previously described and finally resuspended in 200 μ L FACS-EDTA for flow cytometry analysis.

Cells were filtered through a 50 μ m nylon mesh prior to flow cytometry in order to prevent cell aggregation. All flow cytometry was performed using either the FACSCanto™, LSR II™ or LSRFortessa™ (BD Biosciences) and analyzed using the FlowJo vX software (FlowJo LLC).

Target	Fluorophore	Vendor	Catalogue#	Assay
CD8	AF700	eBioscience	56-0086-82	Phenotype
CD4	Pacific Blue	BD Pharm	558116	Phenotype
hulgG	PE	Jackson IR	109-115-098	Phenotype
NGFR/CD271	VioBright FITC	Miltenyi	130-104-847	Phenotype/Proliferation
TCR	APC	BD Pharm	563826	Phenotype
CD4	AF700	eBioscience	56-0048-82	ICS/Proliferation
CD8	PerCPCy5.5	eBioscience	45-0088-42	ICS/Proliferation
NGFR/CD271	BV421	BD Pharm	130-104-847	ICS
IFN γ	APC	BD Pharm	554702	ICS
TNF α	FITC	BD Pharm	554512	ICS
IL-2	PE	BD Pharm	554566	ICS
Cell Trace Violet	BV421	Invitrogen	C34557	Proliferation
Live/Dead Near IR	APC-H7	Invitrogen	L10119	Proliferation
mIlgG	PE	Jackson IR	115-116-146	Phenotype

c-myc	none	Cell Signaling	9B11	Phenotype/IF
-------	------	----------------	------	--------------

Table 3.0 – List of antibodies used in this thesis**2.8 *In vitro* T cell functionality assays****2.8.1 Intracellular cytokine stimulation**

For nonadherent tumour targets (BCMA⁺ KMS-11, CD19⁺ NALM-6, K562) 5x10⁵ T cells were added to a matching number of target tumour cells (E:T ratio of 1:1) in the presence of 1:1000 Brefeldin A (BFA) protein transport inhibitor (Life Technologies) for four hours at 37°C and 5% CO₂. For adherent tumour targets, 50,000 target cells were plated to separate wells of a 96 flat-bottom plate overnight at 37°C and 5% CO₂ in cRPMI media. The next day, 400,000 engineered T cells were added to each well (E:T ratio of 8:1) and incubated for four hours at 37°C and 5% CO₂ in the presence of 1:1000 BFA in T cell media. Stimulation was stopped with the addition of 20 μM EDTA for 15 minutes at room temperature, and the cells were harvested at 500 x g for 5 minutes. Cells were stained for CD4, CD8 and CD271/NGFR surface proteins as described in **Table 3.0** for 30 minutes at room temperature. Cells were washed with FACS-EDTA, harvested (as previously described) and fixed/permeabilized with CytoFix/CytoPerm™ (BD biosciences) for 20 minutes at room temperature. Cells were washed with Perm/Wash buffer (BD Biosciences), harvested and incubated with antibodies against IFNγ, TNFα, and IL-2 (as specified in **Table 3.0**) for 30 minutes at room temperature. Cells were washed with Perm/Wash buffer, harvested and analyzed by flow cytometry. Combinations of parameters were analyzed by the simplified presentation of incredibly complex evaluations (SPICE) software²⁶³.

2.8.2 Killing/Cytotoxicity Assay

Colorimetric (Chapter 3)

Tumour cell lines were seeded at a concentration of 12,500 or 25,000 (in the case of LOXIMVI) cells per well in a 96 well flat bottom plate for 16-18 hours. T cells were added in triplicate two fold serial dilutions from effector: tumour ratios of 8:1 to 0.25:1 and incubated with the tumour cells for 6 hours. Cells were washed three times with sterile PBS and incubated with 10% AlamarBlue® in cRPMI for 3 hours. The plates were then read at 530 nm excitation and 595 nm emission fluorescence on a plate reader. Percent viability was calculated by subtracting the background (AlamarBlue® only) from the absorbance and dividing by the absorbance of the tumour only cells subtracted by the background.

Luminescence (Chapters 4 and 5)

Tumour cells were first transduced with a lentivirus encoding enhanced firefly Luciferase²⁶⁴ and a puromycin selection marker. Tumour cells positive for enhanced firefly Luciferase were selected for by supplementing the media with 2-8 μg/mL of puromycin in cRPMI. The tumour cells were seeded at a concentration of 50,000 cells per well in a 96

well flat bottom plate and engineered T cells were added in triplicate two-fold serial dilutions from effector: tumour ratios of 8:1 to 0.25:1 and incubated with the tumour cells for 16-19 hours. 15 µg/mL of D-Luciferin (Perkin Elmer) was added to each well and incubated at 37°C while shaking for 10 minutes. Total end-point luminescence at all wavelengths was read using the SpectraMax i3 Multi-Mode Platform (Molecular Devices), and percent viability was calculated by subtracting the background (media only) from the absorbance and dividing by the absorbance of the tumour only cells subtracted by the background.

2.8.3 Proliferation Assay

The number of NGFR⁺Receptor⁺ T cells were first determined by phenotypic analysis described above in **Section 2.7**. 0.5×10^6 NGFR⁺Receptor⁺ T cells were then treated with 5 µM of Cell Trace Violet (Invitrogen) for 30 minutes at 37°C and 5% CO₂. T cells were then co-cultured with BCMA⁺ KMS-11 cells at an E:T ratio of 1:1 for 7 days at 37°C and 5% CO₂. After the proliferation period, cells were treated with a 1:1000 dilution of Live/Dead Near IR dye (Invitrogen) in PBS for 15 minutes at room temperature. Cells were then stained for the CD4, CD8 and NGFR surface markers. Gating strategy performed on FCS Express (De Novo Software) was as follows: T cells (FSC-A vs SSC-A) → Live cells (SSC-A vs Live/Dead Near IR) → Single Cells (FSC-H vs FSC-A) → Engineered NGFR⁺ cells (SSC-A vs NGFR) → histogram of live, engineered single T cells on Cell Trace Violet. Division index, proliferation index and percent divided were calculated by the FCS Express algorithm.

2.9 Jurkat immunofluorescence microscopy

The chambers of an 8-chamber micro slide (Ibidi) were treated with 0.1% Poly-L-Lysine (Cultrex) for 15 minutes at room temperature. 5×10^5 Jurkat T cells engineered to express the full-length or tailless TAC receptor were adhered to the separate chambers for 20 minutes at room temperature and then fixed with fresh 4% PFA for 20 minutes. Cells were stained with the mouse anti-c myc antibody (**Table 3.0**) for 1 hour at room temperature, washed and permeabilized with 1X CytoFix/CytoPerm for 20 minutes at room temperature. Cells were washed in 1X Perm Wash, then incubated with the following antibodies (all Abcam) 1:200 rabbit α Rab7a, 1:200 rabbit α Rab5, 1:200 rabbit α Calnexin, 1:50 rabbit α GM130, 1:200 rabbit α CD45, and 1:200 rabbit α Ubiquitin (in Perm/Wash). Cells were washed then stained with a goat anti-mouse AF488 secondary antibody (Thermo Fisher), goat-anti rabbit AF594 secondary antibody (Thermo Fisher) and Hoechst 33342 stain (generously donated by Dr. Karen Mossman, McMaster University) for 30 minutes at room temperature. Cells were treated with a drop of VectaShield anti-fade solution (Vector Labs) and imaged at 60X magnification on the EVOS FL Auto widefield light microscope (Thermo Fisher). 0.3 µm Z stacks were collected for each field of view. Images were compiled and assembled using the Volocity 6.3 software (Perkin Elmer). Pearson coefficients were calculated by Volocity 6.3 by

highlighting regions of interests (single cells) and calculating pixel overlap between the YFP (c-myc) and Texas Red (organelle) channels for at least 30 cells.

2.10 *In vivo* tumour modeling

2.10.1 Mice

Female immunocompromised NOD.Cg-Rag1^{tm1Mom}Il2rg^{tm1Wjl}/SzJ (NRG) mice were purchased (Jackson Laboratories) or bred in-house. All experiments involving mice were pre-approved by the McMaster Animal Research Ethics Board.

2.10.2 KMS-11 model and monitoring

7-11 week old mice were injected subcutaneously with 1.0×10^6 firefly luciferase expressing BCMA⁺ KMS-11 cells and treated intravenously (*i.v*) twelve days later with thawed engineered CTRL TAC, full length TAC or tailless TAC at 1.5×10^6 NGFR⁺ cells per mouse (low cell dose) or 4×10^6 NGFR⁺ cells per mouse (high dose). Tumour burden was monitored weekly by administering 100mg/kg of D-luciferin (Cedarlane) *i.v* into each mouse and measuring the sum of the dorsal and ventral bioluminescence radiance with the IVIS Spectrum In Vivo Imaging System (Perkin Elmer).

2.10.3 OVCAR-3 model and monitoring

6-11 week old mice were implanted with 2.5×10^6 OVCAR-3 cells subcutaneously (s.c.) into the right hind flank. After 35–42 days of tumour growth, mice were optimized into treatment groups based on tumour volume. Engineered T cells (originally cryopreserved as described in **Section 2.6.3**) were infused *i.v* through the tail vein as two doses delivered 48 hours apart. Tumour volume was measured by caliper (Mitutoyo Canada Inc) every 2–3 days post-ACT and calculated as $L \times W \times H$; % change in tumour volume was calculated as $((\text{current volume (mm}^3) - \text{pre-ACT volume (mm}^3)) / \text{pre-ACT volume (mm}^3)) \times 100$. A tumour volume endpoint of $\geq 2000 \text{ mm}^3$ was adhered to.

2.10.4 NALM-6/JEKO model and monitoring

7–11-week-old mice were injected with 0.5×10^6 NALM6-effLuc (or JEKO-1 upon re-challenge) cells intravenously. Two doses of engineered T cells were administered as above after 3 days of tumour growth. Tumour burden was monitored through bioluminescent imaging as described in Section **2.10.2**. $10 \mu\text{L/g}$ of a 15 mg/mL D-Luciferin solution was injected intraperitoneally 14 min prior to dorsal and ventral imaging using an IVIS Spectrum (Caliper Life Sciences; Waltham, MA). Images were analyzed using Living Image Software v4.2 for MacOSX (Perkin Elmer) and dorsal and ventral radiance was summed. Termination criteria included moribundity or hind limb paralysis.

2.11 Statistical Analyses

Student's t test was used to compare the means of two groups, while one-way analysis of variation (ANOVA) was used to compare three or more groups within an experiment. Statistical significance and p values were calculated using GraphPad Prism 6. * $p < 0.05$, ** $p < 0.01$, n.s. indicates no significance.

CHAPTER THREE

SUBSTITUTION OF THE CD4 TAC ANCHOR WITH CD8 VARIANTS

INTRODUCTION

In this chapter, we investigated the functional properties of the TAC anchor (consisting of the transmembrane and intracellular moieties) in order to understand the modular biology of the TAC receptor. While the current TAC configuration consists of the CD4 anchor, the use of CD8, the other endogenous T cell coreceptor, as the TAC anchor remains uninvestigated. Cytotoxic T lymphocytes are CD8⁺, and therefore the CD8 coreceptor might provide additional cytotoxic advantages to CD4 as the TAC anchor^{265,266}. In terms of the natural coreceptor, the CD8 $\alpha\beta$ heterodimer and CD4 monomer both compartmentalize into activation specific membrane microdomains and interact with Lck. Unlike CD4, the CD8 compartmentalization does not require palmitoylation, but instead depends on the presence of an arginine rich motif in the cytoplasmic tail of both CD8 α and CD8 β ²⁶⁷. CD8 α also contains the critical CXCP motif necessary to bind Lck, however this motif is lacking in CD8 β ⁶⁷.

Within the CAR field, the importance of the anchor has been investigated in-depth. Early first-generation CAR constructs used both CD4 and CD8 α as transmembrane and hinge domains, although the use of CD8 α became more prevalent as its longer hinge provided superior response to cell-based antigen stimulation^{234,268}. Two CARs were generated with the same CD19 binding domain and cytoplasmic signaling domains but employing either the CD8 α transmembrane and hinge or a CD28 transmembrane and hinge²⁶⁹. T cells engineered with either CAR displayed similar capacities to clear tumours in mice; however, the CD8 α CAR secreted less pro-inflammatory cytokines and displayed lower activation-induced cell death (AICD) compared to its CD28 counterpart, providing a potentially safer clinical CAR T cell product²⁶⁹. Thus, the choice of transmembrane/hinge regions can have meaningful impact on the functionality of T cells engineered with synthetic antigen receptors.

Here, we investigated the functionality of TAC-engineered T cells containing CD8 as the anchor instead of CD4. Unlike the monomeric CD4, which contains all biologically-relevant domains in a single polypeptide, CD8 is a heterodimer (see **Section 1.3.2** in Chapter 1) where each monomer contains different yet important biochemical properties; as such, a series of “CD8 TAC” constructs were created, which contained various domains from CD8 α and CD8 β .

We continued our characterization of the TAC anchor by creating loss-of-function mutants in both the CD4 and CD8 TAC constructs in order to determine if specific biological features of the anchor were necessary for *in vitro* functionality as previously predicted.

Our results showed that all of the CD8 TAC receptors were expressed on the surface of primary T cells, produce cytokines in response to antigen stimulation and

display *in vitro* anti-tumour killing capabilities. When the intracellular domains theoretically responsible for TAC functionality were mutated in both the CD4 and CD8, engineered T cells retained functionality *in vitro*. These results suggest that the cytoplasmic domains of CD4 and CD8 do not influence the function of the TAC receptor.

RESULTS

CD8 TAC variants express on the surface of primary T cells and functionally respond to cell-based antigen stimulation

The primary objective in this chapter was to replace the CD4 moiety of the TAC with CD8 (while maintaining the biochemical features necessary for functionality) and investigate the resulting CD8 TAC T cell phenotype and functionality *in vitro*. Since CD8 is a heterodimer (with each monomer containing different yet important biochemical properties), the following three CD8 TAC variants were created (**Fig. 3.1**):

- 1) **CD8 Alpha**: monomeric CD8 α subunit, containing CD8 α arginine rich motif for membrane compartmentalization and CXCP motif for Lck interaction
- 2) **CD8 Alpha+R**: monomeric CD8 α subunit, containing CD8 β (not CD8 α) arginine rich motif for membrane compartmentalization and CXCP motif for Lck interaction
- 3) **CD8 Beta+Lck**: monomeric CD8 β subunit, containing CD8 β arginine rich motif for membrane compartmentalization and CXCP motif from CD8 α for Lck interaction

All constructs contain cysteine to serine mutations in the extracellular domain of either CD8 α or CD8 β that prevent receptor dimerization²⁷⁰.

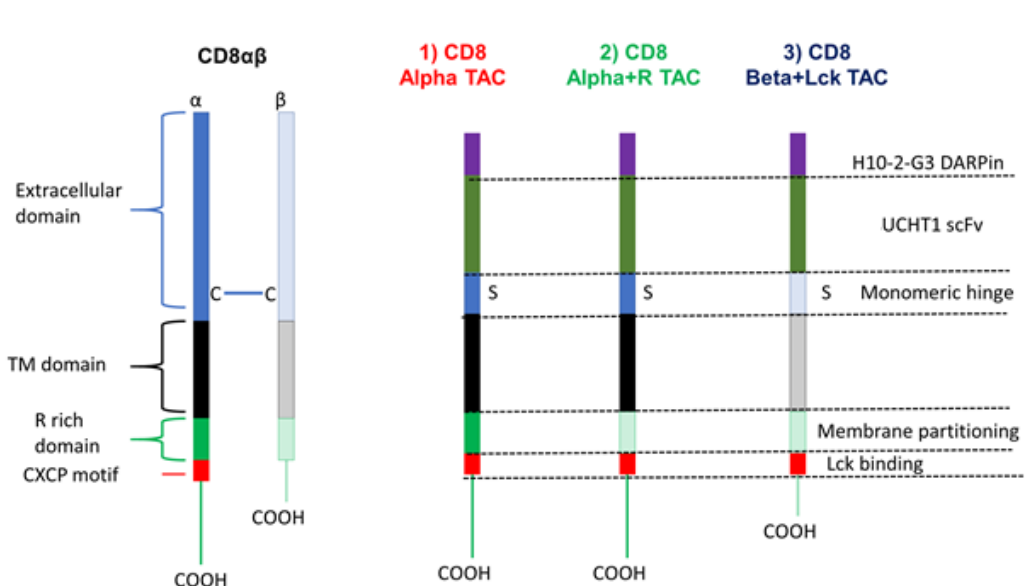


Figure 3.1. Schematic of CD8 TAC Constructs

The three CD8 TAC constructs are shown in addition to the CD8 $\alpha\beta$ heterodimer (alpha opaque, beta translucent). The extracellular anti-Her2 H10-2-G3 DARPIn antigen recognition domain (purple) and CD3 ϵ engager UCHT1 ScFv (orange) remain the same from the CD4 TAC. The CD8 TACs contain cysteine to serine mutations in the extracellular domain (blue) to prevent dimerization, as well as an arginine rich domain (green) for lipid raft association and a CXCP motif (red) for Lck interaction. Constructs not shown to scale.

All CD8 TAC constructs were found to be expressed on the surface of T cells (**Fig. 3.2A**) at levels comparable to the CD4 TAC. When these engineered T cells were co-cultured with the Her2⁺ tumour cell line SKBR3, the T cells were able to lyse the target cells in a dose-dependent manner (**Fig. 3.2B**). The TAC T cells did not lyse the Her2⁻ LOXIMVI cell line beyond background levels. Engineered T cells expressing only the truncated NGFR were a negative control (CTRL) and did not lyse any cell line.

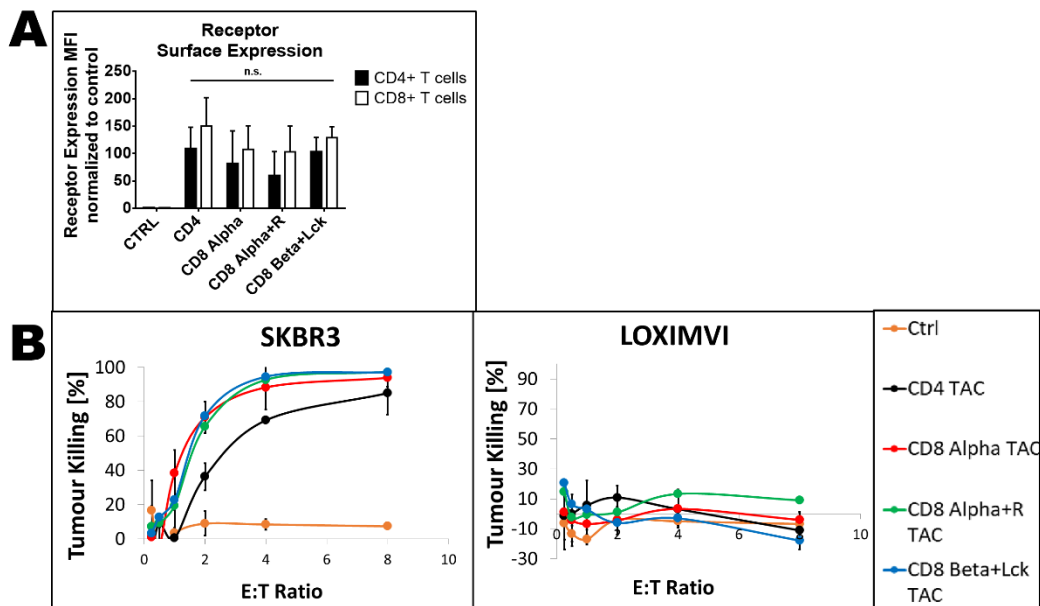


Figure 3.2. CD8 TAC constructs express on the surface of T cells and functionally lyse target cells *in vitro*

Human T cells were transduced with construct-specific lentiviruses, cultured for 14 days, then phenotypically and functionally analyzed for TAC expression and *in vitro* response to antigen stimulation. **(A)** Surface expression of each receptor on CD4⁺ and CD8⁺ T cells, normalized to the transduction control (CTRL). **(B)** Cytotoxicity assays of engineered T cells co-cultured with Her2⁺ SKBR3 target cells and Her2⁻ LOXIMVI target cells for 6 hours at the stated effector to target (E:T) ratio. Error bars represent standard deviation from three independent experiments from the same PBMC donor. n.s = nonsignificant ($p > 0.05$) for all CD4⁺ and CD8⁺ means.

To further assess *in vitro* functionality, we stimulated the engineered T cells with Her2⁺ A549 or Her2⁻ LOXIMVI tumour cells and measured the production of TNF α , IFN γ ,

and IL-2 cytokines. Multivariate data was then analyzed by SPICE software, which displays every combination of cytokine producing cells. The CD4⁺ engineered T cells (**Fig. 3.3A**) are predominantly IL-2⁻/IFN γ ⁺/TNF α ⁻ (purple) and IL-2⁻/IFN γ ⁺/TNF α ⁺ (dark blue) upon tumour stimulation, although the CD8 Alpha+R TAC appears to have a markedly lower population of the latter and therefore less total cytokine producing cells compared to the other constructs. The CD8⁺ engineered cells (**Fig. 3.3B**) are predominantly IL-2⁺/IFN γ ⁻/TNF α ⁻ (light blue) and IL-2⁻/IFN γ ⁺/TNF α ⁻ (purple), and both the CD8 Alpha and CD8 Beta+Lck TAC constructs appear to have larger proportions of cytokine producing cells than the CD4 TAC and CD8 Alpha+R TAC. Taken together, these data demonstrate that the CD4 anchor can be functionally (surface expression and cytokine production) replaced with three CD8 equivalents within the TAC configuration.

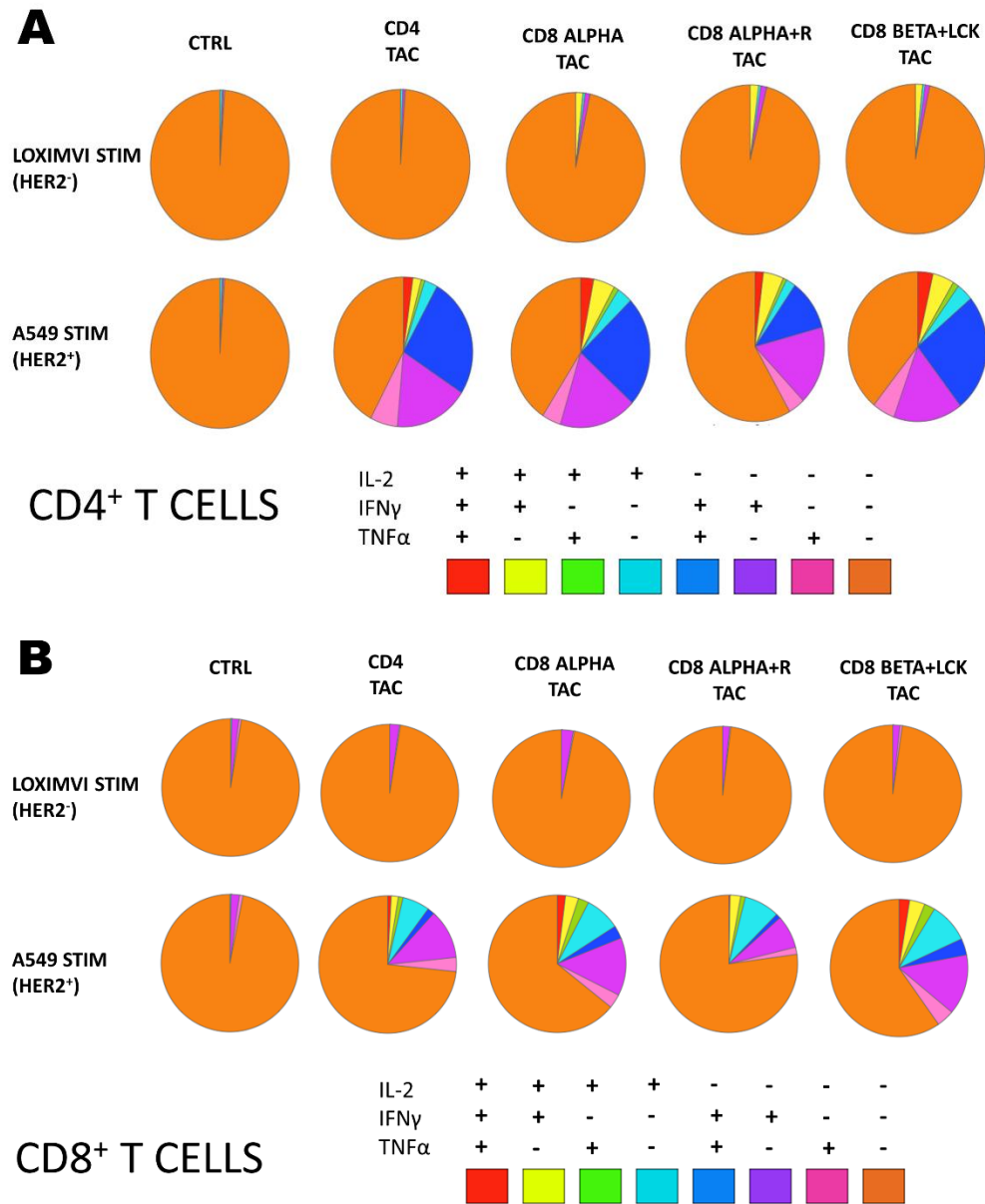


Figure 3.3. CD8 TAC constructs secrete similar cytokines as the CD4 TAC upon antigen stimulation
 Human T cells were functionally analyzed for *in vitro* cytokine production in response to co-culturing with Her2⁺ target cells for 4 hours. Cells were examined by flow cytometry and data was analyzed by SPICE software on transduced CD4⁺ cells. **(A)** Intracellular cytokine profile of transduced CD8⁺ cells analyzed by SPICE. **(B)** Cytokine profile of transduced CD4⁺ cells analyzed by SPICE.

Mutations within the intracellular tail of the TAC receptor have no effect on *in vitro* functionality

The TAC molecule was designed based on certain biological principles, including the role of the intracellular tail of the co-receptor in membrane compartmentalization and Lck interaction during T cell activation^{80,267,271,272}. Given the previous observations, we were interested in investigating the necessity of these intracellular domains to better understand the complete role of the anchor. We therefore generated three different CD8 Beta+Lck TAC (herein referred to as “CD8 TAC”: chosen for its *in vitro* functionality in **Fig. 3.3**) loss-of-function mutants (**Fig. 3.4**): one lacking the arginine rich motif necessary for compartmentalization (CD8ΔR), one lacking the CXCP motif necessary for Lck interaction (CD8ΔL) and one lacking both the arginine and Lck-interaction domains (CD8ΔLR). Additionally, we also created a CD4 TAC 4A mutant (4 cysteines in the cytoplasmic tail mutated to alanines) which has been previously shown to abrogate both lipid raft association and Lck interaction⁶³.

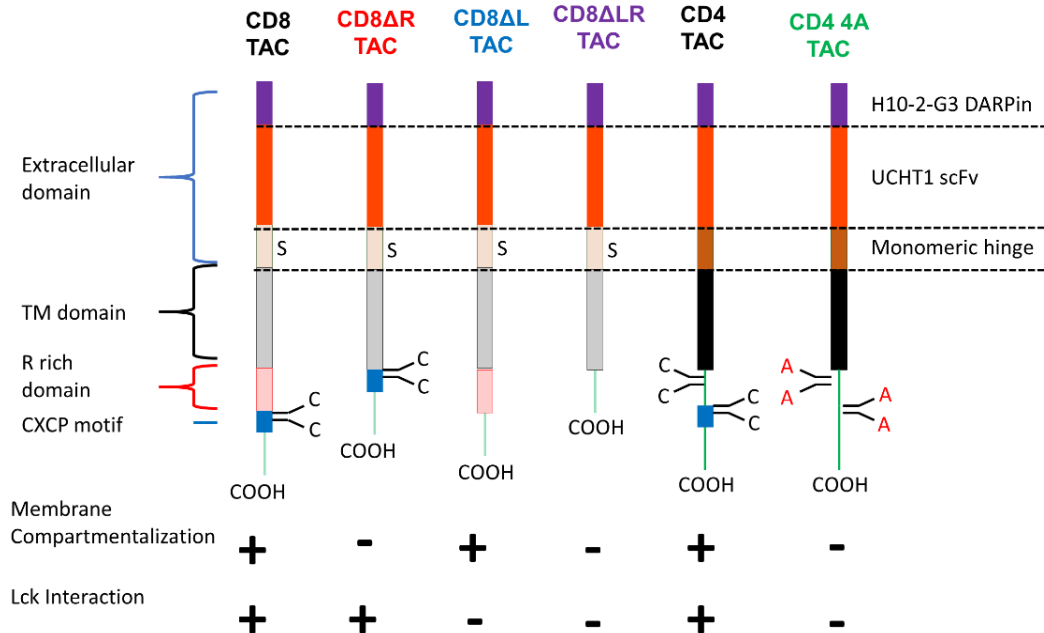
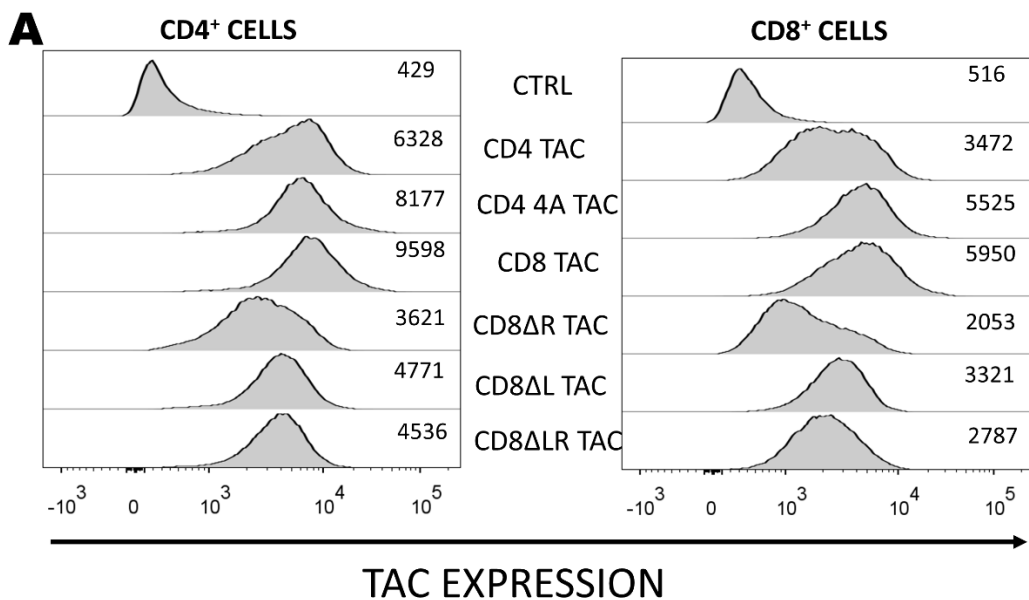


Figure 3.4. Schematic of TAC intracellular tail mutants

Schematic representations of the intracellular tail TAC mutants are shown. The anti-Her2 DARPin is shown in purple, while the UCHT1 scFV is in orange. The CD8 TAC variants consist of the CD8β anchor (hinge in translucent brown, transmembrane in grey) with or without an arginine rich domain (translucent red) or a CXCP motif (blue). The CD4 TAC consists of the CD4 anchor (hinge and transmembrane domain in dark brown and black, respectively), as well as four cysteine residues in the cytoplasmic tail: two for palmitoylation and two in the CXCP motif (blue). The 4A mutant contains C→A point mutations at all four of these sites.

These mutants were all expressed on primary T cells (**Fig. 3.5A**). The CD8 Δ R receptor (lacking the arginine rich domain) displayed poor surface expression in both CD4 $^+$ and CD8 $^+$ cells relative to the other receptors. To assess the functionality of the receptors, an intracellular cytokine stain was performed after co-culturing the engineered T cells with Her2 $^+$ SKOV3 or Her2 $^-$ LOXIMVI for four hours. We observed no appreciable difference in cytokine production between the 4A and parent CD4 TAC, or the CD8 mutant TACs and the parent CD8 TAC in CD4 $^+$ or CD8 $^+$ cells (**Fig. 3.5B**). The ‘loss-of-function’ mutants were also able to successfully lyse Her2 $^+$ SKOV3 (**Fig. 3.5C**) tumour cells in a six-hour cytotoxicity assay comparatively to their respective parent TACs. Despite the plethora of evidence that these domains significantly contribute to the proper functioning of both co-receptors in TCR-pMHC interaction, we found that their omission or mutation had no effect on the modular function of the TAC receptor in redirecting T cells against a tumour.



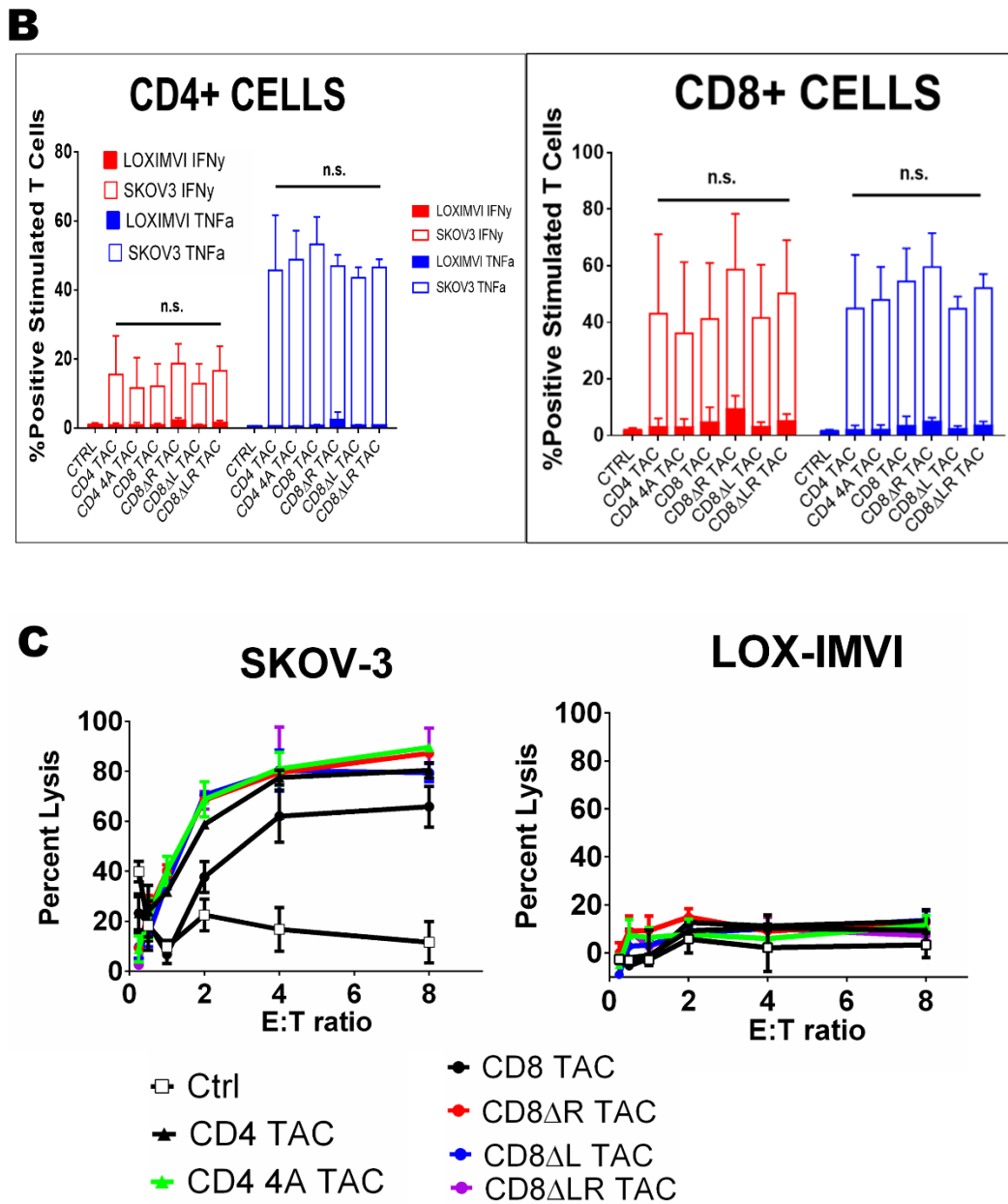


Figure 3.5. TAC mutants retain *in vitro* functionality

Human T cells were transduced with construct specific lentiviruses, cultured for 14 days, then assessed for surface expression and *in vitro* functionality in response to antigen. (A) Receptor surface expression is shown for CD4⁺ and CD8⁺ T cells along with associated mean fluorescence intensity (MFI). (B) Intracellular cytokine production of engineered T cells in response to co-culturing with Her2⁺ SKOV-3 or Her2⁻ LOXIMVI for four hours for CD4⁺ and CD8⁺ cells (C) Engineered

T cells and target cells were co-cultured for 6 hours and lysis of target cells was measured at end point. Error bars represent standard deviation from three independent experiments. n.s. = nonsignificant ($p > 0.05$)

Engineering TAC receptors with low affinity anti-Her2 DARPins

The TAC aims to recapitulate T cell activation, which depends on both the TCR interaction with peptide-MHC and co-receptor binding to MHC. Alone, these two interactions are relatively weak ($K_D \sim 1-99 \mu\text{M}$), therefore T cell activation depends on both binding events²¹⁴. Nevertheless, high affinity TCRs exist which can activate T cells in the absence of CD4/CD8 binding of MHC due to the high affinity of the TCR with pMHC (>100 fold greater than the endogenous affinity)²⁷³. The anti-Her2 DARPin used in previous work (clone H10-2-G3) has an affinity of approximately 91 pM, which is much higher than the endogenous affinity of TCR with pMHC. Due to the high affinity DARPin, the TAC constructs may simply behave as high affinity TCRs, which do not require the contribution of the co-receptor. Therefore, we sought to repeat the experiments with the TAC mutants using a lower affinity binding domain to determine whether the outcomes shown in **Figures 3.4 and 3.5** were simply the result of the affinity of the binding domain. Several variants of the HER-2 DARPin used in these experiments were available in literature and listed in **Table 4.0**.

Clone name	K_D/nM
H10-2-G3	0.091 ± 0.001
G3-D	1.48 ± 0.008
G3-A	1.21 ± 0.006
G3-AVD	10.2 ± 0.055
G3-HAVD	269 ± 1.19
H10-2-G5	0.670 ± 0.005
H10-2-D11	35.8 ± 0.149

Table 4.0. Affinities of different anti-Her2 DARPins²⁶².

The H10-2-G3 clone is the DARPin used in anti-Her2 TAC constructs

We tested three lower affinity DARPin clones (G3-A, G3-AVD and G3-HAVD; **Table 4.0**). We aimed to determine whether functional attributes of the TAC variants were influenced by the affinity of the antigen-binding domain. TACs expressing these DARPins were first expressed on HEK293TM cells and assessed for their expression and ability to bind soluble Her2-Fc. The gene transfer vector encodes truncated NGFR (tNGFR) and the TACs carry an epitope tag from c-myc, allowing us to confirm transfection and TAC expression, independent of the binding domain. NGFR expression revealed that all populations were engineered to a similar degree (**Fig. 3.6A**) and c-myc expression revealed that TAC expression was quite similar across all populations, albeit slightly lower on the cells engineered with G-3A (**Fig. 3.6B**). The binding of Her2-Fc varied considerably between DARPins (**Fig. 3.6**). As expected, the H10-2-G3 DARPin exhibited the highest

Her2-Fc binding, and surprisingly, the G3-A DARPin showed practically no Her2-Fc binding despite having a Her2 K_D in the low nanomolar range (the same as several CAR scFvs^{274,275}). The G3-AVD DARPin exhibited detectable, but considerably lower Her2-Fc binding, while the G3H-AVD (the lowest affinity DARPin) showed practically no antigen binding. When Her2-Fc binding and receptor expression (c-Myc) in terms of MFI is normalized to NGFR MFI (Fig. 3.6D), results indicate that despite comparable transfection efficiencies and receptor expression, the DARPins displayed considerable differences in Her2-FC binding (G3-AVD > G3-A = G3-HAVD).

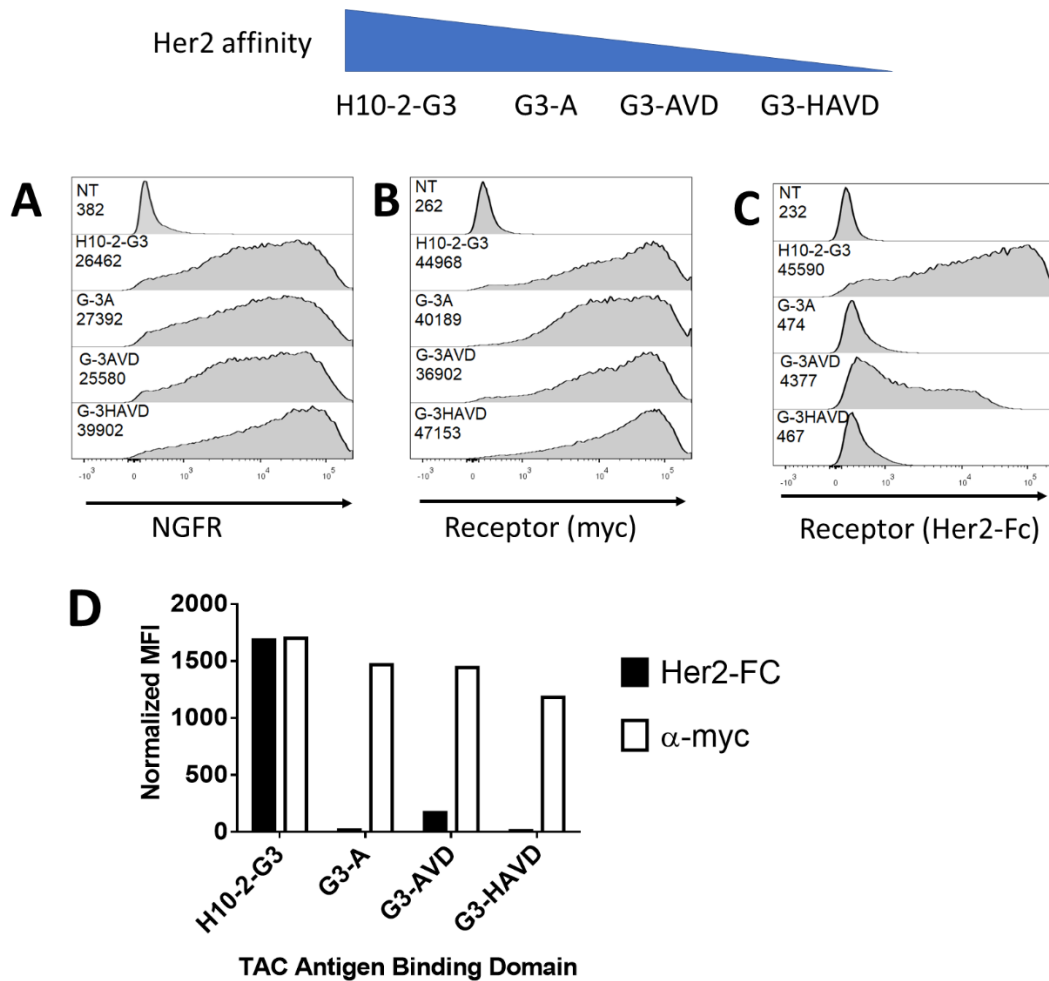


Figure 3.6. The Her2 DARPins as ligand binding domains for the TAC receptor are expressed on HEK293TM cells and exhibit different Her2 binding properties

HEK293TM cells were transiently transfected with plasmids expressing the H10-2-G3, G3A, G3AVD, G3HAVD anti-Her2 DARPins TAC receptors, as well as the anti-Her2 single chain variable fragment (ScFv). Cells were analyzed by flow cytometry for the NGFR transduction marker(A), Myc-tag receptor expression(B) and Her2-Fc binding (C). NT = non transfected, values represent mean

fluorescence intensity. Myc and Her2-Fc MFI were normalized to NGFR MFI in order to compare receptor expression to Her2-Fc binding while accounting for transfection efficiencies (D).

The expression and functional profile of the TAC receptor is influenced by the DARPin

The DARPin TAC constructs were expressed in primary T cells and assessed for surface expression and *in vitro* functionality following antigen stimulation. The H10-2-G3 TAC displayed a relatively high expression profile (Fig. 3.7A), as expected. Similar to the HEK293TM data, The G3-A TAC displayed very poor surface expression and Her2-Fc binding. The G3-AVD TAC had an intermediate profile where some Her2-Fc binding and modest surface expression was detected, while the G3-HAVD TAC showed little to no antigen binding or surface expression. Functionality correlated to surface expression, where the H10-2-G3 TAC showed the highest cytokine response to antigen stimulation, followed by the G3-AVD TAC (Fig. 3.7B). Both the G3-A and G3-HAVD TACs showed little to no cytokine production. Because of this, we chose to pursue the G3-AVD DARPin as the antigen binding domain to test the high affinity TCR hypothesis as it has shown surface expression and Her2-Fc binding on T cells and is within the natural peptide-MHC affinity range (nM). Together with the previous HEK293TM data, these results suggest that well characterized proteins such as these DARPins may behave differently not only in terms of expression, but also in binding with its natural ligand when incorporated into a chimeric receptor module. This is specifically highlighted by the HEK293TM G3-A data: the soluble protein *in vitro* has a relatively strong affinity for Her2 (1.21 ± 0.006 nM), however does not appear to bind to Her2-Fc when expression on the TAC receptor.

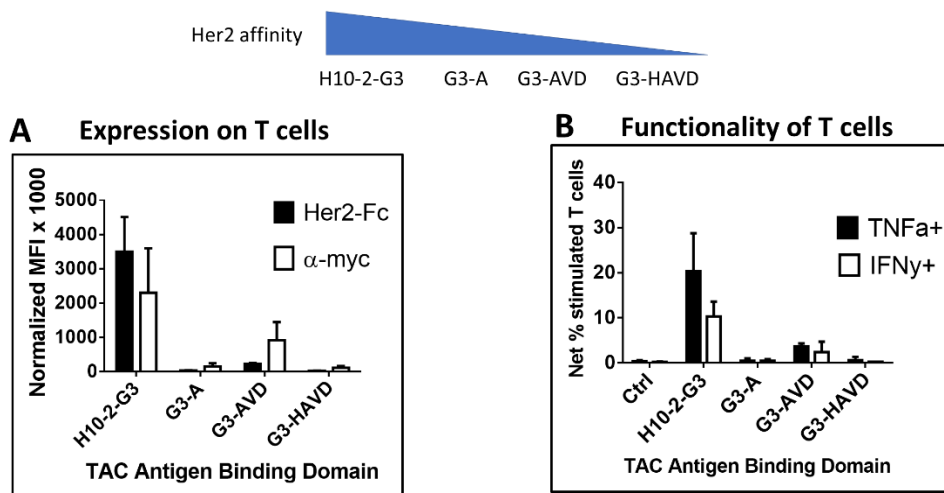
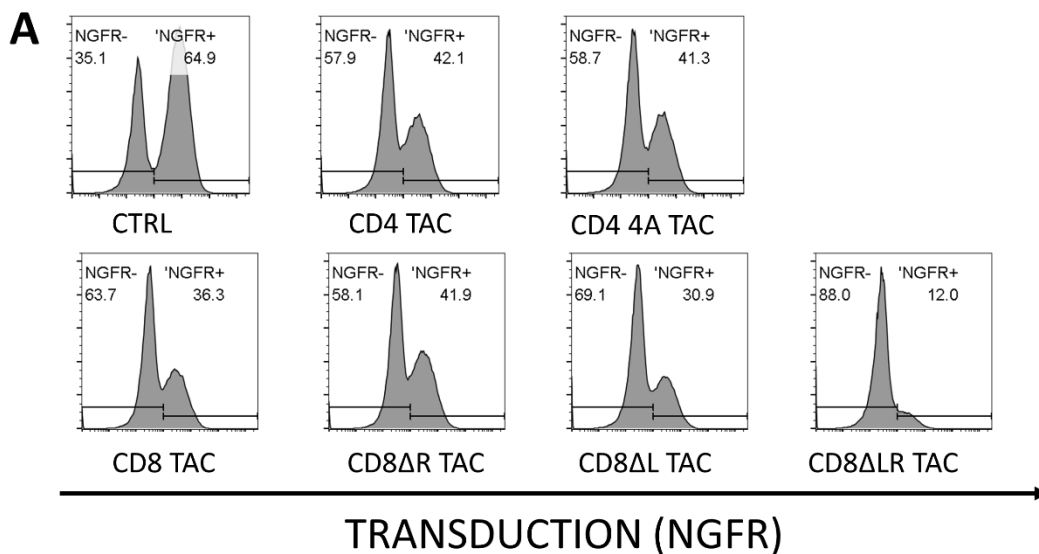


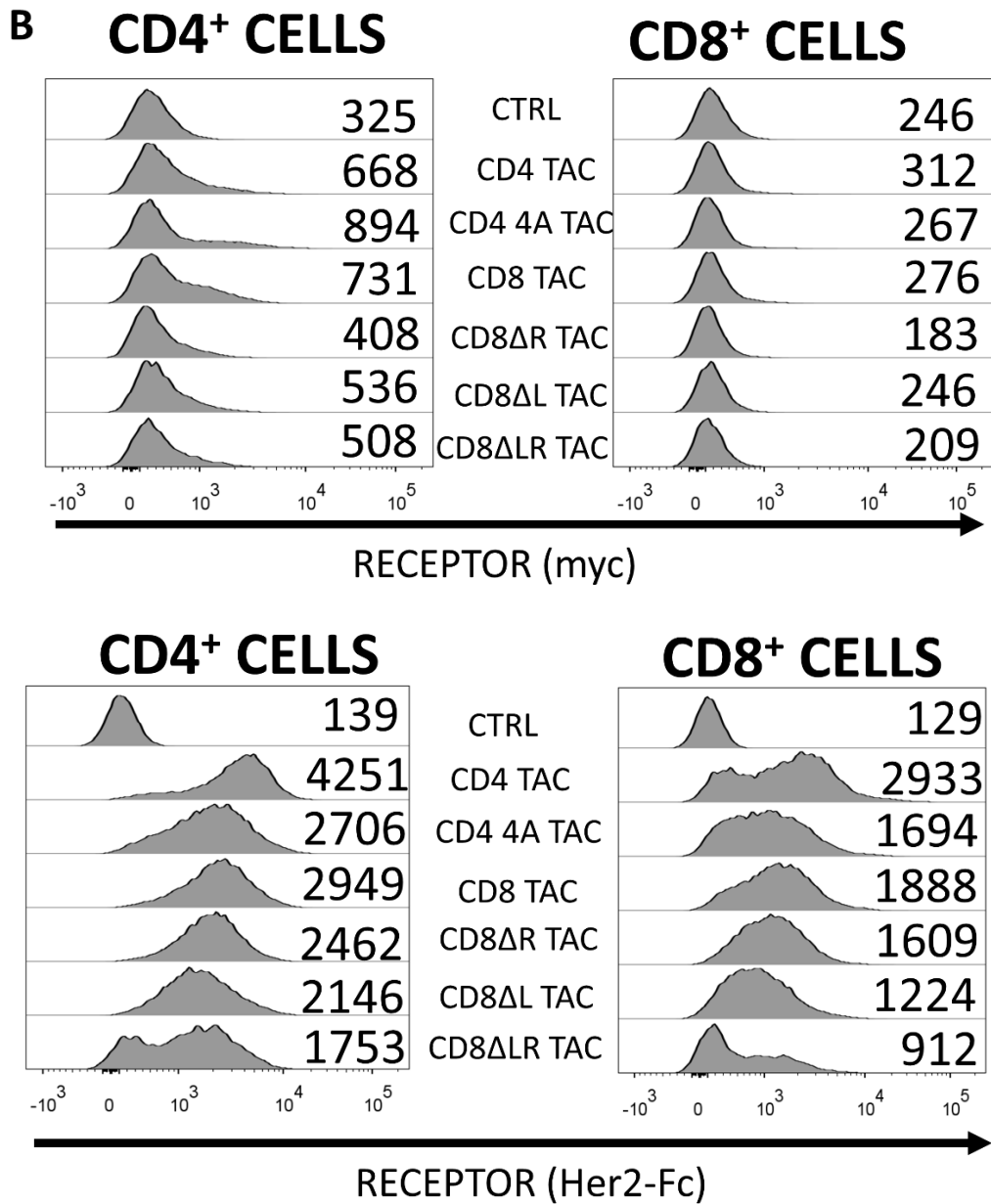
Figure 3.7. DARPins exhibit differential expression and functionality as the antigen binding domain of the TAC receptor on T cells.

HEK293TM cells were transiently transfected with plasmids expressing the H10-2-G3, G3-A, G3-AVD, G3-HAVD anti-Her2 DARPins TAC receptors, as well as the anti-Her2 single chain variable fragment (ScFv). Cells were analyzed by flow cytometry for Her-Fc binding (A), NGFR transfection

marker (B) and Myc-tag receptor expression (C). Myc and Her2-Fc MFI were normalized to NGFR MFI in order to compare receptor expression to Her2-Fc binding while accounting for transfection efficiencies (D).

Based on the results in **Figure 3.7**, we engineered the G3-AVD DARPin on the TAC variants described in **Fig. 3.4**. When surface expression was assessed, the G3-AVD constructs showed variable levels of transduction (**Fig. 3.8A**), namely the CD8 Δ L and CD8 Δ LR TACs which yielded low transduction. Detection of the receptor using the α -myc stain was poor (**Fig. 3.8B**), while receptor binding to Her2-Fc correlated to transduction (lower transduced receptors such as CD8 Δ LR TAC displayed low Her2-Fc receptor binding, while higher transduced constructs displayed higher Her2-Fc binding). When these TAC-engineered T cells were assessed for *in vitro* cytokine production (**Fig. 3.8C**), differences also correlated with transduction efficiencies, making interpretation of the data difficult. For instance, the CD8 Δ LR TAC displayed lower total cytokine production compared to the parent CD8 TAC, but this construct also displayed the low total transduction. This ICS experiment was also conducted on a single donor gated on total (not engineered) T cells. Functionality experiments will need to be repeated with enriched engineered T cells, possibly with transduction selection/sorting as discussed below.





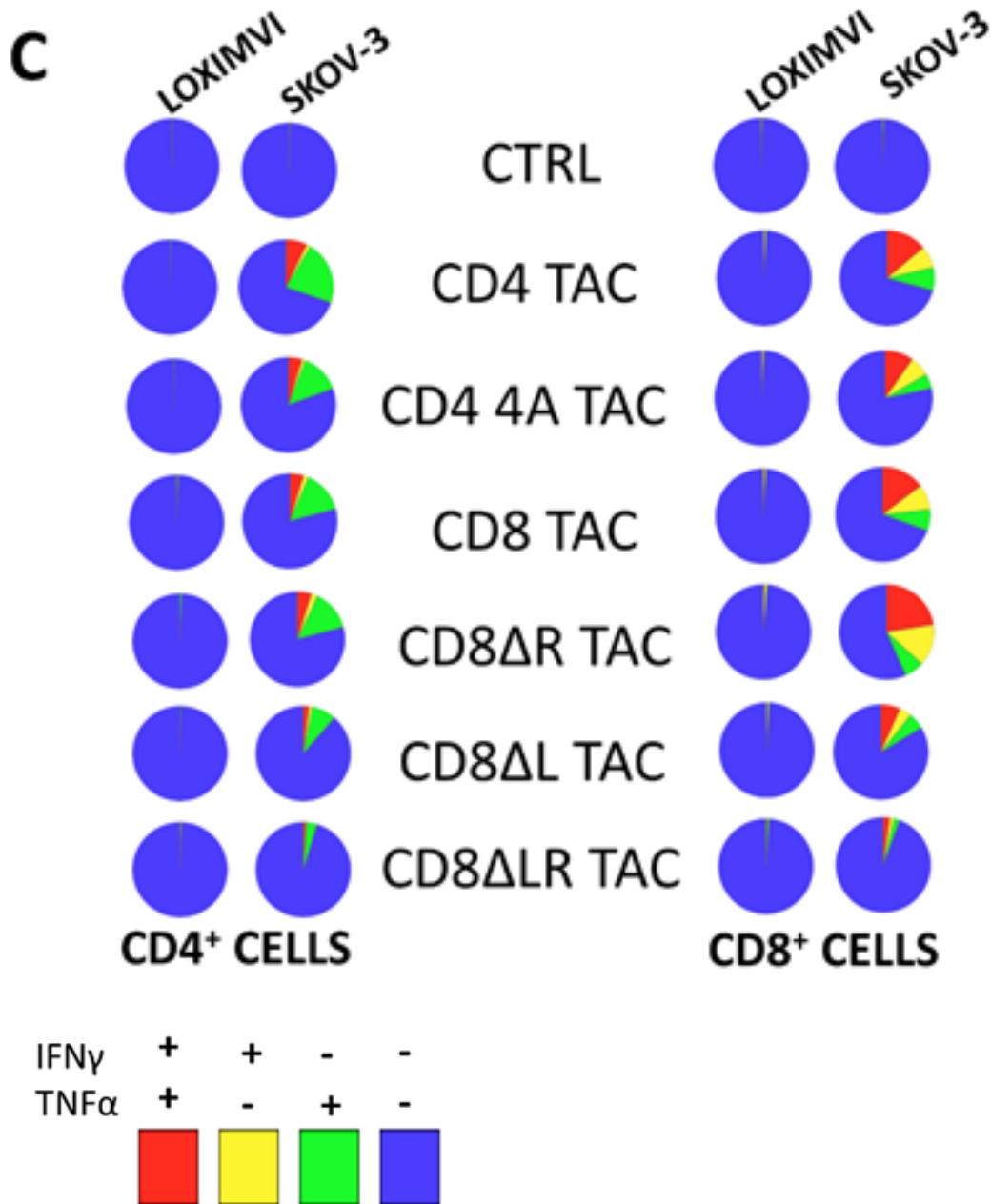


Figure 3.8. *In vitro* functionality of the G3-AVD mutant TAC variants despite generally poor surface expression

The intracellular tail mutants were cloned to express the G3-AVD antigen-binding DARPin and expressed in primary T cells by lentivirus transduction. (A) Transduction efficiency is shown as the number of T cells positive for the NGFR transduction marker. (B) Surface expression of the G3AVD TAC receptor is shown by α -myc and Her2-Fc staining (gated on NGFR⁺ cells from panel A). (C) Engineered T cells were co-cultured with Her2⁺ target cells for 4 hours in the presence of brefeldin

A, and cells were stained for intracellular cytokine production. Cells were examined by flow cytometry and data was analyzed by SPICE software on transduced CD4⁺ and CD8⁺ cells.

DISCUSSION

In this chapter, we sought to understand the biology behind the modular components of the TAC receptor, specifically the coreceptor anchor. The TAC receptor was designed²⁵⁸ with the CD4 transmembrane and cytoplasmic domains for several reasons: i) it is a single pass monomeric transmembrane co-receptor ii) it contains palmitoylated cysteine residues near the C-terminus that facilitate membrane-specific clustering during antigen engagement and activation and iii) it contains an binding domain for Lck, a kinase responsible for phosphorylating ITAMs on the CD3 complex^{62,63,67}. The CAR field is replete with evidence demonstrating the influence of the transmembrane and hinge domains on key biological attributes of the CAR T cell, including *in vivo* persistence, resistance to AICD and antigen engagement on a cell surface^{234,268,269,276}. Given the importance of these domain in the CAR field, we sought to investigate whether replacing the CD4 anchor with alternate structures would influence performance. We designed TACs where the CD4 portion was replaced by three alternate forms of monomeric CD8 (**Fig. 3.1**) and found that TAC T cells with these anchors were expressed well on primary T cells and retained *in vitro* functionality with respect to tumour cytotoxicity (**Fig. 3.2**) and cytokine production (**Fig. 3.3**). These results were expected, as the CD8 TAC variants were specifically designed to recapitulate the biochemical features in CD4.

We then explored the biological features of the cytoplasmic domain that were included specifically for TAC function. To this end, we created TAC variants with deletions and mutations designed to abrogate either lipid raft association or Lck binding or both (**Fig. 3.4**). Contrary to our hypothesis, these constructs all retained functionality *in vitro* compared to the prototypic TAC (**Fig. 3.5**), although deletion of the arginine domain (CD8ΔR) diminished surface expression of the receptor. To account for the possibility that this observation was due to the high affinity H10-2-G3 DARPIn used as the antigen binding domain in the TAC, we used three additional lower affinity DARPins (**Table 4.0**) as antigen engagers on the TAC and first assessed their surface expression and functionality transiently in HEK293TM cells (**Fig. 3.6**). While all constructs showed good transient expression based on flow cytometry analysis using a marker in the receptor (C-myc), two DARPins (G3-A and G3-HAVD) displayed no ability to bind soluble Her2-Fc. While it was not surprising that G-3HAVD failed to bind soluble Her2-Fc, it was a surprise that the G3-A DARPIn failed to bind as its reported affinity for Her2 is in the low nanomole range²⁶², which is higher than the G3-AVD DARPIn that displayed some capacity to bind soluble Her2-Fc. While we cannot explain these data, it is possible that small differences between the DARPIn lead to structural differences in the intact receptor that impair interactions with the DARPIn target. When expressed in primary T cells, all low affinity DARPins

displayed lower receptor expression compared to the H10-2-G3 TAC (**Fig. 3.7**), and the G3-A and G-3HAVD TACs were nearly undetectable. When stimulated in the presence of Her2⁺ tumour cells, the TACs engineered with G3-AVD DARPin (Her2 $K_D = 10.2 \pm 0.055$ nM) could elicit a response from the T cell, whereas the TACs engineered with G3-A and G3-HAVD. We therefore decided to use this DARPin to re-test the biochemical TAC mutants, as it showed detectable expression in primary T cells and has an antigen affinity orders of magnitude lower than high affinity TCRs²⁷³. When these G3-AVD mutant TAC variants were expressed in T cells, they yielded variable transduction efficiencies (12-42% transduced as determined by NGFR positivity) (**Fig. 3.8**), and therefore variable receptor expression. These bulk T cells were assessed for *in vitro* cytokine production, and although we observed differences between TAC constructs, they correlated with differences in transduction, making interpretation difficult.

In the chimeric antigen receptor field, CD8 (specifically the α stalk) plays an important role in receptor design. It is used as the hinge and TM domains of several CAR constructs in the literature due to its flexibility, and even supports antigen recognition on a cell surface better than a CAR using the CD4 TM and hinge domains^{234,277}. It is important to note that we modified monomeric CD8 α in the TAC configuration, which contains a cysteine to serine mutation in the hinge to prevent dimerization of the coreceptor²⁶⁶. Given that the TAC engages CD3 ϵ via the UCHT1 scFV and that two epsilon molecules are present in a single TCR-CD3 complex, we were concerned that a TAC dimer would cause spontaneous clustering of TAC-TCR-CD3 complexes, which would inevitably lead to auto-activation of engineered T cells due to clustering as supported by the kinetic segregation model of activation (see **Section 1.3.4** in Chapter 1)²⁷⁸. Indeed, CARs have previously been shown to form dimers due to the CD28/CD8 α hinge²³³ and are known to transmit a basal signal (tonic signaling). Interestingly, a study found that a CAR containing a modified monomeric CD8 α expressed in the NK-92 cell line expressed better than that containing the unmodified CD8 α dimer²⁷⁹.

These functional modifications of the cytoplasmic domains were specifically chosen based on research demonstrating the importance of the amino acids/domains for TCR activation. Since the TAC receptor aimed to recapitulate the natural activation of the T cell, we hypothesized that the co-receptor as the TAC anchor served the same functional purpose as the co-receptor for the endogenous TCR, and any mutations that render the endogenous coreceptor nonfunctional (i.e. 4A) would render the TAC nonfunctional. The results in this chapter indicate the functionality of mutant receptors may very well be due to the nature of clustering upon antigen engagement: as long as TAC receptor can recognize a tumour associated antigen and recruits the TCR, clustering of these molecules at the site of contact on the tumour cell might be sufficient to initiate a T cell response as predicted by the kinetic segregation model of activation (discussed in Section 1.3.4)²⁸⁰. One important caveat for these results is that the loss of function mechanisms (Lck binding, membrane compartmentalization) for these mutants were not

confirmed. We did not confirm a lack of Lck association or change in membrane compartmentalization in primary T cells for the mutants described herein. The data presented here provide preliminary indication that the intracellular tail may not be required for TAC function.

We considered the possibility that the interaction our high affinity antigen binding domain (H10-2-G3 anti-Her2 DARPin) was so strong that it created a TAC similar to a high affinity TCR, which by definition does not require a coreceptor to respond to peptide-MHC²⁷³. We tested three different DARPins containing 10-fold differences in Her2 affinity as the antigen binding domain for the TAC²⁶². Surprisingly, the G3-A DARPin (KD ~ 1 nM) showed no binding to Her2-Fc despite receptor expression in HEK293TM cells. These DARPins were originally characterized as recombinant proteins purified from *E. coli*. Expression in eukaryotic cells may very well necessitate post translational modifications that do not occur in bacteria, leading to differences in expression and binding. We noted that the G3-A DARPin contained a T55A mutation within the protein not present in H10-2-G3, and considered the possibility that the change of this hydrophilic amino acid to a smaller hydrophobic one may be preventing important post translational modification necessary for proper protein folding²⁶². We tested another DARPin mutant (G3-D, **Table 4.0**) that has a similar affinity for Her2 as G3-A, but contained threonine at position 55 instead of alanine, similar to the H10-2-G3 DARPin. When expressed as the antigen binding domain in TAC T cells, we also observed very poor surface expression, but an *in vitro* cytokine response higher than the G3-AVD TAC and closer to the H10-2-G3 TAC. We also noted a clear downregulation of the TCR, which is a phenotypic hallmark of the TAC observed in our laboratory, suggesting that expression of the G3-D TAC is below our current level of detection by flow cytometry. Surface expression of the G3-AVD TACs was also issue (the percentage of receptor positive cells was below 5%, as detected by flow cytometry), except for a single donor. Future experiments necessitate that we homogenize the population of receptor positive cells by NGFR selection or flow cytometry sorting. Nevertheless, the differences in surface expression of the TAC receptor bearing the lower affinity DARPins made it very difficult to compare the results. Therefore, the possibility that binding affinity may influence the need for particular cytoplasmic functional domains remains unresolved.

Overall, the results in this chapter demonstrate that the CD4 component of the TAC receptor can be replaced by modified variants of CD8 α and CD8 β . Interestingly, TAC receptors retained functionality despite mutation or deletion of key functional domains within the coreceptor, suggesting that the cytoplasmic domain may not be a critical component of the TAC receptor. We explore this idea further in the next chapter where we characterize TAC variants lacking an intracellular tail entirely.

CHAPTER FOUR

CHARACTERIZATION OF THE TAILLESS TAC RECEPTOR

Introduction

In the previous chapter, our work investigating the CD4 component of the TAC receptor lead to observations indicating that the intracellular and transmembrane domains can be replaced with CD8 variants and the receptor could still retain *in vitro* functionality. Moreover, we mutated and/or deleted critical residues within both the intracellular CD4 and CD8 components and likewise observed no abrogation of functionality. In this chapter, we continued the investigation of the CD4 TAC anchor by removing the intracellular cytoplasmic tail in its entirety and observing the resulting functionality of this tailless TAC construct both *in vitro* and within an *in vivo* xenograft mouse model.

The CD4 cytoplasmic tail has been heavily characterized in the literature due to its role in endogenous T cell signaling. The tail contains a C-terminal CXCP motif that has been shown to specifically interact with Lck in the presence of a zinc ion cofactor⁶². The interaction of this motif with Lck is correlated with antigen-dependent production of IL-2. CD4 mutants containing cysteine to alanine substitutions in the CXCP motif or truncation mutants lacking the motif entirely do not interact with Lck, and produce very limited IL-2 in response to antigen²⁸¹. The intracellular domain also contains two membrane proximal cysteine residues that have been shown to be important sites for post translational palmitoylation. Palmitoylation of these cysteines contributes to the localization of the CD4 receptor into membrane specific microdomains that enhance antigen-induced signaling, leading to T cell activation and proliferation⁶³. Given that the cytoplasmic tail of the co-receptor provides important contributions to the functionality of the TCR, we were interested in examining if the tail similarly contributes to the functionality of the TAC receptor and if so, to what capacity?

In this chapter, we focused on TAC receptors for multiple myeloma, a hematological cancer characterized by excessive proliferation of plasma cells in the bone marrow, leading to hypercalcemia, anemia, abnormal immunoglobulin production and osteolytic bone lesions²⁸². B cell maturation antigen (BCMA) is a useful target on multiple myeloma since it is highly and specifically expressed on multiple myeloma cells. BCMA is not expressed on developing B cells or memory B cells, but is expressed on a plasma cells which are dispensable for host immunity²⁸². Importantly, BCMA also contributes to the survival of malignant plasma cells where its upregulation promotes multiple myeloma growth while its downregulation inhibits multiple myeloma survival²⁸³.

Currently, there are two classes of anti-BCMA therapeutics: antibody-based therapies and chimeric antigen T cell therapies. Antibody-based therapeutics includes monoclonal antibodies specific for BCMA, bi-specific T cell engagers (BiTEs) where one arm of the molecule engages the cancer cell (anti-BCMA) while the other engages the T

cell (anti-CD3), and antibody-drug conjugates (ADC) where the antibody specific for BCMA is covalently conjugated to cytotoxic payload that is delivered directly to the tumour cell²⁸³. There are several anti-BCMA CAR variants currently in clinical trials (reviewed by D'Agostino and Raje²⁸⁴). While the first anti-BCMA CAR T cell to enter human clinical trials was a retrovirally transduced 2nd generation CAR with a CD28 co-stimulatory domain²⁸³, the vast majority of current anti-BCMA CAR T cell variants are lentivirus transduced and contain the 4-1BB/CD137 co-stimulatory domain²⁸⁴. These therapies nonetheless continue to struggle with cytokine release syndrome and neurotoxicity discussed in Chapter One²⁸⁴.

Our results demonstrate when the intracellular tail is removed, surface expression of the TAC is profoundly diminished compared to the full-length receptor, and *in vitro* functionality in terms of cytokine production in response to antigen-expressing tumour cells is also diminished. Other measures of *in vitro* functionality (namely proliferation and tumour cytotoxicity) were not diminished, suggesting that this abrogation in response to antigen of the tailless TAC is limited to cytokine production. In our *in vivo* xenograft mouse model however, we found the tailless TAC to be as efficacious as the parent TAC in terms of tumour clearance.

In order to investigate the regions in the cytoplasmic tail of the TAC necessary for surface expression, a progressive tail deletion analysis was performed. Groups of amino acids from the C-terminus of the TAC were successively removed to create cytoplasmic tail truncations. These constructs were phenotypically and functionally analyzed *in vitro* in order to narrow down the critical residues responsible for surface expression. Results in this chapter demonstrate a potential role in TAC surface expression exhibited by the intracellular tail.

RESULTS

The TAC receptor lacking an intracellular cytoplasmic domain results in diminished surface expression and *in vitro* cytokine production on the humanized UCHT1 scaffold

Our previous work studying the TAC receptor used UCHT1, an anti-human CD3ε scFv derived from a murine hybridoma, to recruit the TCR-CD3 complex²⁶⁰. Since the use of mouse scFvs has been associated with anti-mouse antibodies that target engineered T cells, we incorporated a humanized UCHT1 (huUCHT1) scFv into the TAC^{285–287}. This new humanized UCHT1 scFv also contains a tyrosine to threonine mutation in the CDR2 loop of the heavy chain (Y177T)²⁸⁸, a mutation that was identified by our lab through *in vitro* evolution of the UCHT1 domain that sought to improve surface expression and the growth of the engineered T cells. All of the experiments in the chapter also employed the anti-BCMA scFv, C11D5.3 scFv²⁸⁹, which is also used in bluebird bio's BCMA-CAR, bb2121, which is in advanced human trials.

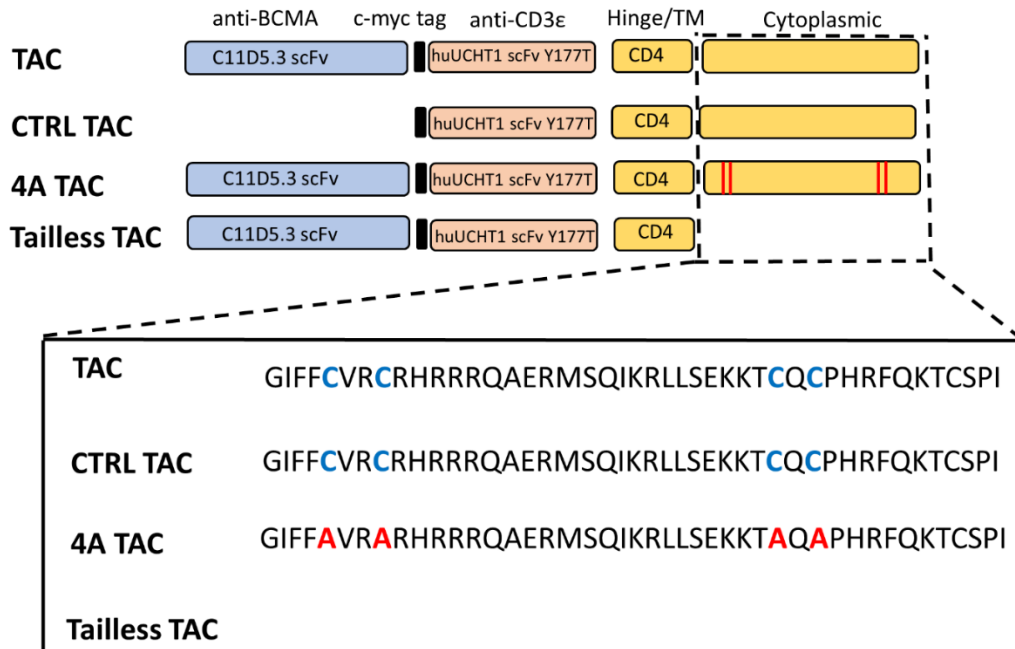


Figure 4.1. Schematic representation of anti-BCMA huUCHT1 Y177T scaffold TAC constructs
 TAC constructs recognize BCMA⁺ targets with the anti-BCMA C11D5.3 scFv antigen binding domain (blue) except for the control (CTRL) TAC which does not contain one. All TAC constructs engage the TCR with a humanized UCHT1 scFv (pink) with a Y177T mutation in the CDR2 loop of the heavy chain and contain a CD4 hinge and transmembrane domain (yellow). The cytoplasmic/intracellular domain for each construct is highlighted by their specific amino acid residues (black box), including the four cysteines in blue and their corresponding alanine mutations (red) in the 4A construct.

We created four constructs on the huUCHT1 Y177T scaffold: full length TAC, a control TAC (CTRL) without an antigen binding domain, the 4A TAC containing intracellular cysteine to alanine mutations that the literature suggests abrogates Lck interaction and membrane compartmentalization and a tailless TAC lacking the entire intracellular domain (**Fig. 4.1**). When expressed in primary T cells, we observed that the tailless TAC had remarkably lower surface expression compared to the full-length TAC (**Fig. 4.2**). The 4A TAC also displayed lower surface expression than the full-length, but not as profound as the tailless TAC.

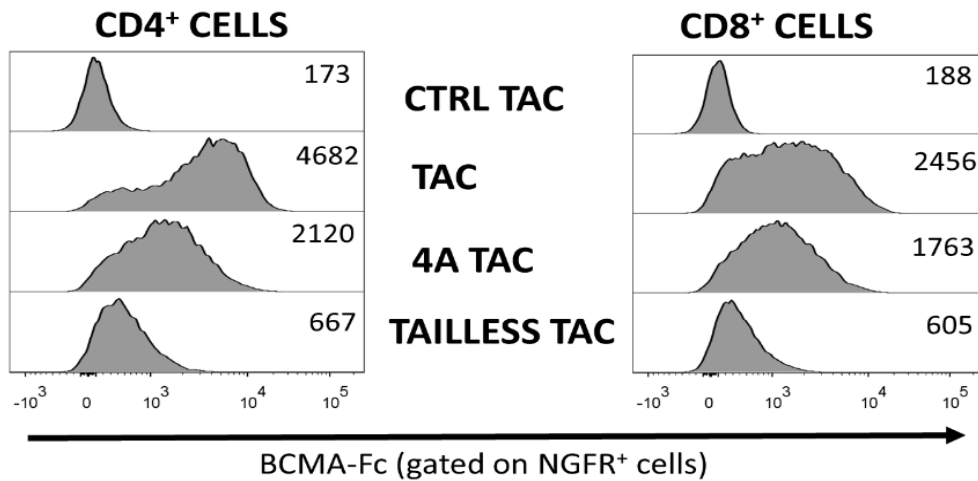


Figure 4.2. Diminished surface expression of the tailless TAC

Diminished surface expression of the tailless TAC in primary T cells and the cellular localization/trafficking of the receptors are shown. Primary T cells were engineered with constructs from Fig. 4.1 and surface expression with associated mean fluorescence intensity (MFI).

The decrease in surface expression of the tailless TAC was investigated by using immunofluorescence (IF) microscopy to determine the trafficking state of both the full-length and parent TAC in resting Jurkat T cells (**Fig. 4.3A**) by localizing the receptor with six separate organelle markers (**Table 5.0**). These experiments revealed that the Tailless TAC had increased accumulation in the endoplasmic reticulum based on Pearson correlation (**Fig. 4.3B**)

Protein	Organelle	Rationale for co-localization
Calnexin	Endoplasmic reticulum ²⁹⁰	Retention in organelle due to misfolding of newly translated protein (i.e. lack of adequate post translational modifications)
CD45	Membrane surface ²⁹¹	Expression on cell surface
Rab5	Early endosome ²⁹²	Internalization from the plasma membrane. Protein can be recycled back to membrane or targeted for degradation
Rab7a	Late endosome ²⁹²	Targeted for degradation by fusion with lysosomes
GM130	Golgi apparatus ²⁹³	Lack of vesicle formation or post translational modifications
Ubiquitin	Proteasome ²⁹⁴	Targeted for degradation, possibly due to aggregation or misfolding

Table 5.0 – Organelle markers for IF trafficking of the tailless TAC

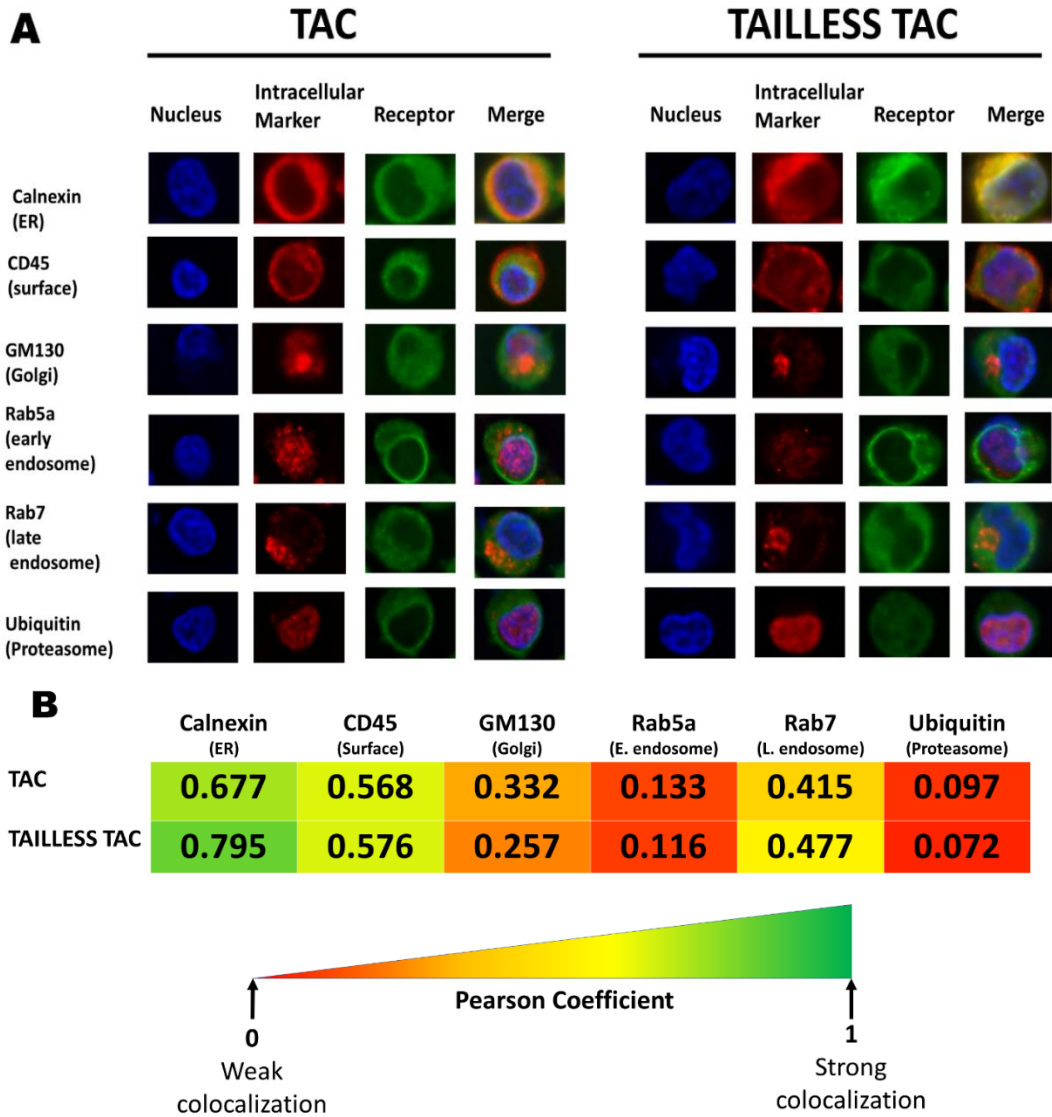


Figure 4.3. Cellular trafficking of the TAC receptor

(A) Jurkats were transduced to express the full-length or tailless TAC, fixed, stained and imaged at 40X oil immersion using IF microscopy. Single-cell images of each stained intracellular marker (red, organelle indicated on the left) and associated nucleus (blue) and receptor (green) staining. Merged images are shown to visualize colocalization. (B) Average Pearson Coefficient²⁹⁵ indicating weak (0 – red) to strong (1 – green) colocalization

When stimulated with BCMA⁺ KMS-11 tumour cells, the tailless and 4A TAC produced less IFN γ and TNF α in both CD4⁺ (Fig. 4.4A) and CD8⁺ (Fig. 4.4B) cells compared to the full-length TAC.

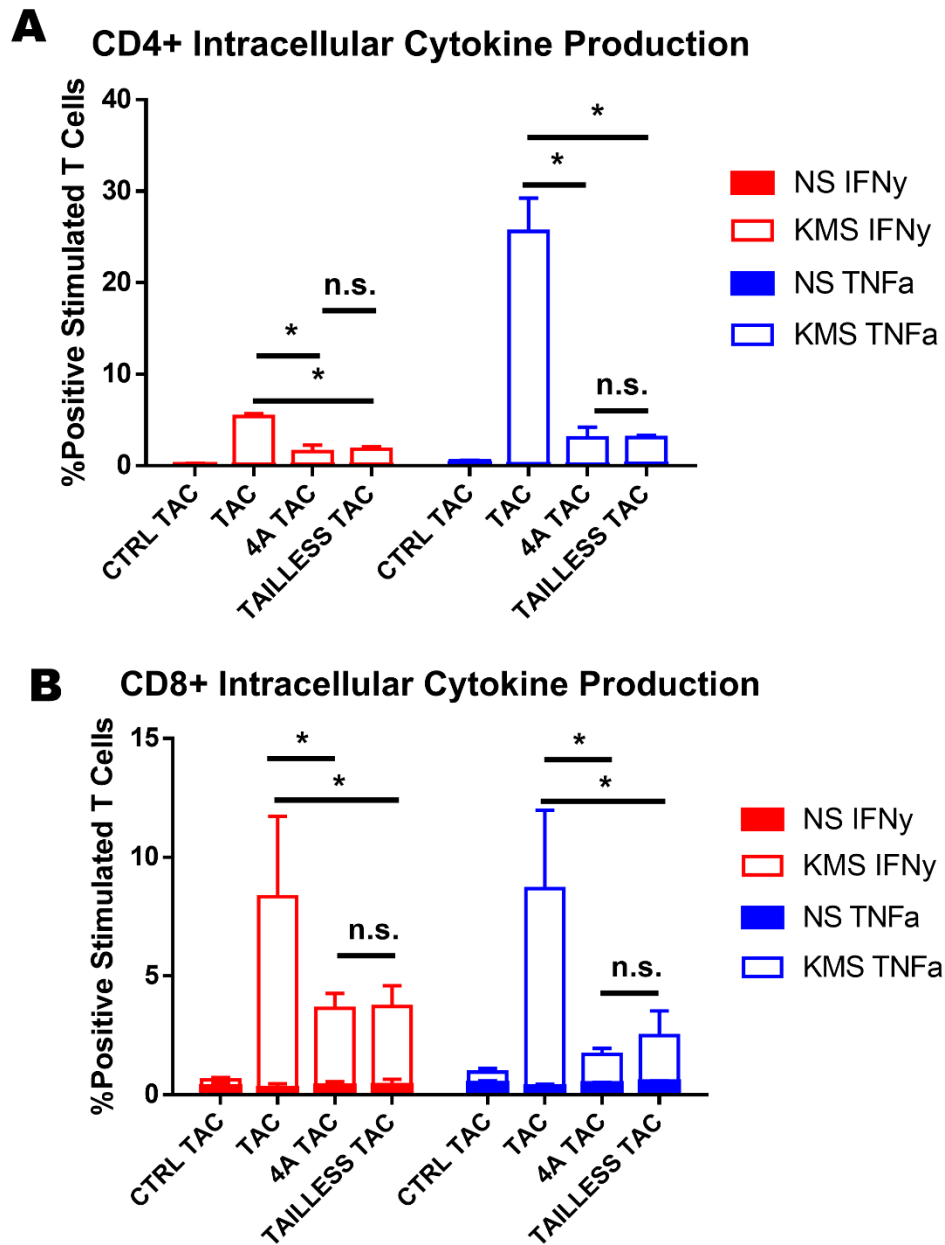
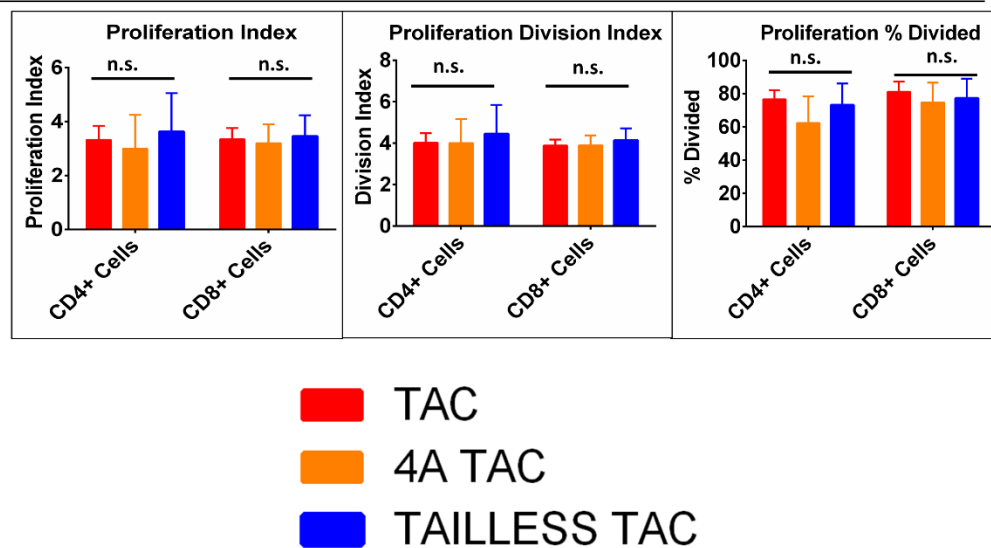


Figure 4.4. Abrogated *in vitro* cytokine production of the tailless TAC

Engineered T cells were co-cultured with KMS-11 cells and IFN γ (red) and TNF α production was measured. (A) Cytokine production for CD4⁺ cells. (B) Cytokine production for CD8⁺ cells. Cells were gated on engineered (NGFR⁺) populations and error bars represent standard deviation of three independent experiments. * = significant ($p < 0.05$), n.s. = nonsignificant ($p < 0.05$) for KMS stimulations.

These experiments were repeated with cell products from three donors that were purified using magnetic selection of NGFR-positive cells. While we continued to observe diminished surface expression and cytokine production, we found no differences in proliferation (**Fig. 4.5A**) or cytotoxicity (**Fig. 4.5B**), indicating that the lack of *in vitro* functionality of the tailless TAC was limited to cytokine production.

A T CELL PROLIFERATION



B TUMOUR CYTOTOXICITY

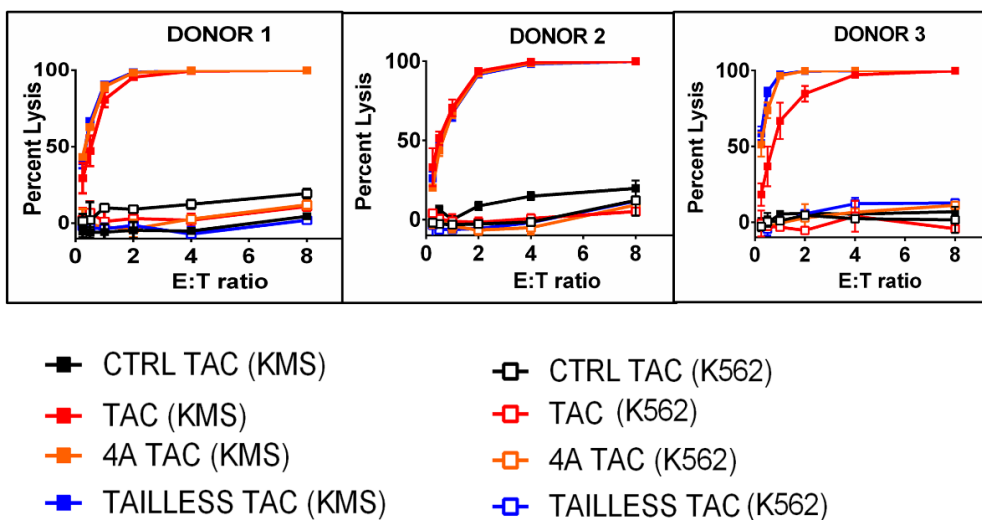


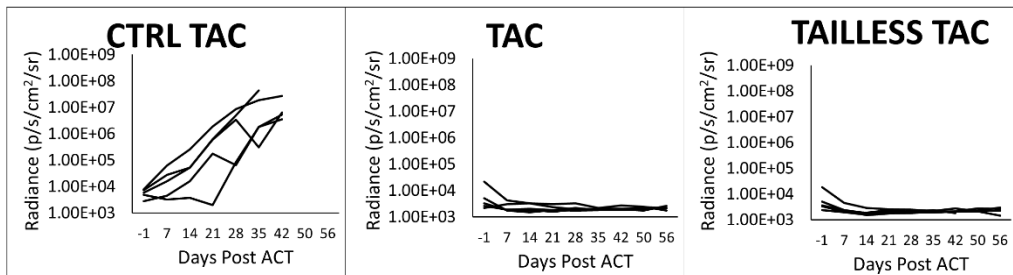
Figure 4.5. *In vitro* proliferation and cytotoxicity of the tailless TAC is not abrogated

TAC constructs were assayed for additional *in vitro* functionality assays. (A) Proliferation of engineered T cells after KMS-11 stimulation is shown as proliferation index, division index and percent divided. Error bars represent standard deviation of three independent experiments with three separate donors. (B) Tumour cytotoxicity was measured after co-incubation of engineered T cells with BCMA⁺ KMS-11 (filled squares) or BCMA⁻ K562 (open squares) across three separate donors. Error bars represent standard deviation. n.s. = nonsignificant ($p > 0.05$) for all means.

The tailless TAC displays robust *in vivo* efficacy in a xenograft mouse model

We were interested in determining if the *in vitro* loss of functionality manifested *in vivo*. To test this, we employed the KMS-11 xenograft human multiple myeloma mouse model. Tumour-bearing mice were treated with either a low (1.5×10^6) or high (4×10^6) dose of NGFR⁺ T cells. Following the high dose treatment (Fig. 4.6A), tumours grew progressively in all mice that received CTRL TAC-T cells and all mice reached end point by 40 days. Tumours regressed in all mice treated with TAC-T cells and tailless TAC-T cells leading to the complete absence of tumour for the duration of the experiment (>50 days). Following low dose treatment (Fig. 4.6B), tumours grew progressively in all mice treated with CTRL TAC-T cells, with most mice reaching end point after 28 days. Tumours were initially controlled in 4/5 mice treated with TAC-T cells, but 3/5 mice ultimately relapsed with tumour growth following TAC-T cell treatment. Surprisingly, all mice treated with the Tailless TAC-T cells were completely cured of their tumours with no relapses observed over the course of the experiment. Therefore, despite an abrogation of surface expression and *in vitro* cytokine production, the tailless TAC maintain *in vivo* functionality and even display increased efficacy over the full length TAC (no tumour growth in any mouse).

A HIGH EFFECTOR DOSE (4×10^6 T CELLS)



B LOW EFFECTOR DOSE (1.5×10^6 T CELLS)

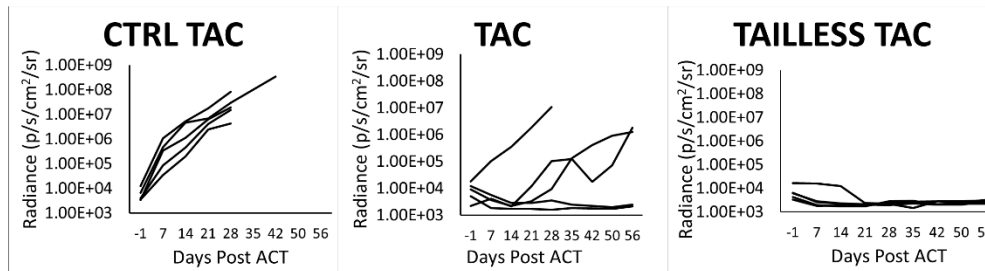


Figure 4.6. The tailless TAC displays *in vivo* efficacy

T cells were engineered with the CTRL, full length or tailless TAC and intravenously injected into immunocompromised NRG mice 12 days after the mice were injected with BCMA⁺ KMS-11 tumour cells and tumour burden was monitored every week. Mice were treated with either a high dose (A) or a low dose (B) of NGFR⁺ T cells, where the number of effector cells injected corresponded to the number of engineered cells as determined by phenotypic analysis.

The experiment was repeated using the same source of T cells, but the mice were challenged with a higher initial tumour burden. In this case, only the high dose (Fig. 4.7A) of T cells displayed efficacy as mice treated with low dose (Fig. 4.7B) of either the full length TAC or tailless TAC eventually reached endpoint by 60 days post ACT. T cells engineered with the Tailless TAC again displayed greater therapeutic benefit than the T cells engineered with the CTRL TAC.

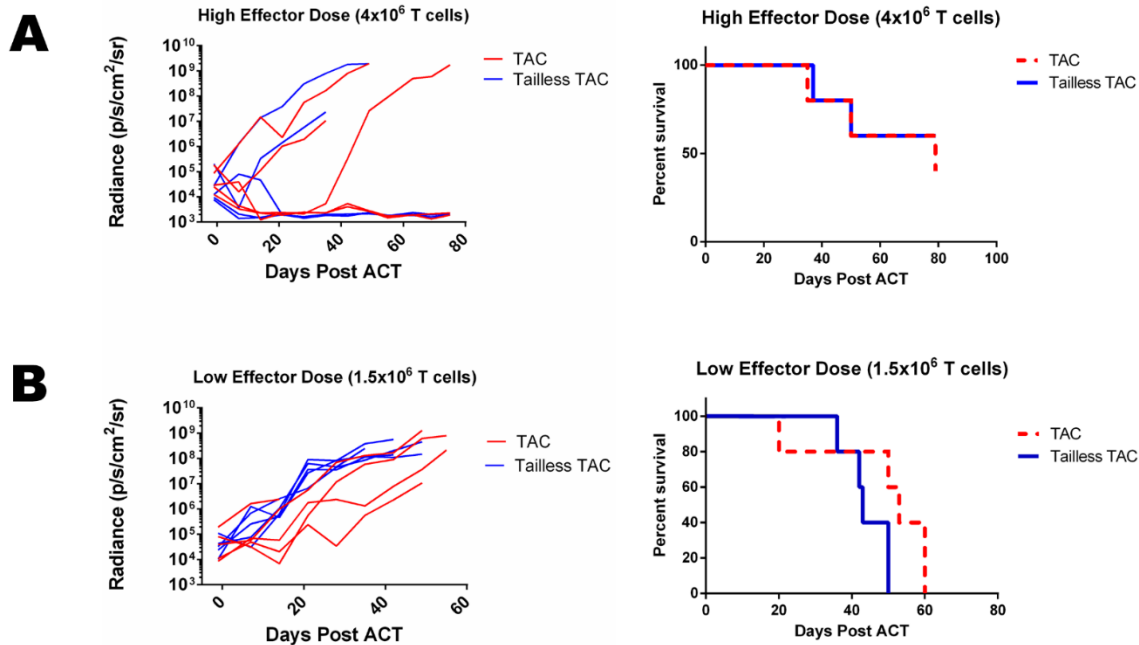


Figure 4.7. The tailless TAC displays *in vivo* efficacy given a higher initial tumour burden

T cells were engineered with the CTRL, full length or tailless TAC and intravenously injected into immunocompromised NRG mice 12 days after the mice were injected with BCMA⁺ KMS-11 tumour cells and tumour burden was monitored every week. Mice were treated with either a high dose (A) or a low dose (B) of NGFR⁺ T cells, where the number of effector cells injected corresponded to the number of engineered cells as determined by phenotypic analysis. Tumour growth curves of individual mice (n=5 per group) are shown on the left and corresponding Kaplan Meier survival curves are shown on the right.

TAC constructs containing truncated intracellular tails exhibit higher surface expression and *in vitro* functionality than the tailless TAC

The cytoplasmic tail consists of 44 amino acids with at least four functional motifs previously described in the literature^{62,63,67,296}. Given the profound loss of TAC on the surface of the engineered T cells when the cytoplasmic domain was removed from the TAC (Fig. 4.2), we sought to determine which elements of the cytoplasmic domain were necessary for surface expression. To this end, we generated 2 TAC mutants with different deletions of the cytoplasmic domain, TAC $\Delta_{516-525}$ and TAC $\Delta_{488-525}$ (Fig. 4.8) and characterized expression in primary T cells. The TAC $\Delta_{516-525}$ mutant lacks the last 10 amino acids from the C-terminus and retains the known functional motifs. The TAC $\Delta_{488-525}$ mutant lacks the last 38 amino acids, including motifs responsible for Lck binding (yellow), membrane clustering during activation (green) and two potential O-linked glycosylation sites (underlined, predicted *in silico*), the latter of which is known to directly affect the surface expression of CD4^{297,298}; this variant retains the two cysteine residues proximal to the transmembrane domain that are necessary for palmitoylation.

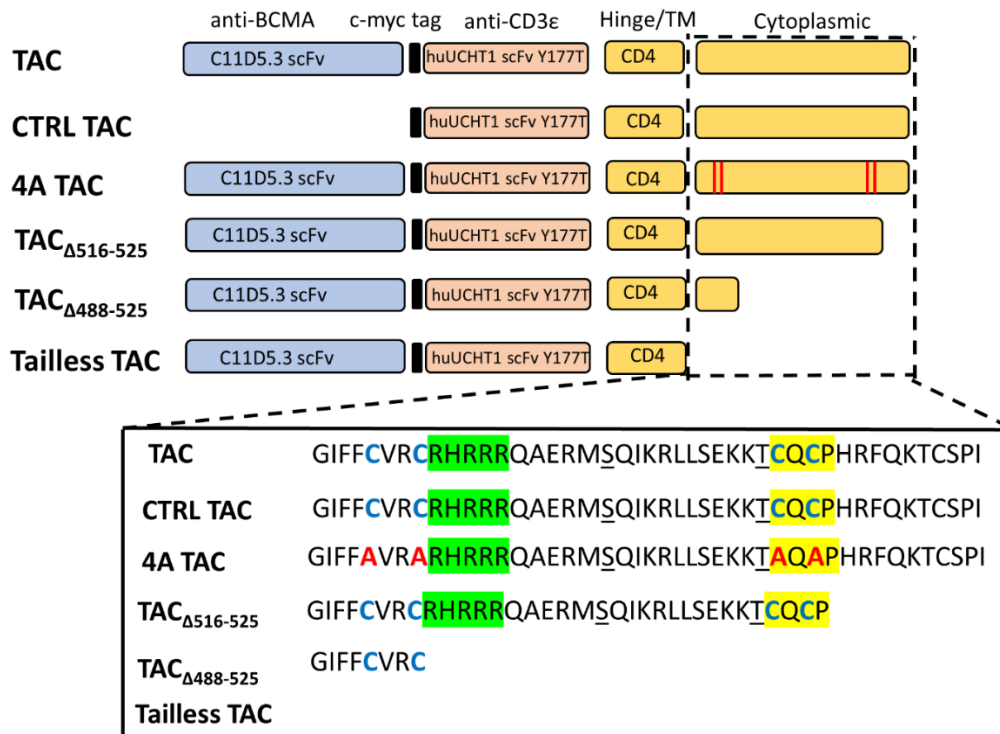
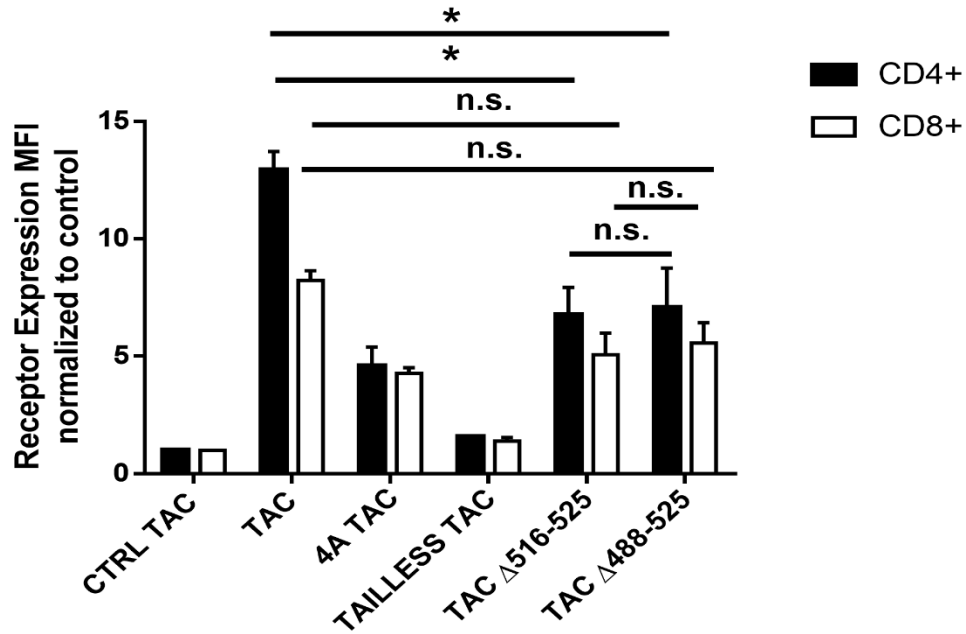


Figure 4.8. Schematic representation of TAC intracellular tail truncation constructs

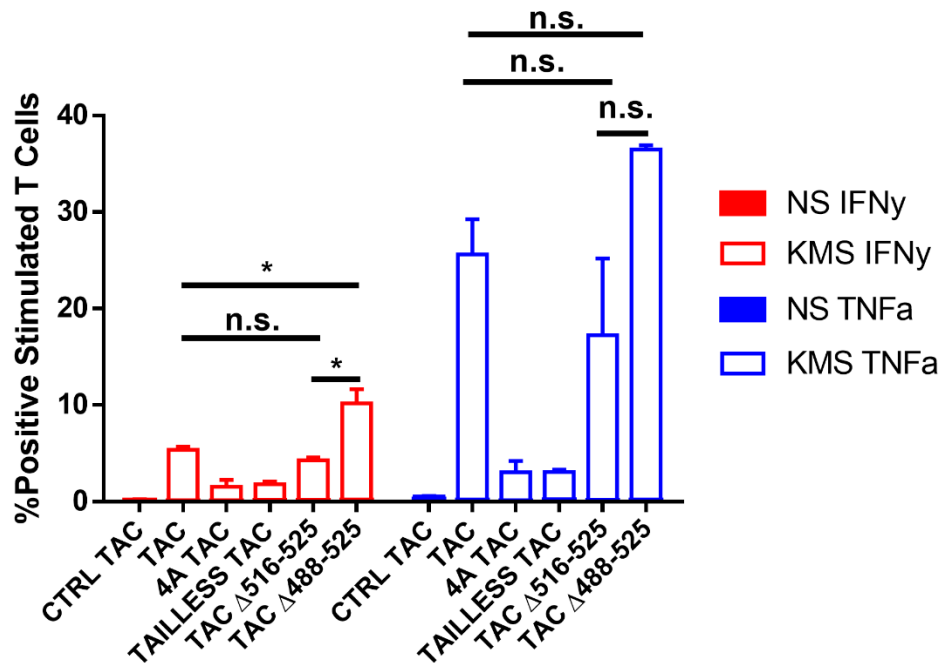
Schematic representation of the TAC tail mutants highlighting the cytoplasmic domains (see text for details).

Together with the previously described TAC constructs, these receptors were expressed in primary T cells and analyzed for surface expression and functionality. Both the TAC truncation constructs exhibited higher surface expression than the tailless TAC but lower expression than the full-length TAC suggesting that the features of the domains in the truncations were required for maximal surface expression (**Fig. 4.9A**). Given the similarity in the expression of TAC_{Δ516-525} and TAC_{Δ488-525}, we reasoned that the domain required for maximal expression is located between residues 516 – 525; nevertheless, the impact of this deletion on surface expression was not as profound as full deletion of the cytoplasmic tail suggesting that the remaining sequence “GIFFCVRC” is central to the surface expression of the TAC. The 4A TAC also displayed diminished surface expression yet retained this region suggesting that maximal surface expression of the TAC is dependent upon the cysteine residues that were mutated in this receptor.

A Receptor Surface Expression



B CD4+ Intracellular Cytokine Production



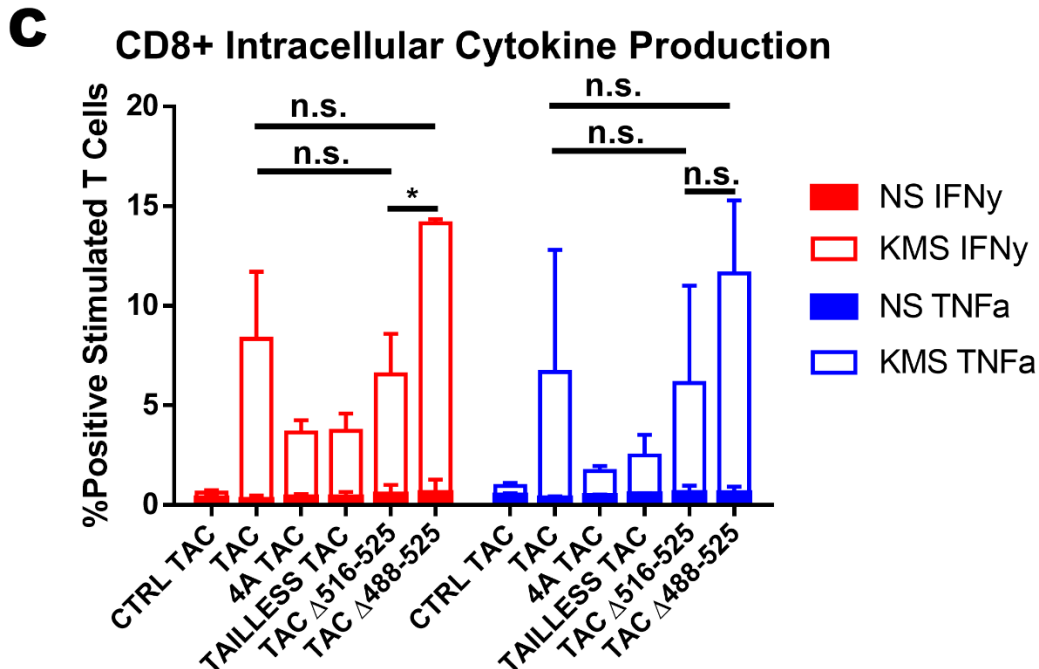


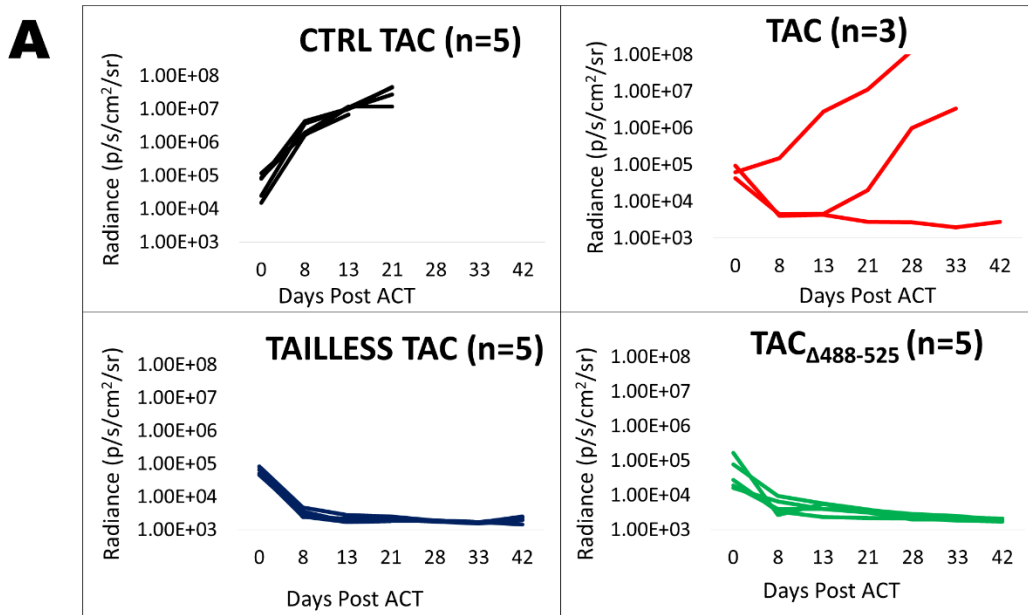
Figure 4.9. Intracellular tail truncation constructs exhibit higher surface expression and *in vitro* functionality than the tailless TAC

Primary T cells were engineered to express the constructs in Fig. 4.8. Surface expression of the receptor was measured by normalizing mean fluorescence intensity to the control TAC (A). *In vitro* functionality in terms of IFN γ and TNF α production in response to tumour stimulation of the receptors was measured for CD4 $^+$ cells (B) and CD8 $^+$ cells (C). Results shown are gated on NGFR $^+$ cells. Error bars represent standard deviation from three independent experiments. n.s. = nonsignificant ($p > 0.05$), * = significant ($p < 0.05$)

In vitro functionality of the deletion mutants was assessed by stimulating the engineered T cells with KMS-11 tumour cells or media (no stim, NS) and measuring IFN γ and TNF α production. Both the TAC Δ 516-525 and TAC Δ 488-525 truncations constructs produced appreciably more cytokines than the tailless TAC in CD4 $^+$ (Fig. 4.9B) and CD8 $^+$ (Fig. 4.9C) T cells. T cells engineered with TAC Δ 516-525 produced cytokine levels comparable to the full-length TAC indicating that the 516-525 region may be required for maximal surface expression, but it is not required for cytokine production. Interestingly, T cells engineered with TAC Δ 488-525 displayed higher cytokine production than T cells engineered with full-length TAC indicating that something within the deleted region opposes TAC function. As described previously, the 4A TAC had a functional profile comparable to the Tailless TAC despite having the same number of amino acid residues as the full-length TAC. Results here suggest that the biochemical features of the 4A TAC, instead of the residues omitted by the truncation mutations, may contribute to the functional profile of the Tailless TAC.

Given the heightened functionality of the TAC $_{\Delta 488-525}$ variant, we sought to determine whether T cells engineered with this variant would have improved therapeutic efficacy in the KMS-11 model. We included the Tailless TAC variant in this experiment because we had previously noted this variant provided greater therapeutic efficacy. T cells were engineered with full-length TAC, CTRL TAC, TAC $_{\Delta 488-525}$ or the tailless TAC and NGFR purified to enrich for engineered T cells. Mice bearing KMS-11 tumours were subsequently treated with varying doses of the 3 products. Interestingly, tailless TAC and TAC $_{\Delta 488-525}$ -engineered T cells displayed comparable *in vivo* tumour clearance, indicating that the improved efficacy of the tailless TAC is not related to either the diminished surface expression or reduced cytokine production. At a high effector cell dose (**Fig. 4.10A**), both the tailless TAC and TAC $_{\Delta 488-525}$ engineered T cells prevented complete tumour growth in all mice, while two of the mice in the full length TAC-engineered T cells reached end point due to tumour burden. With the lowest effector doses (**Fig. 4.10B**) no difference between any TAC construct was observed, while the tailless TAC group had the best survival outcome (4/5 mice) for the medium effector dose throughout the experiment duration.

HIGH EFFECTOR DOSE (3x10⁶ T CELLS)



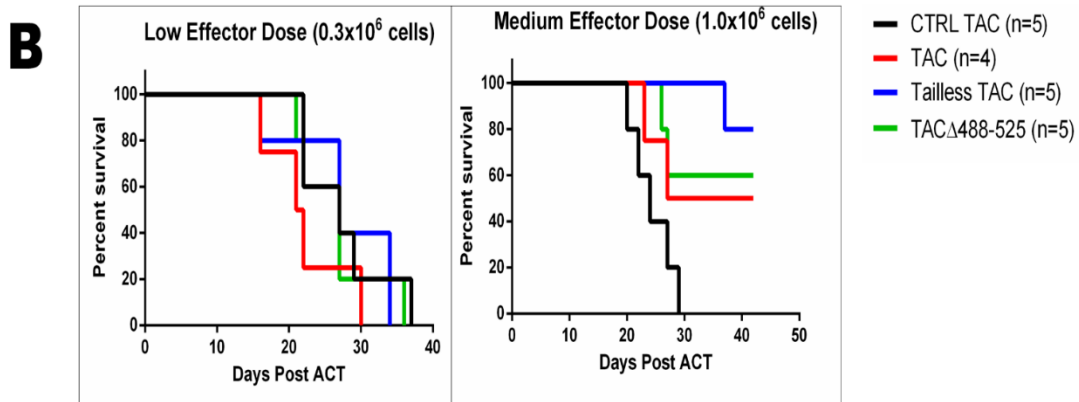


Figure 4.10. The TAC Δ 488-525 truncation displays similar *in vivo* efficacy to the tailless TAC
T cells engineered with either the CTRL (black), full length (red), tailless (blue) or Δ 488-525 truncation (green) TAC were NGFR enriched and injected into mice bearing KMS-11 tumours. (A) Tumour growth at the high effector dose over 42 days post ACT is shown. (B) Kaplan-Meier survival curves of tumour growth from low and medium effector dose over 42 days post ACT is shown.

When the surviving mice from the tailless TAC and TAC Δ 488-525 truncation groups were re-challenged with JEKO-1 cells (another BCMA⁺ tumour cell line), all mice treated with the tailless TAC displayed no tumour expansion or growth (Fig. 4.11). Mice treated with TAC Δ 488-525 truncation T cells displayed evidence of tumour relapse after 9 and 16 days post re-challenge (2 mice each), while all mice not treated with any T cells (NT) displayed immediate tumour growth.

JEKO-1 RE-CHALLENGE

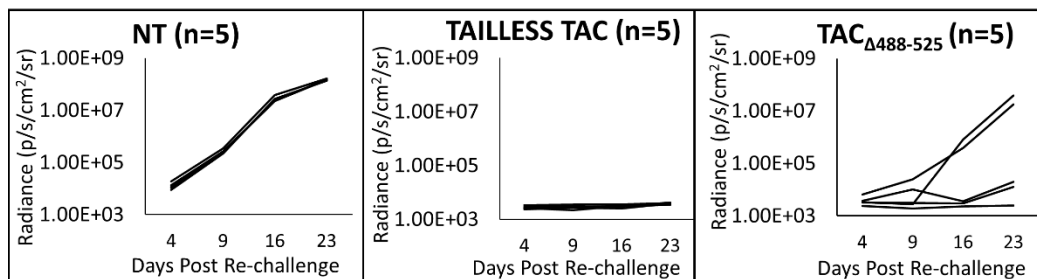


Figure 4.11. The tailless TAC outperforms the TAC Δ 488-525 truncation *in vivo* when mice are re-challenged with BCMA⁺ JEKO-1 tumour cells

Mice surviving the KMS-11 challenge from the tailless or Δ 488-525 truncation TAC groups were re-challenged with BCMA⁺ JEKO-1 cells, and tumour burden was monitored over time. Mice not treated with any T cells (NT) are used as negative controls.

Progressively removing the C-terminal amino acids from the TAC cytoplasmic tail revealed the TAC Δ 516-525 and TAC Δ 488-525 truncation constructs did not share similar

attributes with the tailless TAC. These truncation constructs did display similar *in vitro* cytokine production (Fig. 4.12A) to the full-length TAC. The 4A and tailless TAC constructs phenocopied in terms of *in vitro* cytokine production; these results indicate that the cysteine residues that were mutated in the 4A TAC are absolutely required for full cytokine production. Since TAC $_{\Delta 488-525}$ truncation mutant displayed equally, if not greater, cytokine production relative to full-length TAC, we reasoned that the two cysteines closest to the inner leaflet of the cell membrane were required for full functionality as these residues were present in all truncation mutant and absent from the 4A TAC (cysteine to alanine mutations) and Tailless TAC (omission) (Fig. 4.12B). These cysteines have previously been shown in the literature to be important post-translation palmitoylation sites necessary for full co-receptor functionality (i.e. TCR-specific activation of T cells)^{63,68,298}.

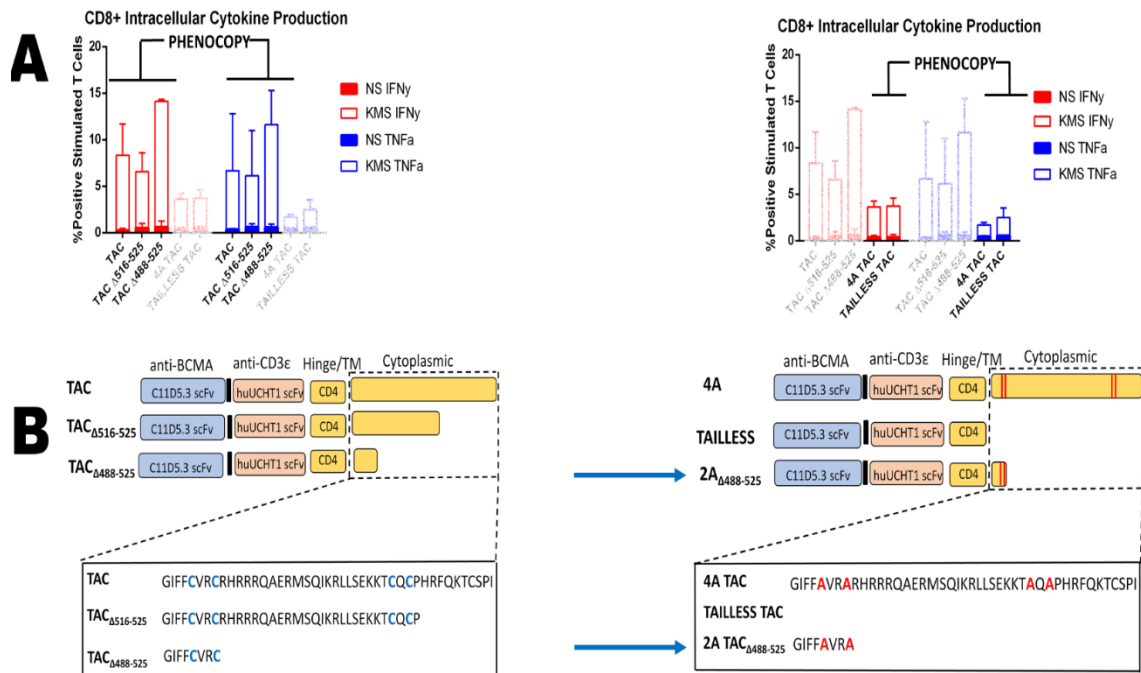


Figure 4.12. Characterization of the role of the palmitoylation cysteines on surface expression and functionality

Functional profiles of the anti-KMS TAC constructs. (A) The full-length TAC and truncations functionally phenocopy, while the 4A and tailless TAC functionally phenocopy. (B) Amino acid analysis of the intracellular tails of these constructs reveal that the full-length TAC and truncation constructs all share the first two palmitoylation cysteines closest to the cell membrane. Conversely, the 4A and tailless TAC constructs have these cysteines either mutated (4A) or omitted (tailless). The “2A TAC $_{\Delta 488-525}$ ” (blue arrow) was designed to phenocopy the 4A and tailless constructs by mutating the 2 cysteines, but still containing $\Delta 488-525$ truncation

We therefore hypothesized that these two palmitoylation cysteines were the residues responsible for the functional impairments of 4A TAC and Tailless TAC. To test this hypothesis, we created a 2A TAC $_{\Delta 488-525}$ construct, similar to TAC $_{\Delta 488-525}$ with the exception that the two cysteines in the GIFFCVRC retained in the cytoplasmic portion of TAC $_{\Delta 488-525}$ were mutated to alanine (**Fig. 4.12B, blue arrow**). If our hypothesis is correct, this construct would phenocopy the 4A and tailless TAC receptors and provide evidence that the membrane proximal cysteines are critical for receptor surface expression and functionality.

Contrary to our hypothesis surface expression of the 2A $_{\Delta 488-525}$ truncation was similar to the full-length TAC (**Fig. 4.13A**). Cytokine production across three separate T cell donors in response to stimulation from BCMA⁺ tumour cells (KMS) or media alone (no stimulation) similarly showed that the 2A truncation phenocopies the full length TAC (**Fig. 4.13B**). Results here demonstrate that despite lacking the two palmitoylation cysteines, the 2A TAC $_{\Delta 488-525}$ phenocopies the full-length and not the tailless TAC which indicates that some other feature of the GIFFCVRC cytoplasmic region retained in TAC $_{\Delta 488-525}$ was responsible for the heightened cytokine production relative to the original TAC.

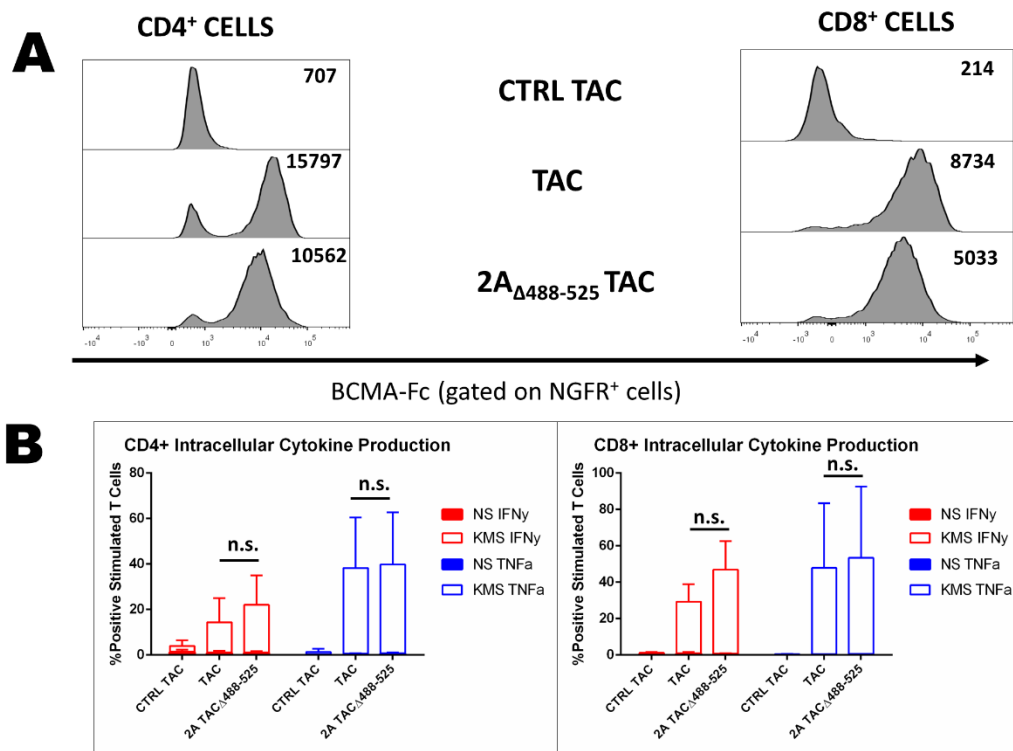


Figure 4.13. The 2A truncation TAC phenocopies the surface expression and *in vitro* functionality (cytokine production) of the full-length TAC

Primary T cells were engineered to express the CTRL, full length and 2A truncation TAC. **(A)** Surface expression and associated mean fluorescence intensity (MFI) of each receptor is shown for CD4⁺ and CD8⁺ T cells gated on engineered (NGFR⁺) cells **(B)** *In vitro* cytokine production in response to KMS-11 (KMS) or no stimulation (NS) is shown for CD4⁺ and CD8⁺ cells. Error bars represent standard deviation of three independent experiments. n.s. = nonsignificant ($p > 0.05$)

DISCUSSION

In this chapter we continued our work to understand the importance of the CD4 intracellular cytoplasmic tail of the TAC anchor. Our results demonstrate that removal of the cytoplasmic tail (tailless TAC) greatly impairs surface expression of the receptor and cytokine production by the engineered T cell. Curiously, the absence of the CD4 tail does not impair antigen-driven cytotoxicity or proliferation. Surprisingly, the removal of the CD4 tail enhanced the therapeutic potency of the engineered T cells in a xenograft model of multiple myeloma. Analysis of the CD4 tail truncation constructs identified the C-terminal amino acids (HRFQKTCSPI) and membrane proximal amino acids (GIFFCVRC) as being important for maximal surface expression and cytokine production. Mutation of the cysteines known for Lck binding (C512 and C514) and palmitoylation (C484 and C487) in the full-length TAC resulted in a functional phenotype comparable to the full deletion of the cytoplasmic tail. When the data from all of these variants were combined, we rationalized that the cysteines in GIFFCVRC were key to surface expression and cytokine function. To test this hypothesis, we generated a truncation mutant that lacks all cytoplasmic components and harbors alanines to replace the cysteines. Our hypothesis proved to be incorrect and this variant displayed a phenotype comparable to full-length TAC indicating that some other feature of the GIFFCVRC was responsible for surface expression and cytokine production.

The TAC platform used in this chapter employed a humanized UCHT1 (huUCHT1) scaffold. Due to the possibility of human anti-mouse antibodies targeting the mouse scFv expressed by engineered T cells, the huUCHT1 allows for a more clinically applicable TAC receptor^{285,286}. Our laboratory has published data showing TAC functionality and surface expression with different scaffolds (all mouse scFvs) in addition to both UCHT1 CD3 ϵ binders: OKT3, L20 and F6A^{258,261}. The huUCHT1 TAC had robust cytokine production in response to antigen stimulation and had the highest surface expression, while other TAC scaffolds such as F6A and L20 had poor surface expression and cytokine production²⁵⁸. The huUCHT1 scFv was “humanized” from the UCHT1 scFv primarily by several point mutations in the framework regions, but also includes a single point mutation in the second complementary determining region loop of both the heavy and light chains^{299–301}. While the anti-BCMA C11D5.3 scFv used as the antigen recognition domain is of mouse origin, the antigen recognition domain (unlike the CD3 engager) allows for exchange flexibility as our group have previously shown²⁵⁸.

Interestingly we note that the 4A TAC here phenocopies the tailless TAC in terms of low surface expression and *in vitro* functionality, unlike the previous chapter where this construct phenocopied the full-length TAC. This difference might be due to the change in scaffold and antigen recognition platform. In the next chapter, we address this possibility by evaluating these constructs with a new antigen recognition domain on the huUCHT1 scaffold to determine if this observation is only unique to this specific anti-BCMA C11D5.3 platform.

We were interested in determining whether loss of functionality *in vitro* for the tailless TAC manifested in an *in vivo* mouse model, as *in vitro* observations do not always manifest as meaningful *in vivo* effects. A study investigating the inclusion and exclusion of an extracellular hinge domain in a second generation CAR targeting five different tumour associated antigens showed that the inclusion of the hinge in all CARs lead to increased cell expansion and *in vitro* migration to the target in a trans well Matrigel chamber. When assessed *in vivo*, there was no difference in tumour clearance capacity for CARs with or without the hinge for four of these CARs³⁰², which supports the notion that results from *in vitro* parameters do not always match *in vivo* outcomes. Despite observing clear improvements in cell expansion and migration *in vitro* with the addition of a hinge in five different CAR targets, the study found no difference in the *in vivo* efficacy of these CARs in four of the five designs. Another study demonstrated that increasing the hinge domain length increased *in vitro* functionality in terms of cytokine production, but inversely decreased *in vivo* anti-tumour clearance³⁰³. Similar to those studies, we observed no loss in *in vivo* functionality of the tailless TAC receptor despite lower surface expression on primary T cells and decreased *in vitro* cytokine production. Not all measures of *in vitro* functionality were impaired however, as we did not find any difference in proliferation or cytotoxicity of the tailless TAC compared to the full length TAC, suggesting that *in vitro* functional impairment is limited to cytokine production.

Although the TAC receptor was originally designed to incorporate the features of the cytoplasmic tail, the functionality of the tailless TAC receptor *in vivo* is clinically intriguing as the possibility of a robust therapeutic with lower cytokine production may lead to a better safety profile for the tailless TAC. As discussed in the Introduction to the previous chapter, T cells engineered with a CD19 CAR with a hinge and transmembrane domain from CD8 α showed comparable *in vivo* activity to T cells engineered with a CD19 CAR with a CD28 hinge and transmembrane domain²⁶⁹. The T cells engineered with the CAR bearing the CD8 α hinge showed lower levels of *in vitro* cytokine release and AICD compared to T cells engineered with the CAR bearing the CD28 hinge, prompting the investigators to use that construct in phase I clinical trials as they hypothesized that it would be less toxic to patients. The tailless TAC similarly displays low *in vitro* cytokine production yet retains *in vivo* efficacy. Due to its smaller size in the size-restricted lentivirus cassette, the tailless TAC construct also allows for the inclusion of additional signaling domains that would increase *in vivo* persistence of the T cell.

The mechanisms involved in CAR signaling is becoming an area of increased interest and discoveries made in the field can potentially relate to observations here. With regards to the co-stimulatory domains of 2nd generation CARs, the field has shown that 4-1BB CARs display more memory-like properties including β -oxidation metabolism, delayed *in vitro* killing kinetics and increased *in vivo* persistence. Conversely, CD28 CARs display effector-like properties including glycolysis metabolism, rapid killing *in vitro* killing kinetics and lower *in vivo* persistence^{198,202,239}. Mutagenesis of the Lck-binding domain of CD28 within the 2nd generation CAR construct by two separate groups have shown that abrogation of Lck binding decreased the antigen-dependent signaling state intensity (phosphorylation of CD3 ζ , SLP-76 and PLC- γ 1) associated with the effector phenotype and lead to an increased *in vivo* persistence phenotype associated with the memory phenotype^{304,305}. Similar to the results in this chapter, the tailless TAC displayed decreased *in vitro* cytokine production, but displayed equal or increased *in vivo* efficacy over the parent TAC. It is conceivable that the interaction of Lck within the receptor complex might be pushing the TAC T cell to an effector-like state (high cytokine production, lower *in vivo* persistence), while the omission of Lck in the tailless TAC complex might be favouring a memory-like state (lower cytokine production, higher *in vivo* persistence). Further work is required to validate this claim, not only in phenotyping the polarization state (effector or memory) of the T cell, but also confirming if either construct directly interacts with Lck.

Through a progressive cytoplasmic tail deletion strategy, we sought to identify the regions responsible for the tailless phenotype, thereby establishing the critical residues necessary for proper surface expression. The rationale for these deletions was based on our understanding of the cytoplasmic tail in the literature. The TAC $\Delta_{516-525}$ truncation omitted the ten amino acids at the C-terminal but includes the domains the literature deems necessary for signaling and compartmentalization. The TAC $\Delta_{488-525}$ truncation omitted the next 38 amino acids including Lck binding^{62,67} and arginine-rich²⁹⁸ domains, the latter of which is important for membrane compartmentalization. This truncation also omitted two potential O-linked glycosylation sites (**Fig. 4.8**, underlined and predicted *in silico*), which we hypothesized to contribute to full surface expression. Glycosylation is a significant post translational modification for the CD4 co-receptor, necessary for its transport and function. Treatment of CD4⁺ T cells with tunicamycin, an antibiotic that inhibits glycosylation causes a 76% decrease in surface expression²⁹⁷. Site-directed mutagenesis of N-linked glycosylation sites in the extracellular domain of CD4 leads to its misfolding and intracellular retention in the endoplasmic reticulum³⁰⁶. Finally, these 38 amino acids also contained the MSQIKRLLSEKKT domain, the binding site for the HIV-1 accessory protein Nef-1, which downregulates CD4 during infection^{307,308}.

None of the truncations could recapitulate the abrogation of surface expression seen in the tailless TAC, and it's possible that the residues responsible may reside in the eight remaining amino acids closest to the inner leaflet.

The functionality and surface expression of the 2A TAC $_{\Delta 488-525}$ was very intriguing when considered with the results from the other cytoplasmic tail constructs. When the entire 44 amino acid cytoplasmic tail is removed (tailless), we see a clear, reproducible phenotype of our TAC receptor. Of these 44 amino acids, five domains or individual residues have been best characterized in the literature (**Fig. 4.8**): the membrane proximal cysteines (blue, important for post translational palmitoylation)^{62,63,67}, arginine rich domain (green, important for membrane compartmentalization)⁶², O-linked glycosylation sites (underlined, important for post translational O-linked glycosylation)^{306,309} and C-terminal cysteines (yellow highlight, important for interaction with Lck)⁶². Of the three truncations (2A TAC $_{\Delta 488-525}$, TAC $_{\Delta 516-525}$ and TAC $_{\Delta 488-525}$), each contain some combination of the mutation or omission of each of those domains, yet neither can phenocopy the tailless TAC. In theory, all intracellular domains are disrupted in both the 2A truncation and tailless receptors, yet the 2A TAC $_{\Delta 488-525}$ expresses quite well and shows no functional defect. Perhaps even more puzzling is the 4A construct, which best phenocopies the tailless TAC despite lacking domains also absent in the 2A truncation. It seems that despite our deep understanding of the CD4 cytoplasmic tail, its contribution to the functionality of the TAC receptor may not be as pronounced as its contribution to the functionality of CD4 as an endogenous co-receptor.

Overall, our results show that omission of the cytoplasmic tail in the TAC receptor leads to abrogated surface expression, lower *in vitro* cytokine production, yet *in vivo* efficacy may be enhanced.

CHAPTER FIVE

FUNCTIONALITY OF THE TAILLESS TAC USING DIFFERENT ANTIGEN BINDING DOMAINS

INTRODUCTION

In the previous chapter, we observed that removal of the intracellular domain of the anti-BCMA TAC lead to diminished surface expression and *in vitro* cytokine production upon antigen stimulation, however *in vivo* efficacy was enhanced compared to the full-length TAC. This chapter continues the investigation of the phenotype and functionality of tailless TAC-engineered T cells across different antigen binding domains using the huUCHT1 Y177T scaffold to see if those results are generalizable against different cancer targets. Within the CAR field, observations on receptor efficacy and functionality made against one cancer target do not always recapitulate against other cancers, especially when differences between *in vitro* functionality and *in vivo* efficacies are compared. For instance, one study investigating the inclusion or exclusion of an extracellular hinge domain within second generation CARs against five cancer targets (mesothelin, CD19, Her2, prostate stem cell antigen, and Mucin1) found increased *in vivo* efficacy of the anti-mesothelin CAR when the hinge was included. However, the study found no difference in the *in vivo* efficacy of the other four CARs with or without a hinge, demonstrating that the increased *in vivo* functionality when the hinge was included was unique to the anti-mesothelin CAR³⁰². Another study investigating hinge lengths found that scFvs that bind membrane-proximal epitopes on cancer antigens require a flexible extracellular hinge domain within the CAR design in order to permit efficient engagement and maximal *in vitro* cytotoxicity and cytokine production, while scFvs that interact with the N-terminus of antigens further from the membrane display maximal *in vitro* cytotoxicity and cytokine production in the absence of a long hinge domain²³¹. This study reiterates the notion that chimeric receptors do not necessarily have a one-size-fits-all basis, and conclusions made about functionality with regards to hinge/spacer domains need to be validated against other cancers/antigens by using different antigen binding domains. In terms of the TAC, our observations of diminished surface expression and cytokine production yet increased *in vivo* efficacy was made against BCMA⁺ targets using the C11D5.3 scFv, and these observations remain to be investigated against other cancer targets.

We use two different antigen binding domains in this chapter: the anti-Her2 H10-2-G3 DARPin²⁶² previously described in **Chapter 3**, and the anti-CD19 FMC63 scFv. Our laboratory has previously demonstrated that the H10-2-G3 DARPin can be successfully used as a CAR antigen-binding domain against Her2⁺ breast cancer lines by producing cytokine in response to target cell stimulation and lysing tumours *in vitro*²¹⁹. CD19 is a critical type I transmembrane protein on the surface of mature B cells responsible for mediating and amplifying signal transduction during B cell activation¹⁶⁸. It is also an important target for B cell lymphoma cancers, and over 70% of CAR T cell products currently in clinical trials in the United States and China are engineered to target CD19³¹⁰. Several mechanistic *in vitro* and *in vivo* studies on CAR T cells, especially those investigating the hinge^{269,302} and co-stimulatory domains^{197,253}, use CARs specific for CD19,

therefore the CD19 serves as a well characterized tumour associated antigen model in the CAR field.

RESULTS

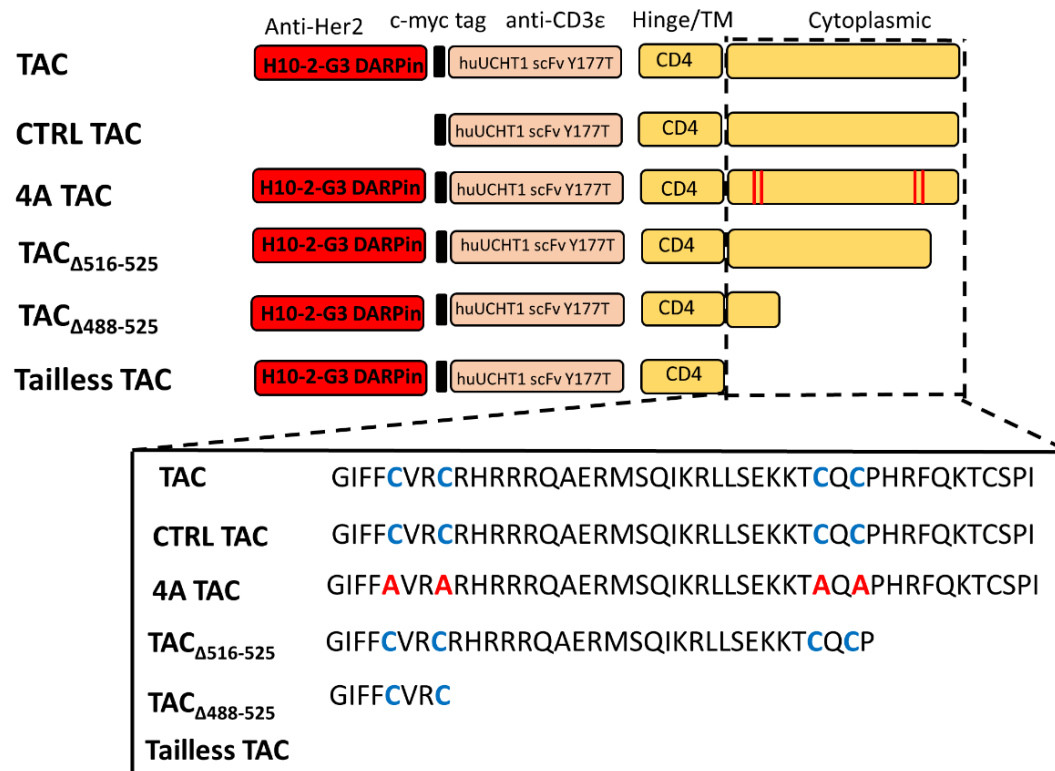


Figure 5.1. Schematic representation of Her-2 specific TAC intracellular tail truncation constructs
Schematic representation of the TAC tail mutants highlighting the cytoplasmic domains (see text for details).

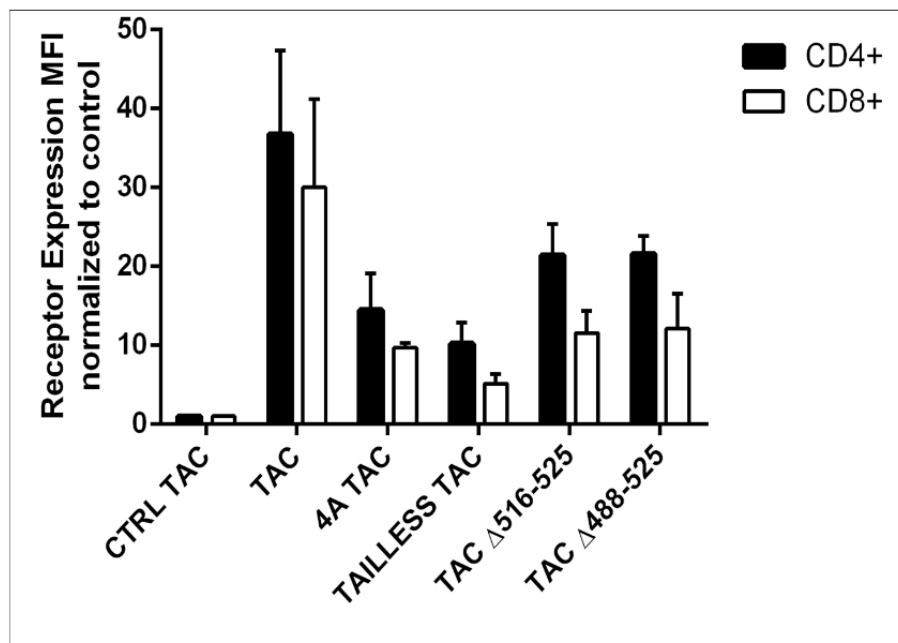
Surface expression of the anti-Her2 tailless TAC is diminished, but *in vitro* cytokine production is not affected compared to the full length TAC

Our previous results demonstrated that removing the intracellular domain (cytoplasmic tail) of the TAC receptor diminished surface expression of the receptor and decreased cytokine production in response to BCMA⁺ tumour stimulation of the engineered T cells. To determine if those functional properties were consistent for TAC engineered T cells against other tumour targets besides BCMA, we created anti-Her2 TAC constructs using the H10-2-G3 DARPIn (described in Chapter 3)^{219,262} antigen recognition domain (**Fig. 5.1**, shown in red). These constructs are on the humanized UCHT1 Y177T scaffold (also described in Chapter 4, shown in **Fig. 4.1**), and consist of the full

length TAC, a control (CTRL) TAC with no antigen binding domain, the 4A TAC with four cysteine to alanine mutations in the Lck binding and membrane partitioning sites^{63,298} of the intracellular tail (red bars), the TAC_{Δ516-525} and TAC_{Δ488-525} cytoplasmic tail truncations and the tailless TAC lacking the entire cytoplasmic tail.

A

Anti-Her2 T cells surface expression



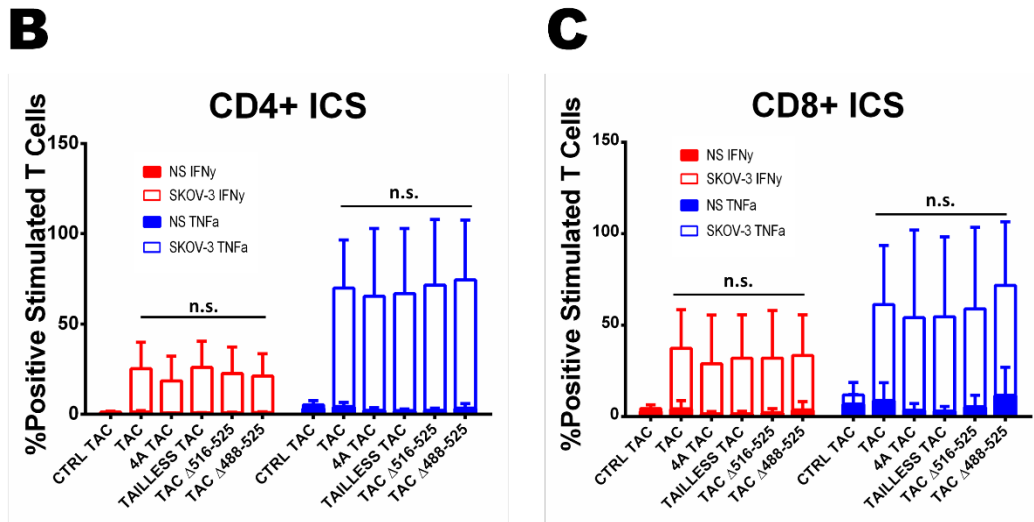
Anti-Her2 T cells *in vitro* cytokine production

Figure 5.2. *In vitro* cytokine production of the Her2-specific tailless TAC is not abrogated despite diminished surface expression

(A) T cells were engineered to express anti-Her2 (DARPin) TAC constructs and receptor surface expression is shown normalized to the CTRL TAC. (B, C) Intracellular IFN γ and TNF α production in response to SKOV-3 (HER2⁺) or no stimulation (NS). Error bars represent standard deviation from three separate experiments. n.s. = nonsignificant ($p > 0.05$)

These constructs were expressed in primary T cells by lentivirus transduction, and the 4A and tailless TAC displayed diminished surface expression compared to the full length TAC in both CD4⁺ and CD8⁺ T cells (Fig. 5.2A). The two truncation constructs displayed higher surface expression than the 4A and tailless TAC-engineered T cells, but less than the full length TAC. When the *in vitro* functionality of these engineered T cells was assessed by IFN γ and TNF α production in response to tumour (Her2⁺ SKOV-3) or no (NS) stimulation, no difference was observed in CD4⁺ cells (Fig 5.2B) or CD8⁺ (Fig. 5.2C). These results demonstrate that the surface expression of the anti-Her2 tailless TAC is diminished, but unlike the anti-BCMA tailless TAC, *in vitro* cytokine production is not affected.

The tailless TAC displays high *in vivo* efficacy against Her2⁺ OVCAR-3 tumours

The anti-BCMA tailless TAC demonstrated enhanced *in vivo* efficacy against established KMS-11 liquid tumours despite diminished *in vitro* cytokine production relative to the full-length TAC. We evaluated the *in vivo* efficacy of the anti-Her2 TAC constructs against OVCAR-3 human xenografts. At the dose of T cells used for this experiment, treatment with T cells engineered with the control receptor, full length, 4A

TAC or TAC $_{\Delta 488-525}$ truncation showed progressive tumour growth throughout the 45 day post adoptive cell transfer monitoring period (**Fig. 5.3**). Mice treated with the tailless TAC showed clear and sustained tumour regression throughout the monitoring period. Therefore, TAC-engineered T cells lacking a cytoplasmic tail domain exhibited increased *in vivo* efficacy against Her2⁺ OVCAR-3 solid tumours compared to TAC-engineered T cells expressing the full length receptor despite comparable *in vitro* properties.

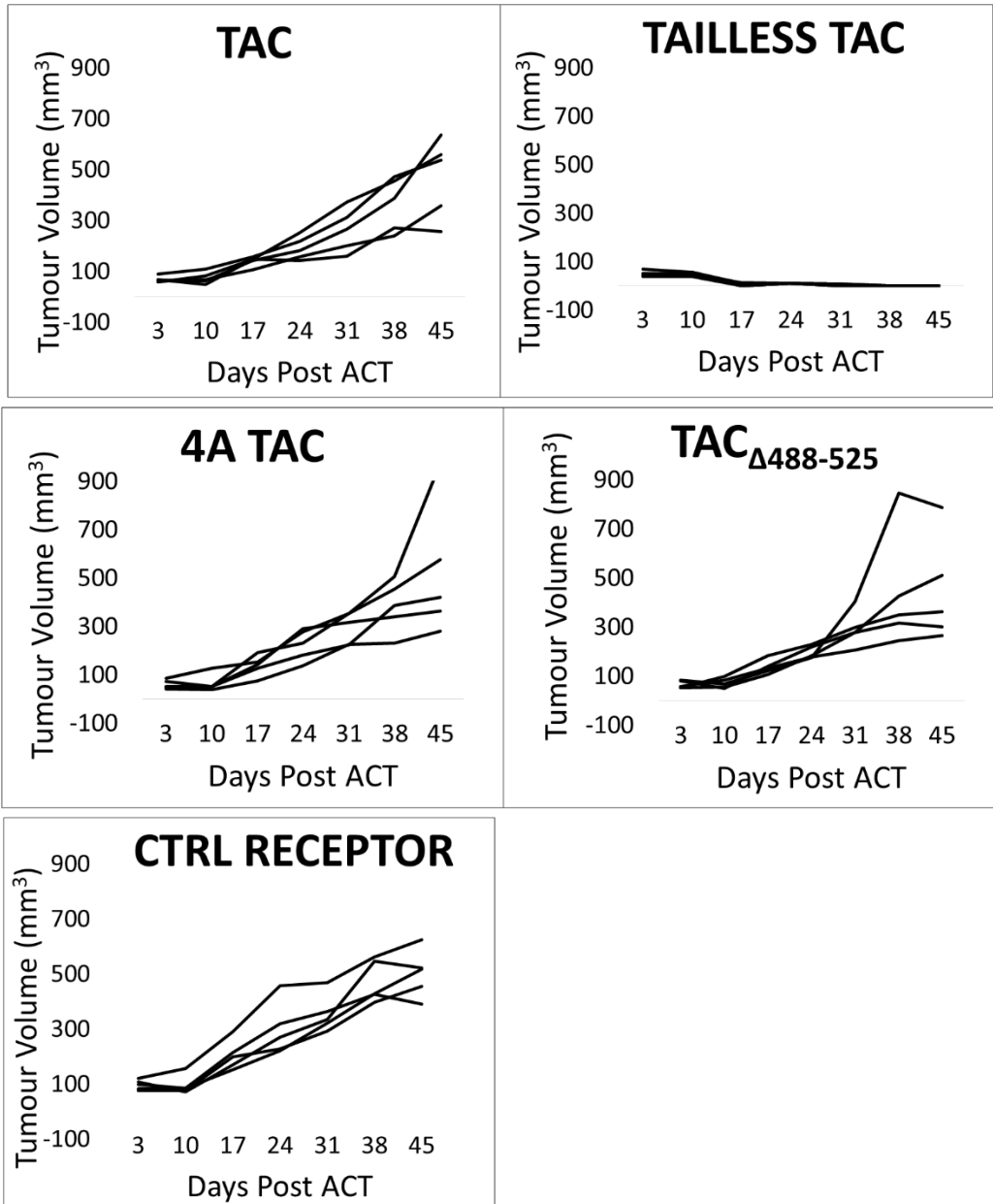


Figure 5.3. The tailless TAC displays increased *in vivo* efficacy compared to other TAC constructs against Her2⁺ OVCAR tumours

Immunocompromised mice were challenged with OVCAR-3 tumour cells and after tumour establishment, were then treated with either a low dose or high dose of TAC-engineered T cells (normalized for NGFR expression, n = 5 for all groups). Graphs show tumour growth measured every 6-7 days until 45 days post ACT.

***In vitro* cytokine production of the anti-CD19 tailless TAC is unchanged compared to the full length TAC despite diminished surface expression**

We sought to investigate the *in vitro* and *in vivo* characteristics of TAC-engineered T cells against the CD19 tumour associated antigen. We created three anti-CD19 TAC constructs using the well characterized FMC63 scFv³¹¹: control TAC lacking the antigen binding domain, the full length TAC and the tailless TAC lacking the intracellular cytoplasmic domain (Fig. 5.4).

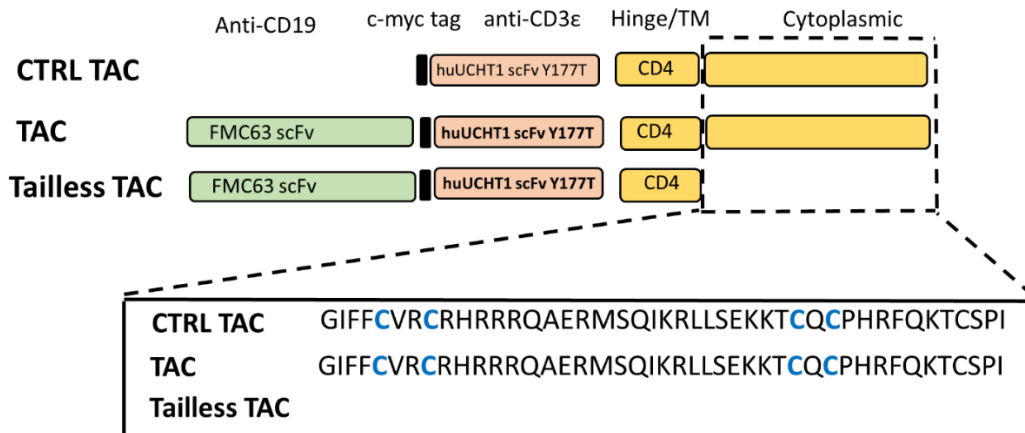


Figure 5.4. Schematic representation of CD19 specific TAC constructs used

Schematic representation of the TAC tail mutants highlighting the cytoplasmic domains (see text for details).

When expressed in primary T cells and enriched for engineered transduction by NGFR selection, the tailless TAC displayed markedly diminished surface expression compared to the full length TAC in both CD4⁺ and CD8⁺ T cells by 6-7 fold (Fig. 5.5A). Because Protein L (a immunoglobulin-binding protein that specifically interacts with the light chain of an scFv)³¹² was used as a receptor marker, T cells transduced with NGFR only (transduction marker, no chimeric receptor) are shown in the phenotypic analysis as a negative control instead of T cells transduced with the CTRL TAC (lacking an antigen binding domain) since the latter would stain positive with Protein L. When stimulated with CD19⁺ NALM-6 tumour cells, T cells engineered with either TAC construct displayed similar multivariate production of IL-2, TNFα and IFNγ (Fig. 5.5B). The CD4⁺ T cells produced large populations of IL-2⁺IFNγ⁺TNFα⁺ (pink pie slice) and IL-2⁺IFNγ⁺TNFα⁺ (green pie slice). The CD8⁺ T cells predominantly produced IL-2⁺IFNγ⁺TNFα⁺ (green pie slice), but also had a larger amount

of single IL-2 producing cells (light blue) compared to the CD4⁺ cells. These results demonstrate that despite diminished surface expression compared to the full length TAC, the tailless TAC exhibits the same *in vitro* production of cytokines upon antigen stimulation.

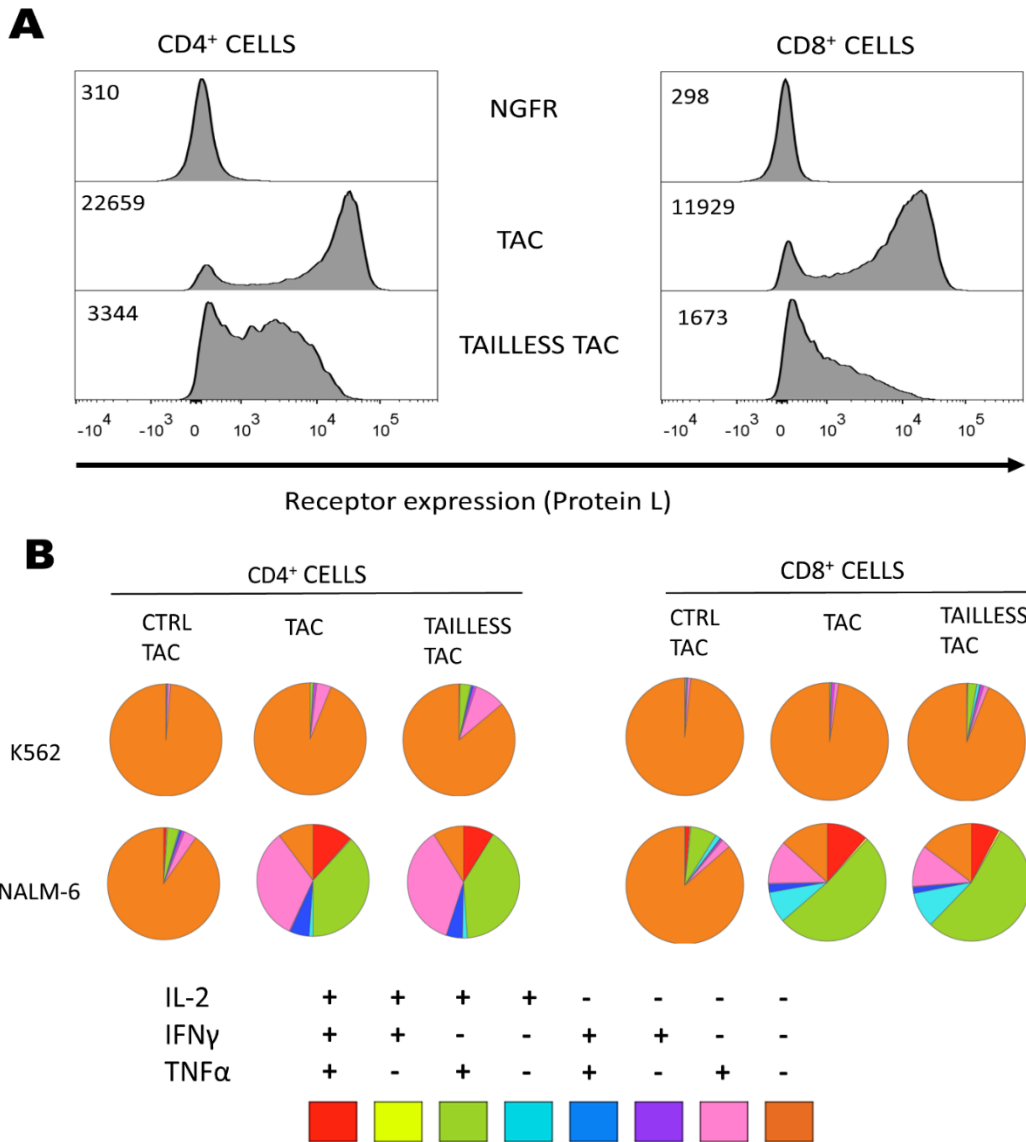


Figure 5.5. CD19-specific tailless TAC displays abrogated surface expression, but similar *in vitro* cytokine production profile compared to the full length TAC

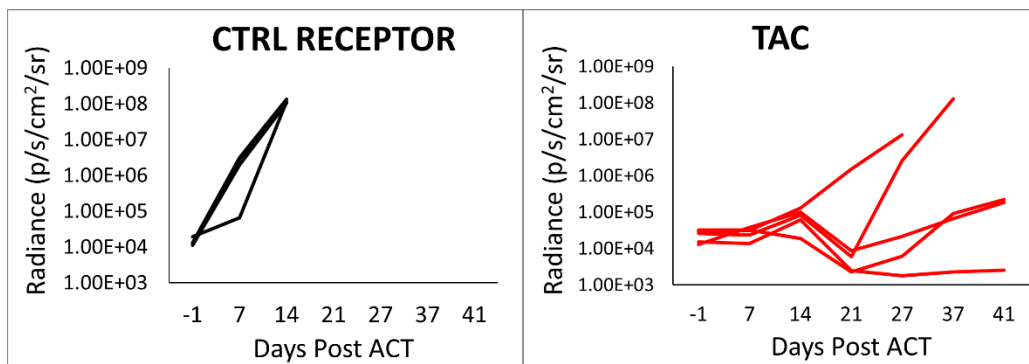
(A) T cells engineered with either the control receptor (NGFR), full length TAC or tailless TAC, enriched for engineered cells by NGFR selection and assessed for surface expression in CD4⁺ and

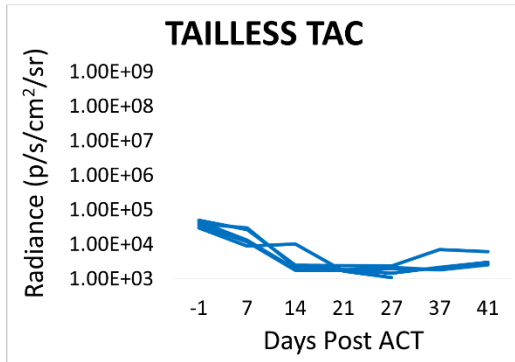
CD8+ cells. Histograms are gated on NGFR+ (engineered) cells and show receptor expression by Protein L staining and corresponding mean fluorescence intensity (MFI). **(B)** *In vitro* cytokine production of IL-2, IFN γ and TNF α was measured after stimulation with NALM-6 (CD19⁺) or K562 (CD19⁻) cells and is shown by multivariate SPICE analysis of CD4⁺ and CD8⁺ cells.

Tailless TAC-engineered T cells display higher *in vivo* efficacy against CD19⁺ NALM-6 tumours compared to full length TAC-engineered T cells

We evaluated the *in vivo* efficacy of the anti-CD19 TAC constructs by treating mice bearing human NALM-6 xenografts. When mice were treated with a low (1.5×10^6) effector dose of T cells (**Fig. 5.6A**), both the full-length and tailless TAC controlled tumour burden relative to the CTRL receptor, in which all mice in the CTRL group reached end point by 14 days post ACT. Nevertheless, while most mice in the TAC group showed tumour regression, three mice displayed tumour relapse in addition to one mouse that exhibited limited overall tumour control and reached end point by 27 days post ACT. In the tailless TAC group, tumour regression was observed for approximately 14 days post adoptive transfer and was sustained for the duration of the monitoring period. When mice were treated with a high (4.0×10^6) effector dose of T cells (**Fig. 5.6B**), we similarly observed initial tumour regression of the full-length and tailless TAC compared to the control TAC, three mice in the TAC group displayed tumour regression above ACT baseline. Within the tailless TAC group, all mice displayed initial and sustained tumour regression throughout the duration of the experiment. Therefore, the mice treated with anti-CD19 tailless TAC-engineered T cells had better *in vivo* outcomes than mice treated with full length TAC-engineered T cells after NALM-6 challenge.

A LOW T CELL DOSE (1.5×10^6 /MOUSE)





B HIGH T CELL DOSE (4x10⁶/MOUSE)

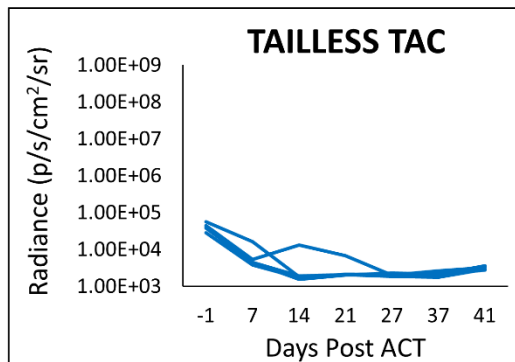
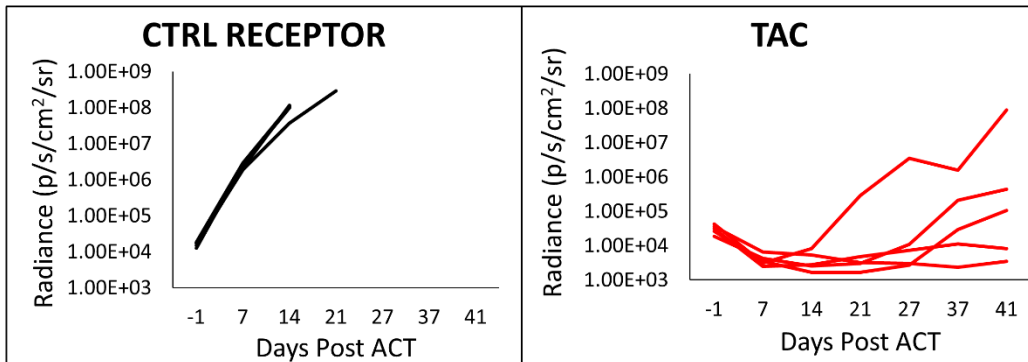
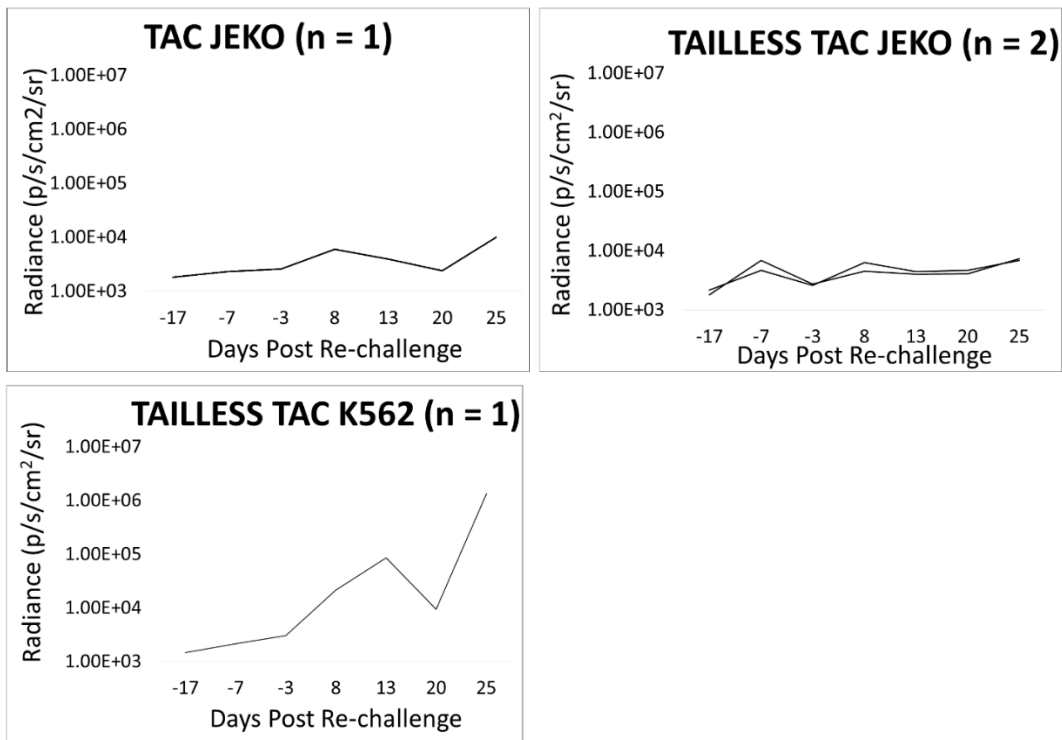


Figure 5.6. The tailless TAC displays increased *in vivo* efficacy compared to other TAC constructs against CD19⁺ NALM-6 tumour cells

Immunocompromised mice with established NALM-6 tumours were treated with either a (A) low dose or (B) high dose of TAC-engineered T cells enriched by NGFR selection. Tumour growth is measured by luminescence every 6-7 days post ACT.

We were next interested in confirming if mice that showed complete NALM-6 remission within both TAC groups could similarly clear another CD19⁺ cell line (JEKO-1)³¹³ when re-challenged. We found that both full-length and tailless TAC could control JEKO-1 tumour burden relative to the tailless TAC re-challenged with a CD19⁻ tumour (K562) in both low T cell dose (**Fig. 5.7A**) and high T cell dose (**Fig. 5.7B**) groups. This result demonstrates that the both the anti-CD19 full-length and tailless TAC can respond *in vivo* to additional tumour challenge.

A CD19⁺ TUMOUR RE-CHALLENGE (LOW T CELL DOSE)



B CD19⁺ TUMOUR RE-CHALLENGE (HIGH T CELL DOSE)

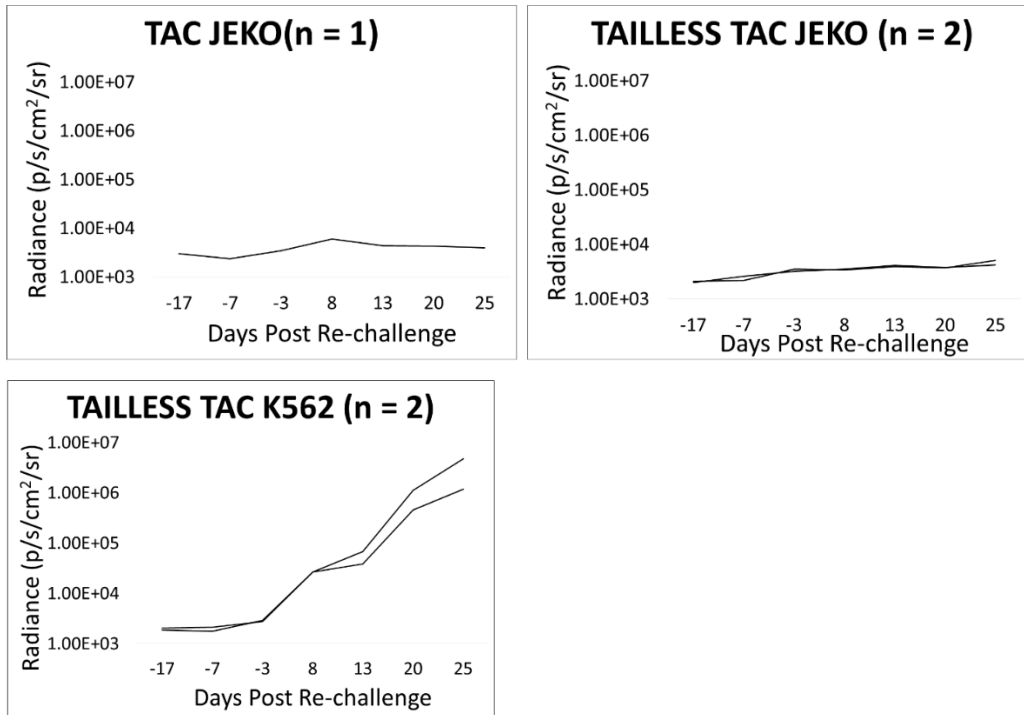


Figure 5.7. Both TAC-engineered T cells can control the tumour burden from a CD19⁺ tumour re-challenge

Mice which survived NALM-6 tumour challenge from Fig. 5.6 were re-challenged with CD19⁺ JEKO-1 or CD19⁻ K562 cells and tumour growth was measured every 5-7 days. Tumour growth curves are shown for (A) mice initially treated with a low T cell dose (1.5×10^6 cells) and (B) mice initially treated with a high T cell dose (4×10^6 cells)

DISCUSSION

The work in this chapter has confirmed across different antigen binders and tumour targets that the tailless TAC exhibits lower surface expression yet increased *in vivo* efficacy compared to the full length TAC. Unlike anti-BCMA engineered T cells, T cells engineered with anti-Her2 and anti-CD19 tailless TAC T cells do not display diminished *in vitro* cytokine production from tumour stimulation relative to T cells engineered with the full-length version of these receptors.

The increased *in vivo* efficacy of the tailless TAC is an intriguing observation. From the receptor biology perspective, the TAC was originally constructed to recapitulate

natural T cell activation, and the modular design of the receptor specifically included the intracellular domain of CD4 due to its functional features described in the literature^{63,67,298,309}. It appears that not only are one or more of these features not necessary for TAC function *in vitro*, the inclusion of the cytoplasmic domain may diminish the *in vivo* efficacy of the TAC regardless of the tumour target. From a T cell engineering perspective, these results question the validity in evaluating a receptor's ultimate clinical performance by *in vitro* assays such as proliferation, cytokine production, or tumour cytotoxicity. We have shown across two tumour types and antigen binders that the tailless TAC shows no difference in tumour stimulated *in vitro* cytokine production compared to the parent TAC, yet clear *in vivo* advantages. Furthermore, phenotypic surface expression is an important parameter in the field used to evaluate CAR T cells, where a high density is often (but not always, discussed below) desired. The tailless TAC consistently exhibited diminished surface expression compared to the full-length TAC, yet T cells engineered with the tailless TAC outperformed T cell engineered with full-length TAC *in vivo*. This demonstrates the possibility of *in vivo* efficacy of an engineered T cell despite poor surface expression of the exogenous receptor. Finally, and most importantly, from a clinical perspective the creation of a T cell product with a high therapeutic index (high efficacy, low toxicity) is the critical objective. The tailless TAC clearly shows increased *in vivo* efficacy, and it merits further investigations to determine its safety profile with regards to any potential toxicities that accompany this efficacy.

The mechanism behind the increased *in vivo* efficacy of the tailless TAC is unknown, however literature on CAR T cells provides potential insights. CAR T cells are susceptible to tonic signaling, which has been shown to increase exhaustion markers on the engineered T cell and therefore decrease long term *in vivo* persistence. This is due primarily to the clustering of antigen-binding scFvs, but this effect is intensified in part by the surface expression levels of the CAR, where less receptor on the surface decreases tonic signaling²¹⁰. By having less CARs on the surface of the T cell, there is less clustering of chimeric receptors and therefore less tonic signaling and T cell exhaustion. Nevertheless, our group has failed to observe evidence of tonic signaling (i.e. upregulation of exhaustion markers) in the full-length TAC across multiple scFvs in head-to-head comparisons with second generation CARs containing either 4-1BB or CD28 co-stimulatory domains²⁵⁸. Therefore, although the decrease in CAR surface expression leads to lower tonic signaling and increased *in vivo* efficacy, the TAC does not appear to be susceptible to tonic signaling to begin with, and the relationship (if any) between diminished TAC expression and increased *in vivo* efficacy needs to be investigated further.

Recently, CRISPR/Cas9 has been used to deliver site-specific integration of the CAR transgene within the T cell genome, specially within the T cell receptor α constant (TRAC) locus³¹⁴. These TRAC CARs showed more uniform and less variable surface expression compared to CARs transduced with a γ -retrovirus, which displayed on average two-fold higher surface expression. TRAC CARs also displayed diminished tonic signaling

and enhanced *in vivo* therapeutic activity, further supporting the notion that ‘fine-tuning’ CAR expression is correlated with increased *in vivo* activity due to a decrease in tonic signaling³¹⁵.

T cells expressing memory-like properties including β -oxidation metabolism and delayed *in vitro* killing kinetics have exhibited greater *in vivo* anti-tumour persistence than T cells expressing effector-like properties such as glucose metabolism, rapid *in vitro* killing kinetics and high cytokine production. The co-stimulatory domain of 2nd generation CARs drives these phenotypes, where 4-1BB promotes memory and CD28 promotes effector^{202,238–240}. The mechanism behind this is unclear, however groups that have mutated the Lck-binding domain of CD28 within the CAR have shown that a lack of Lck interaction leads to a more memory-polarized phenotype and increased *in vivo* persistence^{304,305}. It is conceivable that the interaction of Lck within the receptor complex might be pushing the TAC T cell to an effector-like state, while the omission of Lck in the tailless TAC complex might be favouring a memory-like state (lower cytokine production, higher *in vivo* persistence). Further work will need to be done to validate this claim.

CHAPTER SIX

GENERAL DISCUSSION

6.1 Summary of research findings

The TAC was designed to recapitulate the natural activation of a T cell, consisting of 3 main components: (i) an antigen binding domain, (ii) a CD3 engaging domain and (iii) the transmembrane and cytoplasmic domain of the CD4 co-receptor. Our laboratory has previously²⁵⁸ investigated two of these components, demonstrating that i) while the choice of CD3 engager affects both surface expression and functionality, the TCR-CD3 binding domain is absolutely necessary for full activation and ii) multiple tumours (including solid cancers) can successfully be targeted by changing the antigen binding domain, which is also absolutely critical for full functionality. The TAC receptor does not contain any signaling components (such as CD3 ζ or CD28) and requires the endogenous signaling network of the T cell to function. The transmembrane and cytoplasmic domains of CD4 were incorporated into the TAC to recapitulate the co-receptor features that enable collaborative functions with the TCR-CD3 complex to achieve T cell activation, but the true contribution of these domains to the TAC functionality was unknown. As the CAR field has shown (discussed in **Chapter 1, Section 1.5.1** and additionally in **Section 6.2.2** below) understanding the contribution of each component of a synthetic antigen receptor is important in understanding the biology of both the receptor and the engineered T cell, and therefore critical in designing a safe and effective therapeutic product for cancer patients. Therefore, the work presented in this thesis aimed to investigate the biological function of the TAC receptor cytoplasmic domain.

In **Chapter 3**, the CD4 transmembrane and cytoplasmic domains in the TAC receptor were replaced with sequences from CD8 α and CD8 β based on literature reports of critical intracellular residues and domains required for endogenous TCR signaling. Given that the TAC was designed to recapitulate natural T cell activation, we hypothesized that that these features would also contribute to the functionality of the TAC receptor and tested this hypothesis by creating TAC variants with those features mutated or removed. These variants displayed varying degrees of surface expression and, when expressed in T cells, these variants triggered comparable T cell function *in vitro*, indicating that those specific intracellular residues and domains did not substantially contribute to TAC receptor performance *in vitro*.

In **Chapter 4**, we used a different TAC scaffold that replaced the original UCHT1, an scFv of mouse origin, with a humanized variant of UCHT1 (huUCHT1 Y177T) that contains a mutation selected in the Bramson lab by *in vitro* evolution. Here, I focused on TAC receptors directed against BCMA, a multiple myeloma target, and compared a number of modifications to the CD4 cytoplasmic domain, including full removal of the cytoplasmic domain (*aka* tailless TAC). The most striking phenotype was observed with the tailless TAC, which displayed diminished surface expression and T cells engineered with the tailless TAC exhibited diminished cytokine production in response to antigen stimulation *in vitro*, however other *in vitro* functionality parameters, such as proliferation and

cytotoxicity, were unaffected. Despite the lower surface expression and decreased cytokine production, the tailless TAC nevertheless showed high *in vivo* efficacy against BCMA⁺ tumours.

In **Chapter 5**, we continued the work with the tailless TAC receptor by investigating *in vitro* and *in vivo* functionality of tailless TAC receptors directed against CD19 and Her2; again, we used the huUCHT1 Y177T scaffold. We were ultimately interested in determining if the results with the tailless TAC in the previous chapter could be recapitulated against other cancers or if they were unique to the anti-BCMA scFv used in Chapter 4. Our results showed that similar to the anti-BCMA tailless TAC, the surface expression of the anti-CD19 and anti-Her2 tailless TACs was also abrogated, however there was no difference in *in vitro* antigen-dependent cytokine production compared to the full length TAC. Again, the tailless TAC displayed greater *in vivo* efficacy than the full length TAC against mice bearing established human xenografts. The combined results of Chapters 4 & 5 demonstrated that regardless of the antigen recognition domain, surface expression of the TAC receptor lacking an intracellular tail was diminished, however *in vivo* efficacy was increased.

6.2 Biological Implications

6.2.1 Diminished surface expression of the tailless TAC

One of the major biological outcomes of removing the cytoplasmic tail of the TAC receptor is a clear and reproducible decrease in surface expression compared to the full length TAC receptor. The CD4 intracellular tail is only 44 amino acids in length, yet contains motifs and sites critical for membrane partitioning^{63,316}, post translational modifications (such as palmitoylation⁶³, phosphorylation³¹⁷, and potentially O-linked glycosylation^{297,306}), and important protein-protein interactions (such as Lck-binding^{62,67}), thereby demonstrating important roles in co-receptor functionality. We hypothesized that one or several of these amino acids/motifs were responsible for the abrogation of surface expression. Indeed, many of the changes to the cytoplasmic domain, including the mutation of key cysteine residues to alanines, resulted in reduced surface expression of the TAC receptor (Chapter 4). However, none of truncations and/or amino acid mutations, could reproduce the magnitude of the reduction in surface expression exhibited by the tailless TAC. It is important to note that all of our truncation and mutant constructs except for the tailless TAC contained the GIFFCVRC sequence in the intracellular tail closest to the cell membrane, with the exception of 2A_{Δ488-525}, which carried the sequence GIFFAVRA, (**Figure 4.8**) suggesting that some component of that sequence, other than the cysteine residues, was impacting surface expression of the TAC.

The antigen-independent decrease in surface expression of the tailless TAC can be attributed either to trafficking issues preventing the TAC from reaching the surface after translation, or enhanced internalization of the receptor from the cell surface. We used IF

microscopy to determine the trafficking state of both the full-length and parent TAC in resting Jurkat T cells (**Figure 4.3**) by localizing the receptor with six separate organelle markers. It is interesting to observe that in resting Jurkats, both the full-length and tailless TAC colocalized strongest with Calnexin (endoplasmic reticulum marker) compared to other organelles, although the tailless TAC appeared to localize stronger with the ER based on the Pearson coefficient. This may suggest accumulation in the endoplasmic reticulum, preventing the receptor from reaching the surface of the cell. Furthermore, both TAC receptors appear to colocalize relatively well with Rab7a, a late endosome marker. This may suggest that the receptor is internalized from the surface of the cell, quickly acidified in late endosomal vesicles and finally degraded by lysosomes²⁹¹. Given that the endogenous TCR is continuously recycled from the cell surface in resting T cells³¹⁸ and that the TAC interacts with the TCR complex, a staining pattern consistent with TCR recycling is expected (i.e. association with the early endosome marker Rab5). The TCR has been shown to co-localize specifically with Rab4 in resting T cells, an early endosomal marker involved in transiting proteins from endosome vesicles back to the cell surface³¹⁹. Another group has shown that the TCR co-localizes with Rab11 (a marker of recycling endosomes, which receives endocytosed proteins from early endosomes³²⁰) in both resting primary and Jurkat T cells, further demonstrating that the TCR is constitutively downmodulated and recycled back to the cell surface by protein transiting via endosomal vesicles³²¹. The IF results generated here suggest possible lysosomal degradation of full length and tailless TAC (co-localization with Rab7a), however lysosomal degradation of the TCR has only been observed after TCR ligation, and not in resting T cells³¹⁹.

6.2.2 Increased *in vivo* efficacy of the tailless TAC

The second biological outcome of removing the intracellular tail from the TAC receptor is the enhanced *in vivo* efficacy compared to the full length TAC. Intriguingly, the only difference in *in vitro* functionality we observed between the full-length and tailless TAC was a *decrease* in cytokine production of the tailless TAC when stimulated with BCMA⁺ tumours (**Figure 4.4**). Therefore, despite the *in vitro* functionality data which suggests that the tailless TAC should be equal to or less efficacious than the full-length TAC, T cells engineered with the tailless TAC consistently outperformed T cells engineered with the full-length *in vivo*. The mechanisms behind this unique observation were not elucidated in this thesis and several hypotheses are provided below:

Hypothesis 1: The tailless TAC T cells exist in a more memory-like state

As stated earlier, the CAR field is replete with evidence of engineered T cells with a memory differentiation state having increased *in vivo* persistence compared with engineered T cells with an effector differentiation state²³⁹. Memory T cells are associated with antigen dependent fatty acid oxidation metabolism, slow kinetic killing and high *in vivo* persistence (months-years), while effector T cells use glucose metabolism as a primary energy pathway, display rapid kinetic killing and have relatively low *in vivo* persistence (weeks)^{125,322}. Due to the observation of enhanced *in vivo* efficacy of tailless

TAC-engineered T cells compared to full-length TAC-engineered T cells, and increased *in vivo* efficacy is associated with memory T cells, it is possible that the tailless TAC receptor is promoting a T cell state that is less terminally differentiated and more memory than T cells expressing the full-length TAC. Conversely (for reasons postulated below), T cells expressing the full-length TAC may be more prone to effector differentiation upon antigen engagement. This is perhaps best observed when anti-BCMA T cells were stimulated *in vitro* with BCMA⁺ tumour cells (**Figure 4.4**), and TAC-engineered T cells produced more IFN γ and TNF α (measures of effector function) than tailless TAC-engineered T cells. Since the ultimate goal is to create clinically effective *in vivo* engineered T cells, *in vitro* assays used to assess potential receptors should ideally be evaluating memory features such as antigen-dependent fatty acid oxidation, slow kinetic killing and memory markers instead of effector features such as proliferation, short term cytokine production from antigen stimulation and end-point cytotoxicity (discussed further in **SECTION 6.3**).

If the tailless TAC is promoting a T cell state that is more memory-like than the full-length TAC which is promoting an effector-like T cell state, what is driving this polarization? In the CAR field, the CD28 and 4-1BB co-stimulatory domains of 2nd generation CAR T cells provide potential insights. CD28-CARs display effector characteristics such as rapid tumour killing kinetics, high T cell signaling intensity (phosphorylation of CD3 ζ , SLP-76 and PLC- γ 1), glucose metabolism and therefore have lower persistence compared to 4-1BB-CARs^{237–239}. Conversely, 4-1BB-CARs display memory characteristics such as fatty acid oxidation, lower signaling intensity, slow tumour killing kinetics *in vivo*, and increased *in vivo* persistence. There are many biological differences in the structures and signaling pathways between CD28 and 4-1BB described in great detail elsewhere³²³, however one difference of particular relevance to the work in this thesis is the association with Lck. While neither human CD28 nor 4-1BB contain the intracellular CXCP motif that specifically binds to Lck (found in CD4 and CD8), CD28 does contain a PYAP motif that interacts with the SH2 (binds phosphorylated tyrosines) and SH3 (binds proline rich regions) motifs of all src kinases, including Lck^{304,324}. Indeed, Lck has been shown to directly interact with CD28 in T cells and contribute to downstream CD28 signaling, specifically in recruiting protein kinase C (PKC) to the signalosome and activating it³²⁵. Within the context of CAR T cells, Lck recruitment and signaling by CD28 may be driving CD28-CARs to an effector state, while the lack of Lck recruitment by 4-1BB-CARs may allow them to retain a memory state. Studies that have mutated the PYAP motif in CD28 (thereby preventing Lck interaction) in 2nd generation CD28-CARs have shown that these CARs display memory-like properties such as lower antigen-dependent proximal signaling intensity and higher *in vivo* persistence^{304,305}. By simply abolishing Lck interaction (confirmed by co-immunoprecipitation pull downs), groups have shown that effector-like CD28-CARs can be polarized to a memory state and have increased *in vivo* persistence^{304,305}.

In the context of the TAC receptor, the intracellular tail of the full length TAC contains the CQCP motif (binding site for Lck^{62,67}), while the tailless TAC does not. Similar to the

observations in the CAR field, the recruitment of Lck by the full length TAC might be driving the engineered T cells to an effector-like state (high *in vitro* cytokine production, lower *in vivo* persistence), while the lack of Lck recruitment by the tailless TAC might be favouring a memory-like state (high *in vivo* persistence). Upon antigen binding, the kinetic segregation and proofreading models of T cell activation suggest that phosphorylation of CD3 ζ ITAMs occurs due to the clustering of the CAR/TAC receptors on the surface of T cells. The binding dwell time between the receptor and antigen then allows for these clusters to remain in proximity while passive phosphorylation by Lck of multiple ITAMs initiates the signaling^{77,96,326}. However, if Lck is already associating with these receptor clusters (through the TAC CQCP motif or the PYAP motif on CD28-CARs) during antigen binding, this may potentially allow for increased ITAM phosphorylation, since signaling is no longer only dependent on the passive phosphorylation by Lck away from phosphatases such as CD45. The increase in signaling intensity (CD3 ζ phosphorylation) by Lck association during antigen stimulation has previously been shown to be a key determinate in CAR T cell fate³⁰⁴, and might possibly apply for TAC T cells as well. Future work will need to involve determining the effector/memory subset phenotype of these engineered T cells (discussed further in **Section 6.3**). There are several caveats to this hypothesis however:

- The anti-BCMA TAC $_{\Delta 488-525}$ truncation construct (**Figure 4.8**) lacking the CQCP motif produced significantly more TNF α and IFN γ in response to 4 hour tumour stimulation than the tailless TAC (**Figure 4.9**), a property indicative of effector function.
- The anti-Her2 4A mutant and $\Delta 488-525$ truncation constructs (**Figure 5.1**), which lack Lck interaction by mutation and omission of the CQCP motif (respectively), both did not show any *in vivo* efficacy against OVCAR-3 solid tumours (**Figure 5.3**) while the tailless TAC did.
- The lack of Lck interaction with the tailless TAC or any other truncation/mutant TAC receptor has not been demonstrated. The assumption that the interaction with Lck is eradicated is based on the literature characterizing the intracellular tail of the endogenous CD4 co-receptor and needs to be confirmed.

Hypothesis 2: The tailless TAC is more resistant to downmodulation

One of the hallmarks of T cell regulation is the downmodulation of the TCR-CD3 complex upon antigen ligation which ultimately prevents excessive stimulation³¹⁹. Similarly, the CD4 co-receptor has been shown to downmodulate/internalize upon stimulation, specifically by endocytosis leading to protein degradation³²⁷. One study from the late 1980s found that removal of the CD4 cytoplasmic domain prevented the internalization of the receptor when stimulated with phorbol 12-myristate 13-acetate (PMA), an activator of PKC. Even when the CD4 cytoplasmic domain was replaced with the cytoplasmic domain from IL-2, internalization of CD4 could not be rescued, indicating that critical residues for internalization were contained in the CD4 cytoplasmic tail³²⁸. These

residues were mapped out to be three serine amino acids in the cytoplasmic tail whose phosphorylation by PKC all contribute to CD4 internalization³¹⁷. Serine phosphorylation intensity correlated with internalization and membrane proximity (i.e. the closest serine to the membrane was most phosphorylated, the furthest serine was the least phosphorylated). When a single serine was mutated to alanine, the CD4 receptor with the serine closest to the membrane displayed the least internalization, while the receptor with the serine furthest from the membrane displayed the most internalization. Complete inhibition of CD4 internalization upon stimulation could only be achieved by mutating all serines to alanines. Interestingly, a CD4 variant containing the phosphorylated membrane proximal serine and the rest of the cytoplasmic tail randomized to indiscriminate amino acids showed absolutely no internalization (similar to mutating all the serines to alanines), suggesting that other features on the cytoplasmic tail are critical for internalization in addition to serine phosphorylation. These studies indicate that CD4 is internalized and degraded upon stimulation, and this internalization is dependent on both the intracellular phosphorylation of serine residues and the intact features of the cytoplasmic tail.

With regards to the TAC receptor, the enhanced *in vivo* efficacy of the tailless TAC might be explained by decreased antigen-dependent receptor downmodulation. Upon antigen engagement, the signaling cascade of the T cell is expected to activate PKC, which would be expected to phosphorylate the serine residues on the intracellular tail of the TAC's CD4 co-receptor. Decreased internalization of the TAC may allow more engagement with the tumor cells and enhanced anti-tumor effect. One would therefore expect the TAC $_{\Delta 488-525}$ truncation to recapitulate the performance of the tailless TAC, since it lacks all three serine residues. While this is correct against BCMA⁺ liquid KMS-11 tumours (**Figure 4.10**), the TAC $_{\Delta 488-525}$ truncation showed no efficacy against Her2⁺ OVCAR-3 solid tumours (**Figure 5.3**). However, this truncation still retained the membrane proximal GIFFCVRC residues, and it is conceivable that these residues play a complementary role with the serine residues in internalizing CD4 upon antigen stimulation, and only omission of all residues, as occurs in the tailless TAC, can completely prevent internalization. This is especially obvious against large solid tumours such as OVCAR-3 that require continuous tumour infiltration.

6.3 *In vitro* evaluation of future receptors

Currently, most publications describing a new T cell receptor (synthetic or natural) present *in vitro* data demonstrating: surface expression, cytokine production in response to antigen stimulation, cytotoxicity against tumour targets, proliferation in response to antigen and antigen-independent expansion of the T cell culture after engineering (i.e. lentivirus transduction). If the hypothesis that memory polarization of engineered T cells enhances *in vivo* efficacy is correct, then measures of effector functions (such as the ones stated above) would not necessarily predict *in vivo* performance. For instance IFN γ and TNF α are classical effector molecules produced by CD8⁺ CTLs and CD4⁺ Th1 cells, and

measuring their production in response to relatively short four hour antigen stimulation would not indicate how engineered T cells would persist long term (weeks-months) *in vivo*²⁶. This is important in clinical trials where complete responses (no detectable signs of cancer in response to treatment)³²⁹ are usually measured months after infusion^{244,330}. Furthermore, ITAM phosphorylation upon antigen stimulation drives several signaling pathways within the T cell. There are 10 ITAMS per TCR-CD3 complex: six on the $\zeta\zeta$ dimer (3 per monomer), one on γ , one on δ , and two from the ϵ subunits (one on each)³³¹. One study found that cytokine production and proliferation upon antigen stimulation had different ITAM phosphorylation requirements³³²: the secretion of IL-2, TNF α and IFN γ only required as few as two ITAMs to be phosphorylated upon stimulation. Proliferation could only be achieved when all ten ITAMs were phosphorylated after antigen stimulation, indicating that proliferation requires a higher multiplicity of ITAM phosphorylation (10/10 ITAMS) than cytokine production (2/10 ITAMS). Since effector fate is associated with the strength of ITAM phosphorylation (i.e. more phosphorylation polarizes the cell to an effector state)³⁰⁴, proliferation would therefore be a measure of effector function since it requires more phosphorylated ITAMs to initiate.

In vitro cytotoxicity assays are meant to reflect tumour clearance but cannot reflect *in vivo* performance due to short co-culture periods (hours), and high lymphocyte to tumour ratio within a small surface area (i.e. single well of a 96 well plate). These assays do not address the kinetics of tumour clearance (memory cells associated with slower kinetics) or how the T cells respond to recursive/serial antigen exposure as would be the case *in vivo*.

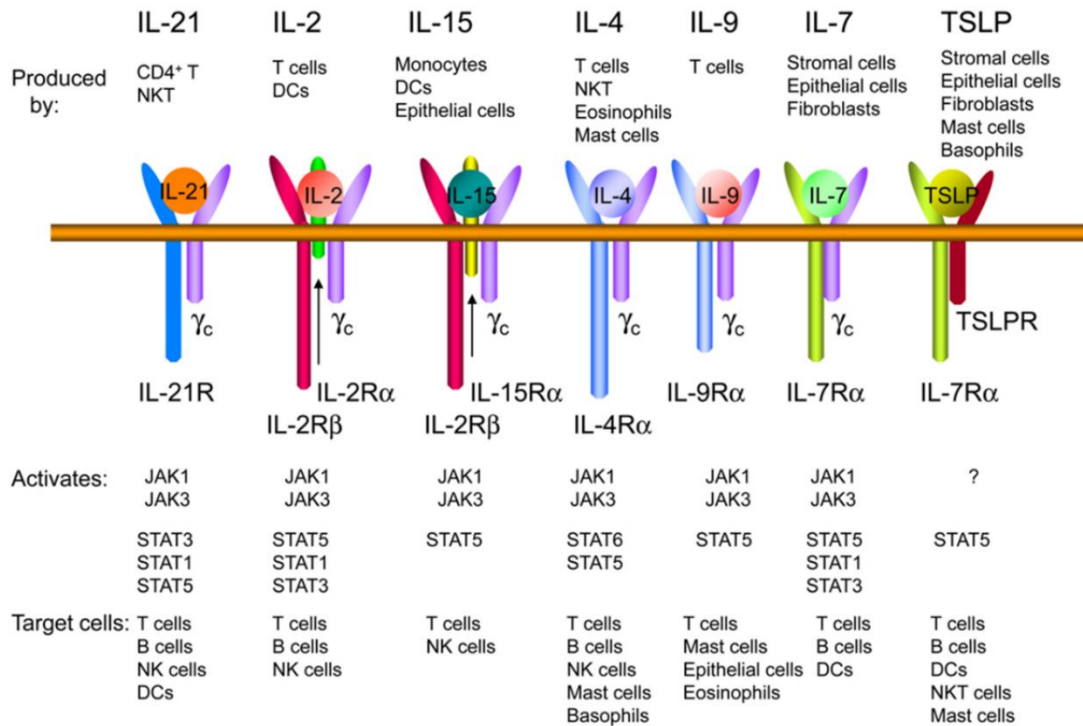
The data presented in this thesis strengthens the notion that specific *in vitro* outcomes do not always manifest *in vivo*. There was no indication from the *in vitro* assays performed for this thesis (cytokine production, proliferation, cytotoxicity, surface expression or expansion) that the tailless TAC would outperform the full-length TAC against human xenografts *in vivo*. This poses the question: are *in vitro* functionality parameters good predictors of *in vivo* efficacy? If so, what are the appropriate *in vitro* parameters to characterize future receptors?

If the memory vs effector polarization hypothesis is correct, then perhaps *in vitro* assays that measure memory-like properties should be used to predict *in vivo* efficacy. For instance, instead of measuring the production of effector cytokines such as TNF α and IFN γ after short-term antigen stimulation, cytoplasmic glycolysis and mitochondrial fatty acid oxidation metabolism of engineered T cells can be measured after long term stimulation²⁴⁰. T cells that preferentially use β -oxidation in the mitochondria are memory polarized, while effector cells prefer to metabolize glucose in the cytoplasm¹²⁸. Furthermore, end-point killing assays should be altered to either real-time or sequential/recursive killing assays. In real-time cytotoxicity assays, viability of the target cells is tracked at specific intervals over the course of the co-culturing period (rather than simply reading end-point viability at the end of the experiment), allowing cytotoxicity

killing rates to be analyzed³³³. Central memory cells display slow killing kinetics, while effector cells display high killing kinetics. Additionally, sequential/recursive killing assays involve re-challenging engineered T cells with new targets over longer periods of time than conventional killing assays and are more indicative of the repeated antigen exposure that T cells endure from tumour cells *in vivo*³³⁴. Finally, phenotypic memory markers should be analyzed after antigen stimulation: endogenous central memory cells home to the lymph node and tend to be CCR7⁺CD62L⁺, while effector cells are CCR7⁻CD62L⁻ as they remain in the periphery³³⁵. These new assays ensure that we are evaluating receptors for memory characteristics instead of effector characteristics in order to predict *in vivo* efficacy.

6.4 Future considerations in TAC design

CARs transmit activation and co-stimulatory signals, but providing a third signal to T cells engineered with second-generation CARs can enhance therapeutic outcomes. T cells normally receive “signal 3” from cytokines, and an important class of cytokines is the common cytokine-receptor γ -chain (γ_c) family (**Supplementary Fig S1**). These cytokines all share γ_c as one of the components of the heterodimeric receptor, and include IL-2, IL-7 and IL-15³³⁶. Together with the cytokine-specific α and/or β receptor, a heterodimer or heterotrimer forms in response to cytokine binding of each separate monomer, leading to activation of JAKs, which autotransphosphorylate their respective receptors. This leads to recruitment of STAT proteins by virtue of their SH2 domains, leading to their own phosphorylation by JAKs and eventual dimerization. Dimerization of the phosphorylated STAT proteins creates a DNA-binding transcription factor, which is then translocated to the nucleus and leads to transcription of several pro-survival genes³³⁷.



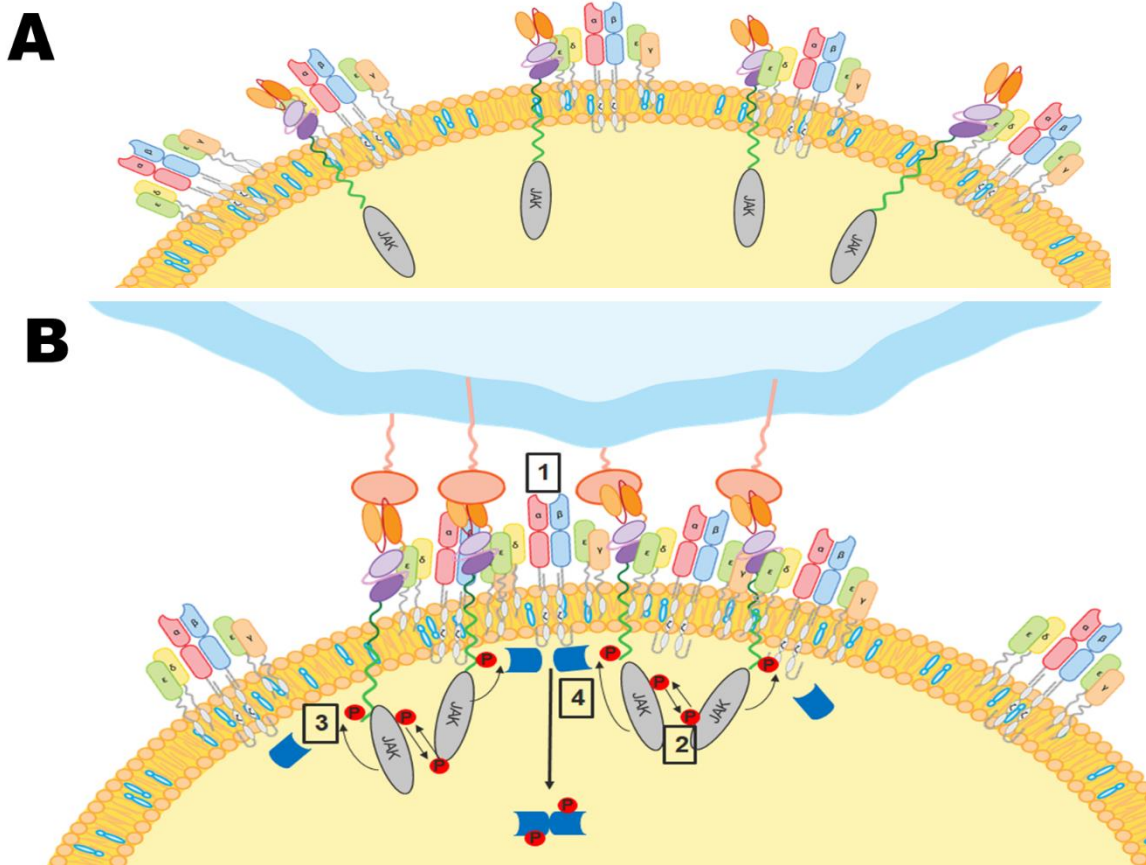
Supplementary Figure S1. Type I cytokine receptors in T cells³³⁶

The heterooligomeric receptors for different Type-I cytokines are shown. In all cases except IL-2 and IL-15, a heterodimer is formed upon antigen binding. The IL-2 and IL-15 receptors form a heterotrimer. Upon cytokine engagement, the separate monomers of the receptor are clustered into close proximity, initiating the signaling cascade of the JAK-STAT pathway (see text for details).

Systemic administration of cytokines to patients is known to cause significant toxicities, therefore strategies to deliver cytokine signaling without administering cytokines themselves are currently being explored in the context of providing signal 3 for CAR T cells. For instance, a CAR encoding a truncated cytoplasmic domain of IL-2Rβ and a STAT3-binding YXXQ motif in addition to CD3ζ and CD28 displayed superior antigen-dependent persistence and proliferation compared to the CARs not expressing these signal 3 domains³³⁸. Another group has shown that constitutive antigen independent STAT5 signaling by expression of an artificially homodimerized IL-7R in addition to a CAR leads to increased T cell proliferation, survival, and anti-tumor activity during repeated exposure to tumour cells, without apparent T cell dysfunction³³⁹.

If the best therapeutic product for cancer patients are engineered T cells with high *in vivo* persistence, then it would be advantageous in incorporating features that promote *in vivo* persistence into engineered T cells. Since signal 3 increases this persistence, the tailless TAC would be an ideal receptor to incorporate additional STAT3/STAT5 signaling moieties since i) incorporation of STAT signaling would contribute to antigen-dependent *in vivo*

persistence and ii) lentivirus vectors have packaging size limits³⁴⁰, therefore swapping the cytoplasmic tail for STAT signaling motifs (as oppose to adding the motifs to an already existing tail that does not contribute to *in vivo* persistence) would prevent the construct from exceeding this size.



Supplementary Figure S2. Antigen-dependent JAK-STAT signaling in TAC T cells

(A) In the absence of antigen engagement, JAK proteins associated with the JAK-binding motifs (such as the truncated cytoplasmic domain of IL-2R β and YXXQ motif described Kagoya et al³³⁸) on the TAC remain spatially excluded and JAK-STAT signaling does not occur. (B) Upon antigen engagement, clustering of the TAC molecules leads to clustering of JAK proteins, which initiates the signaling cascade.

[1] TAC clustering upon antigen engagement

[2] Autotransphosphorylation of TAC cytoplasmic tail by clustered JAK proteins

[3] Recruitment of monomeric STAT (blue) to phosphorylated residues

[4] Phosphorylation of STAT by JAK, leading to dimerization of STAT and translocation to the cell nucleus

Figure adapted from Arya Afsahi

The JAK/STAT signaling cascade within the TAC receptor would capitalize on the clustering of TAC molecules on the T cell surface upon antigen engagement (**Supplementary Figure S2**). In a resting T cell, TAC molecules containing JAK-recruitment motifs would associate with JAK molecules, but no signaling would occur due to spatial segregation. Upon antigen engagement and clustering of TAC molecules, intracellular JAK proteins (now in close proximity with each other) would autotransphosphorylate the tyrosine residues on the adjacent TAC molecule. Phosphorylated tyrosines would recruit monomeric SH2-containing STAT proteins, leading to the phosphorylation of STAT by JAK. Phosphorylated STAT then dimerizes, and translocates to the nucleus where it serves a transcription factor for several survival, growth and persistence genes.

6.5 Closing remarks

The story of TAC development is not unlike that of the CAR. The first generation CAR was designed and described based on minimal features required to redirect a T cell against a target of choice independent of the TCR¹⁹⁴. This construct was improved when the addition of co-stimulatory domains increased *in vivo* persistence. The TAC receptor was also designed based on minimal features required to redirect a T cell against a target of choice, but in a more natural (TCR-dependent) fashion. While the TAC showed unique biological features such as a lack of tonic signaling and efficacy against solid tumours, the tailless TAC described in this thesis has demonstrated that *in vivo* efficacy of the TAC can be improved. Whether the next generation of the TAC molecule will exclude the cytoplasmic tail and/or include STAT signaling, it is evident that this is a powerful receptor in which the full potential and biology remains to be discovered.

REFERENCES

1. National Cancer Institute. What Is Cancer? - National Cancer Institute. Available at: <https://www.cancer.gov/about-cancer/understanding/what-is-cancer>. (Accessed: 10th October 2019)
2. Bertram, J. S. The molecular biology of cancer. *Mol. Aspects Med.* **21**, 167–223 (2000).
3. Canadian Cancer Society. Cancer statistics at a glance. Available at: <http://www.cancer.ca/en/cancer-information/cancer-101/cancer-statistics-at-a-glance/?region=on>. (Accessed: 11th October 2019)
4. Lehmann, A. R., McGibbon, D. & Stefanini, M. Xeroderma pigmentosum. *Orphanet J. Rare Dis.* **6**, 70 (2011).
5. Loeb, L. A. & Harris, C. C. Advances in Chemical Carcinogenesis: A Historical Review and Prospective. *Cancer Res.* **68**, 6863–6872 (2008).
6. Ferguson, L. R. *et al.* Genomic instability in human cancer: Molecular insights and opportunities for therapeutic attack and prevention through diet and nutrition. *Semin. Cancer Biol.* **35 Suppl**, S5–S24 (2015).
7. Ehrlich, M. DNA hypomethylation in cancer cells. *Epigenomics* **1**, 239–59 (2009).
8. Quante, M. & Wang, T. C. Stem cells in gastroenterology and hepatology. *Nat. Rev. Gastroenterol. Hepatol.* **6**, 724–737 (2009).
9. Mbeunkui, F., Johann, D. J. & Jr. Cancer and the tumor microenvironment: a review of an essential relationship. *Cancer Chemother. Pharmacol.* **63**, 571–82 (2009).
10. Karagiannis, G. S. *et al.* Cancer-associated fibroblasts drive the progression of metastasis through both paracrine and mechanical pressure on cancer tissue. *Mol. Cancer Res.* **10**, 1403–18 (2012).
11. Walker, C., Mojares, E. & Del Río Hernández, A. Role of Extracellular Matrix in Development and Cancer Progression. *Int. J. Mol. Sci.* **19**, (2018).
12. Hui, L. & Chen, Y. Tumor microenvironment: Sanctuary of the devil. *Cancer Lett.* **368**, 7–13 (2015).
13. Carmeliet, P. & Jain, R. K. Molecular mechanisms and clinical applications of angiogenesis. *Nature* **473**, 298–307 (2011).
14. Hanahan, D. & Weinberg, R. A. The Hallmarks of Cancer. *Cell* **100**, 57–70 (2000).
15. Hanahan, D. & Weinberg, R. A. Hallmarks of Cancer: The Next Generation. *Cell* **144**, 646–674 (2011).
16. Miller, K. D. *et al.* Cancer treatment and survivorship statistics, 2019. *CA. Cancer J. Clin.* **69**, 363–385 (2019).
17. Tavare, A. N., Perry, N. J. S., Benzonana, L. L., Takata, M. & Ma, D. Cancer recurrence after surgery: Direct and indirect effects of anesthetic agents*. *Int. J. Cancer* **130**, 1237–1250 (2012).
18. Canadian Cancer Society. Surgery in cancer treatment. (2019). Available at: <https://www.cancer.ca/en/cancer-information/diagnosis-and->

- treatment/surgery/?region=on. (Accessed: 18th October 2019)
19. Trimble, E. L. *et al.* Neoadjuvant therapy in cancer treatment. *Cancer* **72**, 3515–24 (1993).
 20. Baskar, R., Lee, K. A., Yeo, R. & Yeoh, K.-W. Cancer and radiation therapy: current advances and future directions. *Int. J. Med. Sci.* **9**, 193–9 (2012).
 21. Begg, A. C., Stewart, F. A. & Vens, C. Strategies to improve radiotherapy with targeted drugs. *Nat. Rev. Cancer* **11**, 239–253 (2011).
 22. Jackson, S. P. & Bartek, J. The DNA-damage response in human biology and disease. *Nature* **461**, 1071–1078 (2009).
 23. Malhotra, V. & Perry, M. C. Classical Chemotherapy: Mechanisms, Toxicities and the Therapeutic Window. *Cancer Biol. Ther.* **2**, 1–3 (2003).
 24. Cosse, J.-P. & Michiels, C. Tumour hypoxia affects the responsiveness of cancer cells to chemotherapy and promotes cancer progression. *Anticancer. Agents Med. Chem.* **8**, 790–7 (2008).
 25. Oiseth, S. J. & Aziz, M. S. Cancer immunotherapy: a brief review of the history, possibilities, and challenges ahead. *J. Cancer Metastasis Treat.* **3**, 250 (2017).
 26. Murphy, K. *Janeway's Immunobiology 8th edition.* (Garland Science, 2012).
 27. Bals, R. & Hiemstra, P. S. Innate immunity in the lung: how epithelial cells fight against respiratory pathogens. *Eur. Respir. J.* **23**, 327–333 (2004).
 28. Bonilla, F. A. & Oettgen, H. C. Adaptive immunity. *J. Allergy Clin. Immunol.* **125**, S33–S40 (2010).
 29. Hopton Cann, S. A., van Netten, J. P. & van Netten, C. Dr William Coley and tumour regression: a place in history or in the future. *Postgrad. Med. J.* **79**, 672–80 (2003).
 30. Gorer, P. A., Lyman, S. & Snell, G. D. Studies on the Genetic and Antigenic Basis of Tumour Transplantation. Linkage between a Histocompatibility Gene and 'Fused' in Mice. *Proc. R. Soc. London. Ser. B - Biol. Sci.* **135**, 499–505 (1948).
 31. Billingham, R. E., Brent, L. & Medawar, P. B. Quantitative Studies on Tissue Transplantation Immunity. III. Actively Acquired Tolerance. *Philos. Trans. R. Soc. Lond. B. Biol. Sci.* **239**, 357–414 (1956).
 32. ISAACS, A. & LINDENMANN, J. Virus interference. I. The interferon. *Proc. R. Soc. London. Ser. B, Biol. Sci.* **147**, 258–67 (1957).
 33. Edelman, G. M. & Poulik, M. D. STUDIES ON STRUCTURAL UNITS OF THE γ -GLOBULINS. *J. Exp. Med.* **113**, 861–884 (1961).
 34. FLEISCHMAN, J., PORTER, R. & PRESS, E. THE ARRANGEMENT OF THE PEPTIDE CHAINS IN γ -GLOBULIN. *Biochem. J.* **88**, 220–228 (1963).
 35. Porter, R. R. The hydrolysis of rabbit γ -globulin and antibodies with crystalline papain. *Biochem. J.* **73**, 119–127 (1959).
 36. Swann, J. B. & Smyth, M. J. Immune surveillance of tumors. *J. Clin. Invest.* **117**, 1137–46 (2007).
 37. Shankaran, V. *et al.* IFN γ and lymphocytes prevent primary tumour development and shape tumour immunogenicity. *Nature* **410**, 1107–1111 (2001).

38. Pagès, F. *et al.* Effector Memory T Cells, Early Metastasis, and Survival in Colorectal Cancer. *N. Engl. J. Med.* **353**, 2654–2666 (2005).
39. Kondo, M. Lymphoid and myeloid lineage commitment in multipotent hematopoietic progenitors. *Immunol. Rev.* **238**, 37–46 (2010).
40. Blom, B. & Spits, H. DEVELOPMENT OF HUMAN LYMPHOID CELLS. *Annu. Rev. Immunol.* **24**, 287–320 (2006).
41. Zlotoff, D. A. & Bhandoola, A. Hematopoietic progenitor migration to the adult thymus. *Ann. N. Y. Acad. Sci.* **1217**, 122–38 (2011).
42. Yan, F. *et al.* Thymic function in the regulation of T cells, and molecular mechanisms underlying the modulation of cytokines and stress signaling. *Mol. Med. Rep.* **16**, 7175–7184 (2017).
43. Ebert, P. J. R., Li, Q.-J., Huppa, J. B. & Davis, M. M. Functional development of the T cell receptor for antigen. *Prog. Mol. Biol. Transl. Sci.* **92**, 65–100 (2010).
44. Bassing, C. H., Swat, W. & Alt, F. W. The Mechanism and Regulation of Chromosomal V(D)J Recombination. *Cell* **109**, S45–S55 (2002).
45. Roth, D. B. V(D)J Recombination: Mechanism, Errors, and Fidelity. *Microbiol. Spectr.* **2**, (2014).
46. Call, M. E., Pyrdol, J. & Wucherpfennig, K. W. Stoichiometry of the T-cell receptor-CD3 complex and key intermediates assembled in the endoplasmic reticulum. *EMBO J.* **23**, 2348–57 (2004).
47. Janas, M. L. *et al.* Thymic development beyond beta-selection requires phosphatidylinositol 3-kinase activation by CXCR4. *J. Exp. Med.* **207**, 247–61 (2010).
48. Klein, L., Kyewski, B., Allen, P. M. & Hogquist, K. A. Positive and negative selection of the T cell repertoire: what thymocytes see (and don't see). *Nat. Rev. Immunol.* **14**, 377–91 (2014).
49. Bridgeman, J. S., Sewell, A. K., Miles, J. J., Price, D. A. & Cole, D. K. Structural and biophysical determinants of $\alpha\beta$ T-cell antigen recognition. *Immunology* **135**, 9–18 (2012).
50. Alberts, B. *et al.* *Molecular Biology of the Cell.* (Garland Science, 2002).
51. Wieczorek, M. *et al.* Major Histocompatibility Complex (MHC) Class I and MHC Class II Proteins: Conformational Plasticity in Antigen Presentation. *Front. Immunol.* **8**, 292 (2017).
52. Sprent, J. Antigen-presenting cells. Professionals and amateurs. *Curr. Biol.* **5**, 1095–7 (1995).
53. Masopust, D. & Schenkel, J. M. The integration of T cell migration, differentiation and function. *Nat. Rev. Immunol.* **13**, 309–320 (2013).
54. Ager, A. & May, M. J. Understanding high endothelial venules: Lessons for cancer immunology. *Oncoimmunology* **4**, e1008791 (2015).
55. Förster, R., Davalos-Misslitz, A. C. & Rot, A. CCR7 and its ligands: balancing immunity and tolerance. *Nat. Rev. Immunol.* **8**, 362–371 (2008).
56. Rosen, S. D. Ligands for L-Selectin: Homing, Inflammation, and Beyond. *Annu.*

- Rev. Immunol.* **22**, 129–156 (2004).
57. Girard, J.-P., Moussion, C. & Förster, R. HEVs, lymphatics and homeostatic immune cell trafficking in lymph nodes. *Nat. Rev. Immunol.* **12**, 762–773 (2012).
 58. Hennecke, J. & Wiley, D. C. T Cell Receptor–MHC Interactions up Close. *Cell* **104**, 1–4 (2001).
 59. Li, Y., Yin, Y. & Mariuzza, R. A. Structural and biophysical insights into the role of CD4 and CD8 in T cell activation. *Front. Immunol.* **4**, 206 (2013).
 60. Wang, J. H. *et al.* Crystal structure of the human CD4 N-terminal two-domain fragment complexed to a class II MHC molecule. *Proc. Natl. Acad. Sci. U. S. A.* **98**, 10799–804 (2001).
 61. Parrish, H. L. *et al.* A Transmembrane Domain GGxxG Motif in CD4 Contributes to Its Lck-Independent Function but Does Not Mediate CD4 Dimerization. *PLoS One* **10**, e0132333 (2015).
 62. Huse, M., Eck, M. J. & Harrison, S. C. A Zn²⁺ ion links the cytoplasmic tail of CD4 and the N-terminal region of Lck. *J. Biol. Chem.* **273**, 18729–33 (1998).
 63. Frago, R. *et al.* Lipid Raft Distribution of CD4 Depends on its Palmitoylation and Association with Lck, and Evidence for CD4-Induced Lipid Raft Aggregation as an Additional Mechanism to Enhance CD3 Signaling. *J. Immunol.* **170**, 913–921 (2003).
 64. Chang, H.-C. *et al.* Structural and Mutational Analyses of a CD8 $\alpha\beta$ Heterodimer and Comparison with the CD8 $\alpha\alpha$ Homodimer. *Immunity* **23**, 661–671 (2005).
 65. Wang, R., Natarajan, K. & Margulies, D. H. Structural basis of the CD8 alpha beta/MHC class I interaction: focused recognition orients CD8 beta to a T cell proximal position. *J. Immunol.* **183**, 2554–64 (2009).
 66. Wong, J. S. *et al.* Stalk Region of γ -Chain Enhances the Coreceptor Function of CD8. *J. Immunol.* **171**, 867–874 (2003).
 67. Kim, P. W., Sun, Z.-Y. J., Blacklow, S. C., Wagner, G. & Eck, M. J. A zinc clasp structure tethers Lck to T cell coreceptors CD4 and CD8. *Science* **301**, 1725–8 (2003).
 68. Pang, D. J., Hayday, A. C. & Bijlmakers, M.-J. CD8 Raft Localization Is Induced by Its Assembly into CD8 $\alpha\beta$ Heterodimers, Not CD8 $\alpha\alpha$ Homodimers. *J. Biol. Chem.* **282**, 13884–13894 (2007).
 69. Palacios, E. H. & Weiss, A. Function of the Src-family kinases, Lck and Fyn, in T-cell development and activation. *Oncogene* **23**, 7990–8000 (2004).
 70. Wang, H. *et al.* ZAP-70: An Essential Kinase in T-cell Signaling. *Cold Spring Harb. Perspect. Biol.* **2**, a002279–a002279 (2010).
 71. Finco, T. S., Kadlecsek, T., Zhang, W., Samelson, L. E. & Weiss, A. LAT Is Required for TCR-Mediated Activation of PLC γ 1 and the Ras Pathway. *Immunity* **9**, 617–626 (1998).
 72. Zhang, W., Sloan-Lancaster, J., Kitchen, J., Tribble, R. P. & Samelson, L. E. LAT: The ZAP-70 Tyrosine Kinase Substrate that Links T Cell Receptor to Cellular Activation. *Cell* **92**, 83–92 (1998).

73. Boomer, J. S. & Green, J. M. An enigmatic tail of CD28 signaling. *Cold Spring Harb. Perspect. Biol.* **2**, a002436 (2010).
74. Wherry, E. J. & Kurachi, M. Molecular and cellular insights into T cell exhaustion. *Nat. Rev. Immunol.* **15**, 486–499 (2015).
75. Schwartz, R. H. T CELL ANERGY. *Annu. Rev. Immunol.* **21**, 305–334 (2003).
76. Beyersdorf, N., Kerkau, T. & Hünig, T. CD28 co-stimulation in T-cell homeostasis: a recent perspective. *ImmunoTargets Ther.* **4**, 111–22 (2015).
77. Lever, M., Maini, P. K., van der Merwe, P. A. & Dushek, O. Phenotypic models of T cell activation. *Nat. Rev. Immunol.* **14**, 619–629 (2014).
78. Jury, E. C., Flores-Borja, F. & Kabouridis, P. S. Lipid rafts in T cell signalling and disease. *Semin. Cell Dev. Biol.* **18**, 608–15 (2007).
79. Kabouridis, P. S. Lipid rafts in T cell receptor signalling (Review). *Mol. Membr. Biol.* **23**, 49–57 (2006).
80. Palacios, E. H. & Weiss, A. Function of the Src-family kinases, Lck and Fyn, in T-cell development and activation. *Oncogene* **23**, 7990–8000 (2004).
81. Marwali, M. R., MacLeod, M. A., Muzia, D. N. & Takei, F. Lipid Rafts Mediate Association of LFA-1 and CD3 and Formation of the Immunological Synapse of CTL. *J. Immunol.* **173**, 2960–2967 (2004).
82. Jin, Z.-X. *et al.* Impaired TCR signaling through dysfunction of lipid rafts in sphingomyelin synthase 1 (SMS1)-knockdown T cells. *Int. Immunol.* **20**, 1427–1437 (2008).
83. Kabouridis, P. S., Magee, A. I. & Ley, S. C. S-acylation of LCK protein tyrosine kinase is essential for its signalling function in T lymphocytes. *EMBO J.* **16**, 4983–4998 (1997).
84. Williams, C. M. *et al.* Normalized Synergy Predicts That CD8 Co-Receptor Contribution to T Cell Receptor (TCR) and pMHC Binding Decreases As TCR Affinity Increases in Human Viral-Specific T Cells. *Front. Immunol.* **8**, 894 (2017).
85. Holler, P. D. *et al.* In vitro evolution of a T cell receptor with high affinity for peptide/MHC. *Proc. Natl. Acad. Sci. U. S. A.* **97**, 5387–92 (2000).
86. Andersen, T. C. B. *et al.* The SH3 domains of the protein kinases ITK and LCK compete for adjacent sites on T cell-specific adapter protein. *J. Biol. Chem.* **294**, 15480–15494 (2019).
87. Rossy, J., Owen, D. M., Williamson, D. J., Yang, Z. & Gaus, K. Conformational states of the kinase Lck regulate clustering in early T cell signaling. *Nat. Immunol.* **14**, 82–89 (2013).
88. Nika, K. *et al.* Constitutively active Lck kinase in T cells drives antigen receptor signal transduction. *Immunity* **32**, 766–77 (2010).
89. Gil, D., Schamel, W. W. A., Montoya, M., Sánchez-Madrid, F. & Alarcón, B. Recruitment of Nck by CD3 ϵ Reveals a Ligand-Induced Conformational Change Essential for T Cell Receptor Signaling and Synapse Formation. *Cell* **109**, 901–912 (2002).
90. Lettau, M., Pieper, J. & Janssen, O. Nck adapter proteins: functional versatility in

- T cells. *Cell Commun. Signal.* **7**, 1 (2009).
91. Borroto, A. *et al.* Relevance of Nck–CD3 ϵ Interaction for T Cell Activation In Vivo. *J. Immunol.* **192**, 2042–2053 (2014).
 92. Risueño, R. M., Schamel, W. W. A. & Alarcón, B. T Cell Receptor Engagement Triggers Its CD3 ϵ and CD3 ζ Subunits to Adopt a Compact, Locked Conformation. *PLoS One* **3**, e1747 (2008).
 93. Swamy, M. *et al.* A Cholesterol-Based Allosteric Model of T Cell Receptor Phosphorylation. *Immunity* **44**, 1091–1101 (2016).
 94. Blanco, R. & Alarcón, B. TCR Nanoclusters as the Framework for Transmission of Conformational Changes and Cooperativity. *Front. Immunol.* **3**, 115 (2012).
 95. Chakraborty, A. K. & Weiss, A. Insights into the initiation of TCR signaling. *Nat. Immunol.* **15**, 798–807 (2014).
 96. Razvag, Y., Neve-Oz, Y., Sajman, J., Rechtes, M. & Sherman, E. Nanoscale kinetic segregation of TCR and CD45 in engaged microvilli facilitates early T cell activation. *Nat. Commun.* **9**, 732 (2018).
 97. Dustin, M. L., Chakraborty, A. K. & Shaw, A. S. Understanding the Structure and Function of the Immunological Synapse. *Cold Spring Harb. Perspect. Biol.* **2**, a002311–a002311 (2010).
 98. Monks, C. R. F., Freiberg, B. A., Kupfer, H., Sciaky, N. & Kupfer, A. Three-dimensional segregation of supramolecular activation clusters in T cells. *Nature* **395**, 82–86 (1998).
 99. Alarcón, B., Mestre, D. & Martínez-Martín, N. The immunological synapse: a cause or consequence of T-cell receptor triggering? *Immunology* **133**, 420–425 (2011).
 100. Yokosuka, T. *et al.* Newly generated T cell receptor microclusters initiate and sustain T cell activation by recruitment of Zap70 and SLP-76. *Nat. Immunol.* **6**, 1253–62 (2005).
 101. Campi, G., Varma, R. & Dustin, M. L. Actin and agonist MHC-peptide complex-dependent T cell receptor microclusters as scaffolds for signaling. *J. Exp. Med.* **202**, 1031–6 (2005).
 102. Lee, K.-H. *et al.* The Immunological Synapse Balances T Cell Receptor Signaling and Degradation. *Science (80-.)*. **302**, 1218–1222 (2003).
 103. Vardhana, S., Choudhuri, K., Varma, R. & Dustin, M. L. Essential Role of Ubiquitin and TSG101 Protein in Formation and Function of the Central Supramolecular Activation Cluster. *Immunity* **32**, 531–540 (2010).
 104. Schamel, W. W. A. *et al.* Coexistence of multivalent and monovalent TCRs explains high sensitivity and wide range of response. *J. Exp. Med.* **202**, 493–503 (2005).
 105. Lillemeier, B. F., Pfeiffer, J. R., Surviladze, Z., Wilson, B. S. & Davis, M. M. Plasma membrane-associated proteins are clustered into islands attached to the cytoskeleton. *Proc. Natl. Acad. Sci. U. S. A.* **103**, 18992–7 (2006).
 106. Lillemeier, B. F. *et al.* TCR and Lat are expressed on separate protein islands on T

- cell membranes and concatenate during activation. *Nat. Immunol.* **11**, 90–96 (2010).
107. Obst, R. The Timing of T Cell Priming and Cycling. *Front. Immunol.* **6**, 563 (2015).
 108. Mempel, T. R., Henrickson, S. E. & von Andrian, U. H. T-cell priming by dendritic cells in lymph nodes occurs in three distinct phases. *Nature* **427**, 154–159 (2004).
 109. Simms, P. E. & Ellis, T. M. Utility of flow cytometric detection of CD69 expression as a rapid method for determining poly- and oligoclonal lymphocyte activation. *Clin. Diagn. Lab. Immunol.* **3**, 301–4 (1996).
 110. Malek, T. R. & Castro, I. Interleukin-2 Receptor Signaling: At the Interface between Tolerance and Immunity. *Immunity* **33**, 153 (2010).
 111. Blair, D. A. & Dustin, M. L. T cell priming goes through a new phase. *Nat. Immunol.* **14**, 311–312 (2013).
 112. Pennock, N. D. *et al.* T cell responses: naive to memory and everything in between. *Adv. Physiol. Educ.* **37**, 273–83 (2013).
 113. Winstead, C. J. & Weaver, C. T. Dwelling on T Cell Fate Decisions. *Cell* **153**, 739–741 (2013).
 114. Kuniyasu, Y. *et al.* Naturally anergic and suppressive CD25+CD4+ T cells as a functionally and phenotypically distinct immunoregulatory T cell subpopulation. *Int. Immunol.* **12**, 1145–1155 (2000).
 115. Curtsinger, J. M. *et al.* Inflammatory cytokines provide a third signal for activation of naive CD4+ and CD8+ T cells. *J. Immunol.* **162**, 3256–62 (1999).
 116. Urban, J. F. *et al.* Local TH1 and TH2 responses to parasitic infection in the intestine: regulation by IFN-gamma and IL-4. *Vet. Immunol. Immunopathol.* **54**, 337–44 (1996).
 117. Taylor-Robinson, A. W. & Phillips, R. S. Functional characterization of protective CD4+ T-cell clones reactive to the murine malaria parasite *Plasmodium chabaudi*. *Immunology* **77**, 99–105 (1992).
 118. Cox, M. A., Harrington, L. E. & Zajac, A. J. Cytokines and the inception of CD8 T cell responses. *Trends Immunol.* **32**, 180–6 (2011).
 119. Henson, S. M. & Akbar, A. N. KLRG1--more than a marker for T cell senescence. *Age (Dordr).* **31**, 285–91 (2009).
 120. Agarwal, P. *et al.* Gene Regulation and Chromatin Remodeling by IL-12 and Type I IFN in Programming for CD8 T Cell Effector Function and Memory. *J. Immunol.* **183**, 1695–1704 (2009).
 121. Chowdhury, D. & Lieberman, J. Death by a thousand cuts: granzyme pathways of programmed cell death. *Annu. Rev. Immunol.* **26**, 389–420 (2008).
 122. Peters, P. J. *et al.* Cytotoxic T lymphocyte granules are secretory lysosomes, containing both perforin and granzymes. *J. Exp. Med.* **173**, 1099–109 (1991).
 123. Volpe, E., Sambucci, M., Battistini, L. & Borsellino, G. Fas–Fas Ligand: Checkpoint of T Cell Functions in Multiple Sclerosis. *Front. Immunol.* **7**, 382 (2016).
 124. Lauvau, G. & Soudja, S. M. Mechanisms of Memory T Cell Activation and Effective Immunity. *Adv. Exp. Med. Biol.* **850**, 73–80 (2015).

125. Arens, R. & Schoenberger, S. P. Plasticity in programming of effector and memory CD8 T-cell formation. *Immunol. Rev.* **235**, 190–205 (2010).
126. Westera, L. *et al.* Closing the gap between T-cell life span estimates from stable isotope-labeling studies in mice and humans. *Blood* **122**, 2205–2212 (2013).
127. Hammarlund, E. *et al.* Duration of antiviral immunity after smallpox vaccination. *Nat. Med.* **9**, 1131–1137 (2003).
128. Gerriets, V. A. & Rathmell, J. C. Metabolic pathways in T cell fate and function. *Trends Immunol.* **33**, 168–73 (2012).
129. Dunn, G. P., Old, L. J. & Schreiber, R. D. The Three Es of Cancer Immunoediting. *Annu. Rev. Immunol.* **22**, 329–360 (2004).
130. Matzinger, P. Tolerance, Danger, and the Extended Family. *Annu. Rev. Immunol.* **12**, 991–1045 (1994).
131. Chow, M. T. & Luster, A. D. Chemokines in Cancer. *Cancer Immunol. Res.* **2**, 1125–1131 (2014).
132. Mittal, D., Gubin, M. M., Schreiber, R. D. & Smyth, M. J. New insights into cancer immunoediting and its three component phases-elimination, equilibrium and escape. *Curr. Opin. Immunol.* **27**, 16–25 (2014).
133. Teng, M. W. L. *et al.* Opposing roles for IL-23 and IL-12 in maintaining occult cancer in an equilibrium state. *Cancer Res.* **72**, 3987–96 (2012).
134. Loeb, L. A., Loeb, K. R. & Anderson, J. P. Multiple mutations and cancer. *Proc. Natl. Acad. Sci.* **100**, 776–781 (2003).
135. Marincola, F. M., Jaffee, E. M., Hicklin, D. J. & Ferrone, S. Escape of Human Solid Tumors from T-Cell Recognition: Molecular Mechanisms and Functional Significance. *Adv. Immunol.* **74**, 181–273 (1999).
136. Hinz, S. *et al.* Bcl-XL protects pancreatic adenocarcinoma cells against CD95- and TRAIL-receptor-mediated apoptosis. *Oncogene* **19**, 5477–5486 (2000).
137. Kataoka, T. *et al.* FLIP prevents apoptosis induced by death receptors but not by perforin/granzyme B, chemotherapeutic drugs, and gamma irradiation. *J. Immunol.* **161**, 3936–42 (1998).
138. Rodriguez, P. C., Quiceno, D. G. & Ochoa, A. C. L-arginine availability regulates T-lymphocyte cell-cycle progression. *Blood* **109**, 1568–1573 (2007).
139. Nagaraj, S. & Gabilovich, D. I. Regulation of suppressive function of myeloid-derived suppressor cells by CD4+ T cells. *Semin. Cancer Biol.* **22**, 282–8 (2012).
140. Otsuji, M., Kimura, Y., Aoe, T., Okamoto, Y. & Saito, T. Oxidative stress by tumor-derived macrophages suppresses the expression of CD3 chain of T-cell receptor complex and antigen-specific T-cell responses. *Proc. Natl. Acad. Sci.* **93**, 13119–13124 (1996).
141. Agostinelli, E. & Seiler, N. Non-irradiation-derived reactive oxygen species (ROS) and cancer: therapeutic implications. *Amino Acids* **31**, 341–355 (2006).
142. Sica, A., Schioppa, T., Mantovani, A. & Allavena, P. Tumour-associated macrophages are a distinct M2 polarised population promoting tumour progression: Potential targets of anti-cancer therapy. *Eur. J. Cancer* **42**, 717–727

- (2006).
143. Vesely, M. D., Kershaw, M. H., Schreiber, R. D. & Smyth, M. J. Natural Innate and Adaptive Immunity to Cancer. *Annu. Rev. Immunol.* **29**, 235–271 (2011).
 144. Mellman, I., Coukos, G. & Dranoff, G. Cancer immunotherapy comes of age. *Nature* **480**, 480–489 (2011).
 145. Couzin-Frankel, J. Cancer Immunotherapy. *Science (80-.)*. **342**, 1432–1433 (2013).
 146. Drake, C. G., Lipson, E. J. & Brahmer, J. R. Breathing new life into immunotherapy: review of melanoma, lung and kidney cancer. *Nat. Rev. Clin. Oncol.* **11**, 24–37 (2014).
 147. Pulendran, B. & Ahmed, R. Immunological mechanisms of vaccination. *Nat. Immunol.* **12**, 509–517 (2011).
 148. Hollingsworth, R. E. & Jansen, K. Turning the corner on therapeutic cancer vaccines. *npj Vaccines* **4**, 7 (2019).
 149. Vigneron, N. Human Tumor Antigens and Cancer Immunotherapy. *Biomed Res. Int.* **2015**, 1–17 (2015).
 150. Disis, M. L. *et al.* Concurrent Trastuzumab and HER2/neu-Specific Vaccination in Patients With Metastatic Breast Cancer. *J. Clin. Oncol.* **27**, 4685–4692 (2009).
 151. De Smet, C. *et al.* Sequence and expression pattern of the human MAGE2 gene. *Immunogenetics* **39**, 121–9 (1994).
 152. Cannuyer, J., Lorient, A., Parvizi, G. K. & De Smet, C. Epigenetic Hierarchy within the MAGEA1 Cancer-Germline Gene: Promoter DNA Methylation Dictates Local Histone Modifications. *PLoS One* **8**, e58743 (2013).
 153. Overwijk, W. W. Cancer vaccines in the era of checkpoint blockade: the magic is in the adjuvant. *Curr. Opin. Immunol.* **47**, 103–109 (2017).
 154. Zhang, H. *et al.* Comparing Pooled Peptides with Intact Protein for Accessing Cross-presentation Pathways for Protective CD8+ and CD4+ T Cells. *J. Biol. Chem.* **284**, 9184–9191 (2009).
 155. Bijker, M. S. *et al.* Superior induction of anti-tumor CTL immunity by extended peptide vaccines involves prolonged, DC-focused antigen presentation. *Eur. J. Immunol.* **38**, 1033–1042 (2008).
 156. Pisetsky, D. S. The origin and properties of extracellular DNA: From PAMP to DAMP. *Clin. Immunol.* **144**, 32–40 (2012).
 157. Karikó, K. *et al.* Incorporation of Pseudouridine Into mRNA Yields Superior Nonimmunogenic Vector With Increased Translational Capacity and Biological Stability. *Mol. Ther.* **16**, 1833–1840 (2008).
 158. Karikó, K. & Weissman, D. Naturally occurring nucleoside modifications suppress the immunostimulatory activity of RNA: implication for therapeutic RNA development. *Curr. Opin. Drug Discov. Devel.* **10**, 523–32 (2007).
 159. Miller, J. D. *et al.* Human Effector and Memory CD8+ T Cell Responses to Smallpox and Yellow Fever Vaccines. *Immunity* **28**, 710–722 (2008).
 160. Scott, A. M., Allison, J. P. & Wolchok, J. D. Monoclonal antibodies in cancer

- therapy. *Cancer Immun.* **12**, 14 (2012).
161. KÖHLER, G. & MILSTEIN, C. Continuous cultures of fused cells secreting antibody of predefined specificity. *Nature* **256**, 495–497 (1975).
 162. Cheson, B. D. & Leonard, J. P. Monoclonal Antibody Therapy for B-Cell Non-Hodgkin's Lymphoma. *N. Engl. J. Med.* **359**, 613–626 (2008).
 163. Van Cutsem, E. *et al.* Cetuximab and Chemotherapy as Initial Treatment for Metastatic Colorectal Cancer. *N. Engl. J. Med.* **360**, 1408–1417 (2009).
 164. Welt, S. *et al.* Antibody targeting in metastatic colon cancer: a phase I study of monoclonal antibody F19 against a cell-surface protein of reactive tumor stromal fibroblasts. *J. Clin. Oncol.* **12**, 1193–1203 (1994).
 165. Weiner, G. J. Rituximab: mechanism of action. *Semin. Hematol.* **47**, 115–23 (2010).
 166. Bou-Assaly, W. & Mukherji, S. Cetuximab (Erbix). *Am. J. Neuroradiol.* **31**, 626–627 (2010).
 167. Labrijn, A. F., Janmaat, M. L., Reichert, J. M. & Parren, P. W. H. I. Bispecific antibodies: a mechanistic review of the pipeline. *Nat. Rev. Drug Discov.* **18**, 585–608 (2019).
 168. Wang, K., Wei, G. & Liu, D. CD19: a biomarker for B cell development, lymphoma diagnosis and therapy. *Exp. Hematol. Oncol.* **1**, 36 (2012).
 169. Wu, J., Fu, J., Zhang, M. & Liu, D. Blinatumomab: a bispecific T cell engager (BiTE) antibody against CD19/CD3 for refractory acute lymphoid leukemia. *J. Hematol. Oncol.* **8**, 104 (2015).
 170. Rudd, C. E., Taylor, A. & Schneider, H. CD28 and CTLA-4 coreceptor expression and signal transduction. *Immunol. Rev.* **229**, 12–26 (2009).
 171. Hodi, F. S. *et al.* Improved Survival with Ipilimumab in Patients with Metastatic Melanoma. *N. Engl. J. Med.* **363**, 711–723 (2010).
 172. McDermott, D. F. *et al.* Atezolizumab, an Anti-Programmed Death-Ligand 1 Antibody, in Metastatic Renal Cell Carcinoma: Long-Term Safety, Clinical Activity, and Immune Correlates From a Phase Ia Study. *J. Clin. Oncol.* **34**, 833–42 (2016).
 173. Guo, L., Zhang, H. & Chen, B. Nivolumab as Programmed Death-1 (PD-1) Inhibitor for Targeted Immunotherapy in Tumor. *J. Cancer* **8**, 410–416 (2017).
 174. Raja, J., Ludwig, J. M., Gettinger, S. N., Schalper, K. A. & Kim, H. S. Oncolytic virus immunotherapy: future prospects for oncology. *J. Immunother. Cancer* **6**, 140 (2018).
 175. Nguyen, T., Avci, N. G., Shin, D. H., Martinez-Velez, N. & Jiang, H. Tune Up In Situ Autovaccination against Solid Tumors with Oncolytic Viruses. *Cancers (Basel)*. **10**, (2018).
 176. Fink, S. L. & Cookson, B. T. Apoptosis, pyroptosis, and necrosis: mechanistic description of dead and dying eukaryotic cells. *Infect. Immun.* **73**, 1907–16 (2005).
 177. Russell, S. J., Peng, K.-W. & Bell, J. C. Oncolytic virotherapy. *Nat. Biotechnol.* **30**, 658–670 (2012).

178. Bommareddy, P. K., Shettigar, M. & Kaufman, H. L. Integrating oncolytic viruses in combination cancer immunotherapy. *Nat. Rev. Immunol.* **18**, 498–513 (2018).
179. Guo, Z. S. *et al.* Vaccinia virus-mediated cancer immunotherapy: cancer vaccines and oncolytics. *J. Immunother. Cancer* **7**, 6 (2019).
180. Tsang, K. Y. Analyses of Recombinant Vaccinia and Fowlpox Vaccine Vectors Expressing Transgenes for Two Human Tumor Antigens and Three Human Costimulatory Molecules. *Clin. Cancer Res.* **11**, 1597–1607 (2005).
181. Kalos, M. & June, C. Adoptive T Cell Transfer for Cancer Immunotherapy in the Era of Synthetic Biology. *Immunity* **39**, 49–60 (2013).
182. June, C. H. Adoptive T cell therapy for cancer in the clinic. *J. Clin. Invest.* **117**, 1466–76 (2007).
183. Kalos, M. & June, C. H. Adoptive T cell transfer for cancer immunotherapy in the era of synthetic biology. *Immunity* **39**, 49–60 (2013).
184. Restifo, N. P., Dudley, M. E. & Rosenberg, S. A. Adoptive immunotherapy for cancer: harnessing the T cell response. *Nat. Rev. Immunol.* **12**, 269–281 (2012).
185. Rosenberg, S. A., Restifo, N. P., Yang, J. C., Morgan, R. A. & Dudley, M. E. Adoptive cell transfer: a clinical path to effective cancer immunotherapy. *Nat. Rev. Cancer* **8**, 299–308 (2008).
186. Dudley, M. E. *et al.* Cancer Regression and Autoimmunity in Patients After Clonal Repopulation with Antitumor Lymphocytes. *Science (80-.)*. **298**, 850–854 (2002).
187. Restifo, N. P., Dudley, M. E. & Rosenberg, S. a. Adoptive immunotherapy for cancer: harnessing the T cell response. *Nat. Rev. Immunol.* **12**, 269–281 (2012).
188. Badalamenti, G. *et al.* Role of tumor-infiltrating lymphocytes in patients with solid tumors: Can a drop dig a stone? *Cell. Immunol.* **343**, 103753 (2019).
189. Morgan, R. A. *et al.* Cancer Regression in Patients After Transfer of Genetically Engineered Lymphocytes. *Science (80-.)*. **314**, 126–129 (2006).
190. Rosenberg, S. A. & Restifo, N. P. Adoptive cell transfer as personalized immunotherapy for human cancer. *Science (80-.)*. **348**, 62–68 (2015).
191. Bubeník, J. Tumour MHC class I downregulation and immunotherapy (Review). *Oncol. Rep.* **10**, 2005–8
192. Garfall, A. L., Fraietta, J. A. & Maus, M. V. Immunotherapy with chimeric antigen receptors for multiple myeloma. *Discov. Med.* **17**, 37–46 (2014).
193. Eshhar, Z., Waks, T., Gross, G. & Schindler, D. G. Specific activation and targeting of cytotoxic lymphocytes through chimeric single chains consisting of antibody-binding domains and the gamma or zeta subunits of the immunoglobulin and T-cell receptors. *Proc. Natl. Acad. Sci.* **90**, 720–724 (1993).
194. Irving, B. A. & Weiss, A. The cytoplasmic domain of the T cell receptor ζ chain is sufficient to couple to receptor-associated signal transduction pathways. *Cell* **64**, 891–901 (1991).
195. Lamers, C. H. J. *et al.* Treatment of metastatic renal cell carcinoma with autologous T-lymphocytes genetically retargeted against carbonic anhydrase IX: first clinical experience. *J. Clin. Oncol.* **24**, e20-2 (2006).

196. Kershaw, M. H. *et al.* A phase I study on adoptive immunotherapy using gene-modified T cells for ovarian cancer. *Clin. Cancer Res.* **12**, 6106–15 (2006).
197. Kowolik, C. M. *et al.* CD28 costimulation provided through a CD19-specific chimeric antigen receptor enhances in vivo persistence and antitumor efficacy of adoptively transferred T cells. *Cancer Res.* **66**, 10995–1004 (2006).
198. Milone, M. C. *et al.* Chimeric Receptors Containing CD137 Signal Transduction Domains Mediate Enhanced Survival of T Cells and Increased Antileukemic Efficacy In Vivo. *Mol. Ther.* **17**, 1453–1464 (2009).
199. Brentjens, R. J. *et al.* Genetically targeted T cells eradicate systemic acute lymphoblastic leukemia xenografts. *Clin. Cancer Res.* **13**, 5426–35 (2007).
200. Sadelain, M., Brentjens, R. & Rivière, I. The Basic Principles of Chimeric Antigen Receptor Design. *Cancer Discov.* **3**, 388–398 (2013).
201. Watts, T. H. Staying alive: T cell costimulation, CD28, and Bcl-xL. *J. Immunol.* **185**, 3785–7 (2010).
202. Carpenito, C. *et al.* Control of large, established tumor xenografts with genetically retargeted human T cells containing CD28 and CD137 domains. *Proc. Natl. Acad. Sci.* **106**, 3360–3365 (2009).
203. Zhong, X.-S., Matsushita, M., Plotkin, J., Riviere, I. & Sadelain, M. Chimeric Antigen Receptors Combining 4-1BB and CD28 Signaling Domains Augment PI3kinase/AKT/Bcl-XL Activation and CD8+ T Cell-mediated Tumor Eradication. *Mol. Ther.* **18**, 413–420 (2010).
204. Stoiber, S. *et al.* Limitations in the Design of Chimeric Antigen Receptors for Cancer Therapy. *Cells* **8**, (2019).
205. Huston, J. S. *et al.* Protein engineering of antibody binding sites: recovery of specific activity in an anti-digoxin single-chain Fv analogue produced in *Escherichia coli*. *Proc. Natl. Acad. Sci.* **85**, 5879–5883 (1988).
206. Bird, R. *et al.* Single-chain antigen-binding proteins. *Science (80-.)*. **242**, 423–426 (1988).
207. Richman, S. A. *et al.* High-Affinity GD2-Specific CAR T Cells Induce Fatal Encephalitis in a Preclinical Neuroblastoma Model. *Cancer Immunol. Res.* **6**, 36–46 (2018).
208. Chen, X., Zaro, J. L. & Shen, W.-C. Fusion protein linkers: Property, design and functionality. *Adv. Drug Deliv. Rev.* **65**, 1357–1369 (2013).
209. Argos, P. An investigation of oligopeptides linking domains in protein tertiary structures and possible candidates for general gene fusion. *J. Mol. Biol.* **211**, 943–958 (1990).
210. Ajina, A. & Maher, J. Strategies to Address Chimeric Antigen Receptor Tonic Signaling. *Mol. Cancer Ther.* **17**, 1795–1815 (2018).
211. Dolezal, O. *et al.* ScFv multimers of the anti-neuraminidase antibody NC10: shortening of the linker in single-chain Fv fragment assembled in VL to VH orientation drives the formation of dimers, trimers, tetramers and higher molecular mass multimers. *Protein Eng. Des. Sel.* **13**, 565–574 (2000).

212. Whitlow, M., Filpula, D., Rollence, M. L., Feng, S.-L. & Wood, J. F. Multivalent Fvs: characterization of single-chain Fv oligomers and preparation of a bispecific Fv. *Protein Eng. Des. Sel.* **7**, 1017–1026 (1994).
213. Rafiq, S. *et al.* Optimized T-cell receptor-mimic chimeric antigen receptor T cells directed toward the intracellular Wilms Tumor 1 antigen. *Leukemia* **31**, 1788–1797 (2017).
214. Willcox, B. E. *et al.* TCR binding to peptide-MHC stabilizes a flexible recognition interface. *Immunity* **10**, 357–65 (1999).
215. Lynn, R. C. *et al.* High-affinity FR β -specific CAR T cells eradicate AML and normal myeloid lineage without HSC toxicity. *Leukemia* **30**, 1355–1364 (2016).
216. Hudecek, M. *et al.* Receptor Affinity and Extracellular Domain Modifications Affect Tumor Recognition by ROR1-Specific Chimeric Antigen Receptor T Cells. *Clin. Cancer Res.* **19**, 3153–3164 (2013).
217. Chmielewski, M., Hombach, A., Heuser, C., Adams, G. P. & Abken, H. T Cell Activation by Antibody-Like Immunoreceptors: Increase in Affinity of the Single-Chain Fragment Domain above Threshold Does Not Increase T Cell Activation against Antigen-Positive Target Cells but Decreases Selectivity. *J. Immunol.* **173**, 7647–7653 (2004).
218. Liu, X. *et al.* Affinity-Tuned ErbB2 or EGFR Chimeric Antigen Receptor T Cells Exhibit an Increased Therapeutic Index against Tumors in Mice. *Cancer Res.* **75**, 3596–3607 (2015).
219. Hammill, J. A. *et al.* Designed ankyrin repeat proteins are effective targeting elements for chimeric antigen receptors. *J. Immunother. Cancer* **3**, 55 (2015).
220. Balakrishnan, A. *et al.* Multispecific targeting with synthetic ankyrin repeat motif chimeric antigen receptors. *Clin. Cancer Res.* clincanres.1479.2019 (2019). doi:10.1158/1078-0432.ccr-19-1479
221. Krebs, S. *et al.* T cells redirected to interleukin-13R α 2 with interleukin-13 mutein-chimeric antigen receptors have anti-glioma activity but also recognize interleukin-13R α 1. *Cytotherapy* **16**, 1121–1131 (2014).
222. Hudecek, M. *et al.* The Nonsignaling Extracellular Spacer Domain of Chimeric Antigen Receptors Is Decisive for In Vivo Antitumor Activity. *Cancer Immunol. Res.* **3**, 125–135 (2015).
223. Almasbak, H. *et al.* Inclusion of an IgG1-Fc spacer abrogates efficacy of CD19 CAR T cells in a xenograft mouse model. *Gene Ther.* **22**, 391–403 (2015).
224. Hombach, A., Hombach, A. A. & Abken, H. Adoptive immunotherapy with genetically engineered T cells: modification of the IgG1 Fc ‘spacer’ domain in the extracellular moiety of chimeric antigen receptors avoids ‘off-target’ activation and unintended initiation of an innate immune response. *Gene Ther.* **17**, 1206–1213 (2010).
225. Watanabe, N. *et al.* Fine-tuning the CAR spacer improves T-cell potency. *Oncoimmunology* **5**, e1253656 (2016).
226. Jonnalagadda, M. *et al.* Chimeric Antigen Receptors With Mutated IgG4 Fc Spacer

- Avoid Fc Receptor Binding and Improve T Cell Persistence and Antitumor Efficacy. *Mol. Ther.* **23**, 757–768 (2015).
227. Hombach, A. A. *et al.* T Cell Activation by Antibody-Like Immunoreceptors: The Position of the Binding Epitope within the Target Molecule Determines the Efficiency of Activation of Redirected T Cells. *J. Immunol.* **178**, 4650–4657 (2007).
228. James, S. E. *et al.* Antigen Sensitivity of CD22-Specific Chimeric TCR Is Modulated by Target Epitope Distance from the Cell Membrane. *J. Immunol.* **180**, 7028–7038 (2008).
229. James, J. R. & Vale, R. D. Biophysical mechanism of T-cell receptor triggering in a reconstituted system. *Nature* **487**, 64–69 (2012).
230. Wilkie, S. *et al.* Retargeting of Human T Cells to Tumor-Associated MUC1: The Evolution of a Chimeric Antigen Receptor. *J. Immunol.* **180**, 4901–4909 (2008).
231. Guest, R. D. *et al.* The Role of Extracellular Spacer Regions in the Optimal Design of Chimeric Immune Receptors. *J. Immunother.* **28**, 203–211 (2005).
232. Lazar-Molnar, E., Almo, S. C. & Nathenson, S. G. The interchain disulfide linkage is not a prerequisite but enhances CD28 costimulatory function. *Cell. Immunol.* **244**, 125–9 (2006).
233. Maher, J., Brentjens, R. J., Gunset, G., Rivière, I. & Sadelain, M. Human T-lymphocyte cytotoxicity and proliferation directed by a single chimeric TCR ζ /CD28 receptor. *Nat. Biotechnol.* **20**, 70–75 (2002).
234. Fitzer-attas, C. J., Schindler, D. G., Waks, T. & Eshhar, Z. for Chimeric Single Chain of the Variable Domain Receptors : Optimal Design for T Cell Activation 1. *Immunology* **160**, 145–154 (2011).
235. Guedan, S., Calderon, H., Posey, A. D. & Maus, M. V. Engineering and Design of Chimeric Antigen Receptors. *Mol. Ther. - Methods Clin. Dev.* **12**, 145–156 (2019).
236. Pulè, M. A. *et al.* A chimeric T cell antigen receptor that augments cytokine release and supports clonal expansion of primary human T cells. *Mol. Ther.* **12**, 933–941 (2005).
237. Carpenito, C. *et al.* Control of large, established tumor xenografts with genetically retargeted human T cells containing CD28 and CD137 domains. *Proc. Natl. Acad. Sci.* **106**, 3360–3365 (2009).
238. Milone, M. C. *et al.* Chimeric Receptors Containing CD137 Signal Transduction Domains Mediate Enhanced Survival of T Cells and Increased Antileukemic Efficacy In Vivo. *Mol. Ther.* **17**, 1453–1464 (2009).
239. Zhao, Z. *et al.* Structural Design of Engineered Costimulation Determines Tumor Rejection Kinetics and Persistence of CAR T Cells. *Cancer Cell* **28**, 415–428 (2015).
240. Kawalekar, O. U. *et al.* Distinct Signaling of Coreceptors Regulates Specific Metabolism Pathways and Impacts Memory Development in CAR T Cells. *Immunity* **44**, 380–390 (2016).
241. Park, J. H. *et al.* Long-Term Follow-up of CD19 CAR Therapy in Acute Lymphoblastic Leukemia. *N. Engl. J. Med.* **378**, 449–459 (2018).
242. Lee, D. W. *et al.* T cells expressing CD19 chimeric antigen receptors for acute

- lymphoblastic leukaemia in children and young adults: a phase 1 dose-escalation trial. *Lancet* **385**, 517–528 (2015).
243. Fraietta, J. A. *et al.* Determinants of response and resistance to CD19 chimeric antigen receptor (CAR) T cell therapy of chronic lymphocytic leukemia. *Nat. Med.* **24**, 563–571 (2018).
244. Maude, S. L. *et al.* Tisagenlecleucel in Children and Young Adults with B-Cell Lymphoblastic Leukemia. *N. Engl. J. Med.* **378**, 439–448 (2018).
245. Hematti, P. *et al.* Distinct genomic integration of MLV and SIV vectors in primate hematopoietic stem and progenitor cells. *PLoS Biol.* **2**, e423 (2004).
246. Wu, X., Li, Y., Crise, B. & Burgess, S. M. Transcription Start Regions in the Human Genome Are Favored Targets for MLV Integration. *Science (80-.).* **300**, 1749–1751 (2003).
247. Schröder, A. R. W. *et al.* HIV-1 integration in the human genome favors active genes and local hotspots. *Cell* **110**, 521–9 (2002).
248. Riet, T. *et al.* Nonviral RNA Transfection to Transiently Modify T Cells with Chimeric Antigen Receptors for Adoptive Therapy. in *Methods in molecular biology (Clifton, N.J.)* **969**, 187–201 (2013).
249. Monjezi, R. *et al.* Enhanced CAR T-cell engineering using non-viral Sleeping Beauty transposition from minicircle vectors. *Leukemia* **31**, 186–194 (2017).
250. Frigault, M. J. *et al.* Identification of Chimeric Antigen Receptors That Mediate Constitutive or Inducible Proliferation of T Cells. *Cancer Immunol. Res.* **3**, 356–367 (2015).
251. Shah, N. N. *et al.* Minimal Residual Disease Negative Complete Remissions Following Anti-CD22 Chimeric Antigen Receptor (CAR) in Children and Young Adults with Relapsed/Refractory Acute Lymphoblastic Leukemia (ALL). *Blood* **128**, 650–650 (2016).
252. Porter, D. L. *et al.* Chimeric antigen receptor T cells persist and induce sustained remissions in relapsed refractory chronic lymphocytic leukemia. *Sci. Transl. Med.* **7**, 303ra139-303ra139 (2015).
253. Locke, F. L. *et al.* Phase 1 Results of ZUMA-1: A Multicenter Study of KTE-C19 Anti-CD19 CAR T Cell Therapy in Refractory Aggressive Lymphoma. *Mol. Ther.* **25**, 285–295 (2017).
254. Lamers, C. H. J. *et al.* Treatment of metastatic renal cell carcinoma with autologous T-lymphocytes genetically retargeted against carbonic anhydrase IX: first clinical experience. *J. Clin. Oncol.* **24**, e20-2 (2006).
255. Yáñez, L., Sánchez-Escamilla, M. & Perales, M.-A. CAR T Cell Toxicity: Current Management and Future Directions. *HemaSphere* **3**, e186 (2019).
256. Shimabukuro-Vornhagen, A. *et al.* Cytokine release syndrome. *J. Immunother. Cancer* **6**, 56 (2018).
257. Gust, J., Taraseviciute, A. & Turtle, C. J. Neurotoxicity Associated with CD19-Targeted CAR-T Cell Therapies. *CNS Drugs* **32**, 1091–1101 (2018).
258. Helsen, C. W. *et al.* The chimeric TAC receptor co-opts the T cell receptor yielding

- robust anti-tumor activity without toxicity. *Nat. Commun.* **9**, 3049 (2018).
259. Baeuerle, P. A. *et al.* Synthetic TRuC receptors engaging the complete T cell receptor for potent anti-tumor response. *Nat. Commun.* **10**, 1–12 (2019).
260. Arnett, K. L., Harrison, S. C. & Wiley, D. C. Crystal structure of a human CD3-epsilon/delta dimer in complex with a UCHT1 single-chain antibody fragment. *Proc. Natl. Acad. Sci. U. S. A.* **101**, 16268–73 (2004).
261. Kipriyanov, S. M., Moldenhauer, G., Martin, A. C., Kupriyanova, O. A. & Little, M. Two amino acid mutations in an anti-human CD3 single chain Fv antibody fragment that affect the yield on bacterial secretion but not the affinity. *Protein Eng.* **10**, 445–53 (1997).
262. Zahnd, C. *et al.* A designed ankyrin repeat protein evolved to picomolar affinity to Her2. *J. Mol. Biol.* **369**, 1015–28 (2007).
263. Roederer, M., Nozzi, J. L. & Nason, M. C. SPICE: Exploration and analysis of post-cytometric complex multivariate datasets. *Cytom. Part A* **79A**, 167–174 (2011).
264. Rabinovich, B. A. *et al.* Visualizing fewer than 10 mouse T cells with an enhanced firefly luciferase in immunocompetent mouse models of cancer. *Proc. Natl. Acad. Sci. U. S. A.* **105**, 14342–14346 (2008).
265. Andersen, M. H., Schrama, D., Thor Straten, P. & Becker, J. C. Cytotoxic T Cells. *J. Invest. Dermatol.* **126**, 32–41 (2006).
266. Purbhoo, M. A. *et al.* The human CD8 coreceptor effects cytotoxic T cell activation and antigen sensitivity primarily by mediating complete phosphorylation of the T cell receptor zeta chain. *J. Biol. Chem.* **276**, 32786–92 (2001).
267. Dick, J. P., Hayday, A. C. & Bijlmakers, M. J. CD8 raft localization is induced by its assembly into CD8 $\alpha\beta$ heterodimers, not CD8 $\alpha\alpha$ homodimers. *J. Biol. Chem.* **282**, 13884–13894 (2007).
268. van der Stegen, S. J. C., Hamieh, M. & Sadelain, M. The pharmacology of second-generation chimeric antigen receptors. *Nat. Rev. Drug Discov.* **14**, 499–509 (2015).
269. Alabanza, L. *et al.* Function of Novel Anti-CD19 Chimeric Antigen Receptors with Human Variable Regions Is Affected by Hinge and Transmembrane Domains. *Mol. Ther.* **25**, 2452–2465 (2017).
270. Devine, L., Kieffer, L. J., Aitken, V. & Kavathas, P. B. Human CD8 β , But Not Mouse CD8 β , Can Be Expressed in the Absence of CD8 α as a $\beta\beta$ Homodimer. *J. Immunol.* **164**, 833 (2000).
271. Zhang, M. *et al.* CD45 Signals outside of Lipid Rafts to Promote ERK Activation, Synaptic Raft Clustering, and IL-2 Production. *J. Immunol.* **174**, 1479–1490 (2005).
272. Kabouridis, P. S. Lipid rafts in T cell receptor signalling (Review). *Mol. Membr. Biol.* **23**, 49–57 (2006).
273. Holler, P. D. *et al.* In vitro evolution of a T cell receptor with high affinity for peptide/MHC. *Proc. Natl. Acad. Sci.* **97**, 5387–5392 (2000).
274. Turtle, C. J. *et al.* Immunotherapy of non-Hodgkin's lymphoma with a defined

- ratio of CD8⁺ and CD4⁺ CD19-specific chimeric antigen receptor–modified T cells. *Sci. Transl. Med.* **8**, 355ra116-355ra116 (2016).
275. Du, X., Beers, R., Fitzgerald, D. J. & Pastan, I. Differential cellular internalization of anti-CD19 and -CD22 immunotoxins results in different cytotoxic activity. *Cancer Res.* **68**, 6300–5 (2008).
 276. Shirasu, N. & Kuroki, M. Functional design of chimeric T-cell antigen receptors for adoptive immunotherapy of cancer: architecture and outcomes. *Anticancer Res.* **32**, 2377–83 (2012).
 277. Ajina, A. & Maher, J. Strategies to Address Chimeric Antigen Receptor Tonic Signaling. *Mol. Cancer Ther.* **17**, 1795–1815 (2018).
 278. Lee, M. S. *et al.* A Mechanical Switch Couples T Cell Receptor Triggering to the Cytoplasmic Juxtamembrane Regions of CD3 ζ . *Immunity* **43**, 227–239 (2015).
 279. Schönfeld, K. *et al.* Selective inhibition of tumor growth by clonal NK cells expressing an ErbB2/HER2-specific chimeric antigen receptor. *Mol. Ther.* **23**, 330–8 (2015).
 280. Gaud, G., Lesourne, R. & Love, P. E. Regulatory mechanisms in T cell receptor signalling. *Nat. Rev. Immunol.* **18**, 485–497 (2018).
 281. Glaichenhaus, N., Shastri, N., Littman, D. R. & Turner, J. M. Requirement for association of p56lck with CD4 in antigen-specific signal transduction in T cells. *Cell* **64**, 511–520 (1991).
 282. Eckhert, E., Hewitt, R. & Liedtke, M. B-cell maturation antigen directed monoclonal antibody therapies for multiple myeloma. *Immunotherapy* **11**, 801–811 (2019).
 283. Nishida, H. & Yamada, T. Monoclonal Antibody Therapies in Multiple Myeloma: A Challenge to Develop Novel Targets. *J. Oncol.* **2019**, 1–10 (2019).
 284. D’Agostino, M. & Raje, N. Anti-BCMA CAR T-cell therapy in multiple myeloma: can we do better? *Leukemia* 1–14 (2019). doi:10.1038/s41375-019-0669-4
 285. Maus, M. V. *et al.* T Cells Expressing Chimeric Antigen Receptors Can Cause Anaphylaxis in Humans. *Cancer Immunol. Res.* **1**, 26–31 (2013).
 286. Shalaby, M. R. *et al.* Development of humanized bispecific antibodies reactive with cytotoxic lymphocytes and tumor cells overexpressing the HER2 protooncogene. *J. Exp. Med.* **175**, 217–225 (1992).
 287. Zhu, Z. & Carter, P. Identification of heavy chain residues in a humanized anti-CD3 antibody important for efficient antigen binding and T cell activation. *J. Immunol.* **155**, 1903–10 (1995).
 288. HELSEN, C. W. *et al.* T CELL-ANTIGEN COUPLER WITH Y182T MUTATION AND METHODS AND USES THEREOF. PATENT WO2019071358. (2019).
 289. Carpenter, R. O. *et al.* B-cell maturation antigen is a promising target for adoptive T-cell therapy of multiple myeloma. *Clin. Cancer Res.* **19**, 2048–60 (2013).
 290. Müller-Taubenberger, A. *et al.* Calreticulin and calnexin in the endoplasmic reticulum are important for phagocytosis. *EMBO J.* **20**, 6772–6782 (2001).
 291. Clark, M. C. & Baum, L. G. T cells modulate glycans on CD43 and CD45 during

- development and activation, signal regulation, and survival. *Annals of the New York Academy of Sciences* **1253**, 58–67 (2012).
292. Jovic, M., Sharma, M., Rahajeng, J. & Caplan, S. The early endosome: A busy sorting station for proteins at the crossroads. *Histology and Histopathology* **25**, 99–112 (2010).
293. Nakamura, N. *et al.* Characterization of a cis-Golgi matrix protein, GM130. *J. Cell Biol.* **131**, 1715–1726 (1995).
294. Melvin, A. T., Woss, G. S., Park, J. H., Waters, M. L. & Allbritton, N. L. Measuring activity in the ubiquitin-proteasome system: from large scale discoveries to single cells analysis. *Cell Biochem. Biophys.* **67**, 75–89 (2013).
295. Dunn, K. W., Kamocka, M. M. & McDonald, J. H. A practical guide to evaluating colocalization in biological microscopy. *American Journal of Physiology - Cell Physiology* **300**, (2011).
296. Bentham, M., Mazaleyrat, S. & Harris, M. The di-leucine motif in the cytoplasmic tail of CD4 is not required for binding to human immunodeficiency virus type 1 Nef, but is critical for CD4 down-modulation. *J. Gen. Virol.* **84**, 2705–2713 (2003).
297. König, R., Ashwell, G. & Hanover, J. A. Glycosylation of CD4. Tunicamycin inhibits surface expression. *J. Biol. Chem.* **263**, 9502–7 (1988).
298. Popik, W. & Alce, T. M. CD4 receptor localized to non-raft membrane microdomains supports HIV-1 entry. Identification of a novel raft localization marker in CD4. *J. Biol. Chem.* **279**, 704–12 (2004).
299. Zhu, Z. & Carter, P. Identification of heavy chain residues in a humanized anti-CD3 antibody important for efficient antigen binding and T cell activation. *J. Immunol.* **155**, 1903–1910 (1995).
300. Carter, P. *et al.* Humanization of an anti-p185HER2 antibody for human cancer therapy. *Proc. Natl. Acad. Sci.* **89**, 4285–4289 (1992).
301. Shalaby, M. R. Development of humanized bispecific antibodies reactive with cytotoxic lymphocytes and tumor cells overexpressing the HER2 protooncogene. *J. Exp. Med.* **175**, 217–225 (1992).
302. Qin, L. *et al.* Incorporation of a hinge domain improves the expansion of chimeric antigen receptor T cells. *J. Hematol. Oncol.* **10**, 68 (2017).
303. Kunkle, A. *et al.* Functional Tuning of CARs Reveals Signaling Threshold above Which CD8+ CTL Antitumor Potency Is Attenuated due to Cell Fas-FasL-Dependent AICD. *Cancer Immunol. Res.* **3**, 368–379 (2015).
304. Salter, A. I. *et al.* Phosphoproteomic analysis of chimeric antigen receptor signaling reveals kinetic and quantitative differences that affect cell function. *Sci. Signal.* **11**, 1–18 (2018).
305. Gulati, P. *et al.* Aberrant Lck signal via CD28 Costimulation augments antigen-specific functionality and tumor control by redirected T cells with PD-1 blockade in humanized mice. *Clin. Cancer Res.* **24**, 3981–3993 (2018).
306. Tifft, C. J., Proia, R. L. & Camerini-Otero, R. D. The folding and cell surface expression of CD4 requires glycosylation. *J. Biol. Chem.* **267**, 3268–73 (1992).

307. Grzesiek, S., Stahl, S. J., Wingfield, P. T. & Bax, A. The CD4 Determinant for Downregulation by HIV-1 Nef Directly Binds to Nef. Mapping of the Nef Binding Surface by NMR [†]. *Biochemistry* **35**, 10256–10261 (1996).
308. Lundquist, C. A., Tobiume, M., Zhou, J., Unutmaz, D. & Aiken, C. Nef-mediated downregulation of CD4 enhances human immunodeficiency virus type 1 replication in primary T lymphocytes. *J. Virol.* **76**, 4625–33 (2002).
309. König, R., Ashwell, G. & Hanover, J. A. Glycosylation of CD4. Tunicamycin inhibits surface expression. *J. Biol. Chem.* **263**, 9502–7 (1988).
310. Zhao, L. & Cao, Y. J. Engineered T Cell Therapy for Cancer in the Clinic. *Front. Immunol.* **10**, 2250 (2019).
311. Nicholson, I. C. *et al.* Construction and characterisation of a functional CD19 specific single chain Fv fragment for immunotherapy of B lineage leukaemia and lymphoma. *Mol. Immunol.* **34**, 1157–1165 (1997).
312. Zheng, Z., Chinnasamy, N. & Morgan, R. A. Protein L: a novel reagent for the detection of chimeric antigen receptor (CAR) expression by flow cytometry. *J. Transl. Med.* **10**, 29 (2012).
313. Amin, H. M. *et al.* Characterization of 4 mantle cell lymphoma cell lines: Establishment of an in vitro study model. *Arch. Pathol. Lab. Med.* **127**, 424–431 (2003).
314. Eyquem, J. *et al.* Targeting a CAR to the TRAC locus with CRISPR/Cas9 enhances tumour rejection. *Nature* **543**, 113–117 (2017).
315. Liu, J., Zhou, G., Zhang, L. & Zhao, Q. Building potent chimeric antigen receptor T cells with CRISPR genome editing. *Frontiers in Immunology* **10**, (2019).
316. Popik, W. & Alce, T. M. CD4 receptor localized to non-raft membrane microdomains supports HIV-1 entry. Identification of a novel raft localization marker in CD4. *J. Biol. Chem.* **279**, 704–12 (2004).
317. Shin, J., Doyle, C., Yang, Z., Kappes, D. & Strominger, J. L. Structural features of the cytoplasmic region of CD4 required for internalization. *EMBO J.* **9**, 425–434 (1990).
318. Benzing, C., Rossy, J. & Gaus, K. Do signalling endosomes play a role in T cell activation? *FEBS J.* **280**, 5164–5176 (2013).
319. Liu, H., Rhodes, M., Wiest, D. L. & Vignali, D. A. A. On the dynamics of TCR:CD3 complex cell surface expression and downmodulation. *Immunity* **13**, 665–675 (2000).
320. Onnis, A., Finetti, F. & Baldari, C. T. Vesicular trafficking to the immune synapse: How to assemble receptor-tailored pathways from a basic building set. *Frontiers in Immunology* **7**, (2016).
321. Kumar, A., Kremer, K. N., Dominguez, D., Tadi, M. & Hedin, K. E. Gα13 and Rho Mediate Endosomal Trafficking of CXCR4 into Rab11 + Vesicles upon Stromal Cell-Derived Factor-1 Stimulation. *J. Immunol.* **186**, 951–958 (2011).
322. Gerriets, V. A. & Rathmell, J. C. Metabolic pathways in T cell fate and function. *Trends Immunol.* **33**, 168–73 (2012).

323. Chen, L. & Flies, D. B. Molecular mechanisms of T cell co-stimulation and co-inhibition. *Nat. Rev. Immunol.* **13**, 227–42 (2013).
324. Mustelin, T. & Taskén, K. Positive and negative regulation of T-cell activation through kinases and phosphatases. *Biochemical Journal* **371**, 15–27 (2003).
325. Dobbins, J. *et al.* Binding of the cytoplasmic domain of CD28 to the plasma membrane inhibits Lck recruitment and signaling. *Sci. Signal.* **9**, (2016).
326. McKeithan, T. W. Kinetic proofreading in T-cell receptor signal transduction. *Proc. Natl. Acad. Sci.* **92**, 5042–5046 (1995).
327. Ruegg, C. L., Rajasekar, S., Stein, B. S. & Engleman, E. G. Degradation of CD4 following phorbol-induced internalization in human T lymphocytes. Evidence for distinct endocytic routing of CD4 and CD3. *J. Biol. Chem.* **267**, 18837–43 (1992).
328. Sleckman, B. P., Bigby, M., Greenstein, J. L., Burakoff, S. J. & Sy, M. S. Requirements for modulation of the CD4 molecule in response to phorbol myristate acetate. Role of the cytoplasmic domain. *J. Immunol.* **142**, 1457–62 (1989).
329. Kogan, A. J. & Haren, M. Translating cancer trial endpoints into the language of managed care. *Biotechnol. Healthc.* **5**, 22–35 (2008).
330. Schuster, S. J. *et al.* Tisagenlecleucel in Adult Relapsed or Refractory Diffuse Large B-Cell Lymphoma. *N. Engl. J. Med.* **380**, 45–56 (2019).
331. Pitcher, L. A. & Van Oers, N. S. C. T-cell receptor signal transmission: Who gives an ITAM? *Trends in Immunology* **24**, 554–560 (2003).
332. Guy, C. S. *et al.* Distinct TCR signaling pathways drive proliferation and cytokine production in T cells. *Nat. Immunol.* **14**, 262–270 (2013).
333. Cerignoli, F. *et al.* In vitro immunotherapy potency assays using real-time cell analysis. *PLoS One* **13**, e0193498 (2018).
334. Wang, D. *et al.* In Vitro Tumor Cell Rechallenge For Predictive Evaluation of Chimeric Antigen Receptor T Cell Antitumor Function. *J. Vis. Exp.* (2019). doi:10.3791/59275
335. Unsoeld, H. & Pircher, H. Complex Memory T-Cell Phenotypes Revealed by Coexpression of CD62L and CCR7. *J. Virol.* **79**, 4510–4513 (2005).
336. Rochman, Y., Spolski, R. & Leonard, W. J. New insights into the regulation of T cells by γ c family cytokines. *Nature Reviews Immunology* **9**, 480–490 (2009).
337. Leonard, W. J. Cytokines and immunodeficiency diseases. *Nature Reviews Immunology* **1**, 200–208 (2001).
338. Kagoya, Y. *et al.* A novel chimeric antigen receptor containing a JAK-STAT signaling domain mediates superior antitumor effects. *Nat. Med.* **24**, 352–359 (2018).
339. Shum, T. *et al.* Constitutive signaling from an engineered IL7 receptor promotes durable tumor elimination by tumor-redirected T cells. *Cancer Discov.* **7**, 1238–1247 (2017).
340. Kumar, M., Keller, B., Makalou, N. & Sutton, R. E. Systematic determination of the packaging limit of lentiviral vectors. *Hum. Gene Ther.* **12**, 1893–1905 (2001).

